X-644-68-282
PREPRINT

ACHIEVEMENTS IN PLANETOLOGY
1967

JULY 1968

GSFC
GODDARD SPACE FLIGHT CENTER
GREENBELT, MARYLAND

X-644-68-282
Preprint

ACHIEVEMENTS IN PLANETOLOGY

1967

Planetology Branch
Laboratory for Theoretical Studies

July 1968

GODDARD SPACE FLIGHT CENTER
Greenbelt, Maryland

Achievements in Planetology—1967

This report on the significant progress in the field of planetology has been compiled by the staff of the Planetology Branch of the Laboratory for Theoretical Studies of the Goddard Space Flight Center. The various sections have been prepared by scientists with some degree of expertise in these fields. In order of the sections as they appear, they are: Planets - R. Mueller; terrestrial geochemistry and geophysics - C. R. Seeger, C. Schnetzler and L. S. Walter; the moon - P. D. Lowman; impact cratering and metamorphism - N. Short; iron and stony-iron meteorites - J. Goldstein; stony meteorites and tektites - L. S. Walter and C. Schnetzler. The manuscript was edited by L. S. Walter, B. M. French, and P. D. Lowman. The staff of the Branch felt that a more complete and penetrating evaluation of the achievements could be made by a team of experts in the diverse fields of planetology. The editors feel that, indeed, the product will be of greater use to investigators in the field as well as to laymen interested in keeping up with the progress in planetology.

Planetology is taken to refer to the study of the condensed matter of the solar system. As such, the field encompasses not only the subjects reviewed in this section (i.e., the planets, including their satellites and the asteroids and meteorites) but interplanetary condensed matter and the sun itself. Since research on the former has generally been restricted to particle counting and the latter is held to be within the purview of the solar astronomers, they have been neglected in our report. In addition, the section on the earth (geochemistry and

geophysics) is relatively short in comparison to the large amount of literature which appears on the subject every year. As opposed to other areas of planetology, however, papers on the earth are more often of restricted interest and applicability and, having confined our scope to papers of broad interest, much of the work concerning the earth has been passed over.

On the other hand, and despite the large number of references in this section, much work of great value and of general interest concerning the earth and other subjects in this section has, unwillingly, been overlooked. The mass of data and ideas appearing in planetology makes this unavoidable but the editor would like to apologize for any omissions.

The section falls naturally into two general sections: the planets and meteorites. Separate sections on the earth and the moon fall under the category of "planetary studies" and work under "meteorites" has been divided into irons, stony-irons, stones and tektites. The latter have been included in this section because tektites are related to meteorites in that they contain meteoritic iron. A section on impact cratering and metamorphism spans the gap between planetary studies and meteorites.

THE PLANETS

The high point in the study of the planets during 1967 was, undoubtedly, the first sounding of the Venus atmosphere by the Soviet planetary probe Venera 4 and the simultaneous fly-by of the U. S. Mariner 5. However, other planetary research activities of both an experimental and theoretical nature also moved at an accelerated pace.

MARS

Most activity was concentrated on sifting, correcting and refining of physical and chemical data on the Martian atmosphere and surface. Barker (1) concluded from a further study of infrared spectra taken earlier that the Martian atmosphere consists of nearly pure CO_2 at a surface pressure of approximately 5 mb. Schorn and Gray (2) on the other hand sought to explain certain apparent variations in the observed pressure by a freezing-out of CO_2. Although it is not yet clear whether the ice caps on Mars consist of CO_2 or H_2O, Wells (3) pointed out a relation between the caps and the frequency of occurrence of the white clouds of the atmosphere. He suggested that the maximum rate of mass transfer from each pole corresponded to the maximum frequency of these clouds.

The nature of the Martian surface was the subject of studies by de Vaucouleurs (4) and by Sinton (5). The work of de Vaucouleurs resulted in a detailed photometric map of Mars based on 3500 visual estimates in white, green, and red light made near favorable oppositions in 1941 and 1958. It is stressed that this map will aid in evaluating the atmospheric and surface temperatures. Sinton, on the other hand, offered an explanation for the color variation and absorption spectrum of the surface in terms of the mineral deposits. He concluded, as a result of observations with a birefringence interferometer, that the surface consists at least in part of hydrous minerals. Also, although iron oxides are regarded as only minor constituents of the surface, they probably account for the red colors observed.

The relation of the surface features to the deep-seated subcrustal processes was sought by Miyamoto (6). His conclusion is that the surface structures are consistent with convection cells which adhere to third order spherical harmonics.

MERCURY

Observational data on this planet continued to be sparse in 1967. Attempts to detect or place an upper limit on the atmospheric density were made by O'Leary and Rea (7) using a polarimetric method. Although no evidence for an atmosphere was obtained in these experiments, an upper limit of one mb for the surface pressure was proposed.

VENUS

The outstanding result of the Soviet probe Venera 4 is its confirmation of the high surface temperatures previously inferred from Mariner 2 data and a variety of terrestrial measurements. Other important results of this and the U. S. probe, Mariner 5, (8) include the total pressure, atmospheric composition, exospheric temperature and composition and the strength of the magnetic field. All of these data have a critical bearing on the present physico-chemical state and evolutionary history of the planet. They also provide us with interesting comparisons with our own planet since, in many ways, Venus is another "Earth experiment" run at a higher temperature.

Venera 4 entered the Venusian atmosphere on the dark side within 10 degrees of the equator and approximately 80 degrees from the terminator (9,10,11). At an altitude of 26 km, as determined by a radar altimeter, temperature, total

pressure and atmospheric chemistry measurements were made. A second and third set of measurements were made at 23 km and very near the surface. The results of these measurements are presented in Table 1 and in Figs. 1 and 2. These results are in general agreement with the data from Mariner 5 except for the altitudes to which they refer. However, no explanation for these altitude inconsistencies has yet been proposed.

One of the most significant Mariner 5 results is that the intrinsic magnetic dipole of Venus is almost certainly less than 0.01 and probably less than 0.001 of that of Earth (12). It is likely that this is directly related to the slow rotation which corresponds to a sidereal period of 243 days. Another highly significant result of this experiment is the relatively low temperature (600-1100°K) inferred for the upper atmosphere (13, 14) since it is this temperature which, in part, governs the rate of escape of hydrogen and helium. However, it is likely that these low upper atmospheric temperatures are more than compensated for by the high temperature of the lower atmosphere which favors a rapid upward transport of these constituents.

A terrestrial observation that supplements the planetary probe data in an interesting way is the detection and measurement of HCl and HF in the Venus atmosphere (15). It was estimated by these workers that in the atmospheric region observed the following mixing ratios obtain:

$$\frac{HCl}{CO_2} \simeq 6 \times 10^{-7}$$

$$\frac{HF}{CO_2} \simeq 5 \times 10$$

It was also reported by the same authors that CH_4, CH_3Cl, CH_3F, C_2H_2 and HCN, whose spectra all fall in favorable region, were not detected and were thus estimated to be present in concentrations of less than a part per million.

The foregoing observations are of great interest to theoretical planetology because of their bearing on both meterological and chemical model atmospheres and on the chemical and mineralogical nature of the surface. Indeed Reese and Swan (11) have already obtained a fair fit of the pressure-altitude and temperature-altitude data (figs. 1 and 2) by assuming either constant or adiabatic lapse rate models for the atmosphere. Of primary interest, however, are the chemical consequences which may be inferred from the high surface temperatures and the atmospheric temperature profile. Because the kinetics of many inorganic chemical reactions are favored by the high surface temperatures, a chemical interaction between the lower atmosphere and the lithospheric minerals seems virtually assured (16, 17). Furthermore, the rapid falling off of the temperature with height favors a trizonal chemical model (17). According to this interaction model, the surface CO_2 pressure is likely to fall within the range 1-50 atm, so that the observed measurements are in good agreement with those expected from an interaction with typical crustal material. Similarly the low measured water and oxygen contents of the atmosphere are also in agreement since these substances show a great affinity for silicate and oxide phases of the lithosphere.

However, it seems likely that the measured oxygen content (Table 1) is still much too high because of errors inherent in the instrumentation.

It has also been shown (17) that the conditions of high temperatures, low water pressure and the relatively oxidizing atmosphere implied by the high CO_2/CO ratio militate strongly against the occurrence of most hydrogen compounds so that the failure to detect them is also in harmony with pervasive chemical interaction with the lithosphere.

The idea of an approach to chemical equilibrium in the lower atmosphere of Venus was accepted by Lippincott, Eck, Dayhoff and Sagan (18). They have, in fact, emphasized the equilibrium aspects of the problem to the virtual exclusion of the non-equilibrium processes. However, the rapid decrease of temperature with height shown by the Venera 4 and Mariner 5 data shows conclusively that the greatest part of the atmosphere cannot be in thermodynamic equilibrium. Indeed it seems unlikely that even local equilibrium could prevail at more than a few kilometers above the surface. The molecular abundances in the greatest part of the atmosphere probably represent quenched equilibrium established in that part of the atmosphere immediately above or within the lithosphere.

In their discussion, Lippincott et al. (18) ignore the possibility of the interaction of certain gases such as CO_2 and H_2O with the lithosphere. In fact, they attempted to trace an evolutionary path for the atmosphere based solely on the escape of hydrogen and reaction of oxygen with surface materials. If the interaction model holds, however, it is clear that the independent reaction of CO_2 and H_2O with the lithospheric minerals make all such evolutionary schemes meaningless.

An area of research which connects the contemporary state of Venus with its time of origin is the work of Goldreich and Peale (19). These authors suggest that the sidereal period of Venus (~243 days) results from a resonance established with the period of Earth's revolution, since at approximately this resonance period (~243.16 days) the same axis of Venus would always point toward Earth at inferior conjunction. According to the authors this type of resonance results from a quadrupole component of the Venus gravity field and might be explained by an irregular geometric figure or by internal density variations. In the latter case it is shown that trapping at the resonance can be understood if Venus possesses a fluid core similar to Earth's. Maximum capture probability occurs if the core responds to changes in angular velocity of the mantle with a time lag of about 3×10^4 yr. An interesting consequence of this is that if Venus is in such a resonance, then mapping of its gravitational field will determine the direction of its primordial rotation and may also provide an estimate of the magnitude.

THE MAJOR PLANETS

Continued efforts were made to understand the atmospheres of the major planets. Saslaw and Wildey (20) emphasized the interaction of ultraviolet radiation with the highly reducing atmosphere of Jupiter and concluded that photochemical processes should result in the production of C_2H_4, C_2H_6, C_3H_8 and higher polymers. Trafton (21) discussed model atmospheres for the major planets and found that in the case of Jupiter he should dominate over H_2, although a postulated small heat flux from the planet's interior would be consistent with a value of $(He/H_2) < 2$.

Further attempts were also made to understand the complex radio wave emissions from Jupiter. From his analysis of the Io-related emission, Dulk (22) concluded that apparent change in Jupiter's rotation rate, as determined by these emissions, resulted from a beam in the form of a conical sheet which intersects the plane of the ecliptic.

ORIGIN OF THE PLANETS

The general problem of the origin and development of the planets was the subject of a number of theoretical papers. Marcus (23) applied statistical methods to the accretion process and found planetary nuclei of from 0.42 to 0.60 of the mass of the whole planet. However, the same problem was approached quite differently by Harris and Tozer (24) who suggested that particle size fractionation and magnetic forces between metallic grains played a role in the enrichment of iron in the region of the inner planets.

The chemical aspects of the problem were taken up again by Shimazu (25). However, his deduced scheme of mineral formation $Fe_2\ SiO_4 \rightarrow Fe \rightarrow Fe_2\ SiO_4$, with progressive loss of hydrogen, is probably of very limited applicability because it fails to take account of important complicating factors such as the non-stoichiometry of the phases involved.

An observation of some interest relative to the dynamics of the formation of the Solar System was made by Hartmann and Larson (26). They found that if the asteroids are plotted for an angular momentum-mass diagram of logarithmic scales, they fall near a straight line curve whose extension also represents the

large planets fairly well. According to the authors the observation agrees with the law of constant period proposed by Alfvén (27) and is explicable either by magnetohydrodynamic effects or by an approach to rotational instability at the time of origin.

SUMMARY

In the confirmation of the high Venus temperatures, the planetary probes have brought us face to face with the concept of an "active planet" since, upon it, chemical and petrogenic processes have the immediacy of laboratory experiments. The recorded temperatures of 500-600° K are encountered in large regions of the solid Earth during regional metamorphism and then only at great depths within the crust where pressures are also high. However, on Venus, the analogous conditions should occur over wide regions of the surface where the pressure is comparatively low (by geologic standards) and the atmospheric chemistry relatively constant.

The early evolution and continued development of the atmospheres of the terrestrial planets may be considered in terms of certain critical reactions between their gases and the lithosphere. Three of the most important reactions are the following:

(1) oxidized rock $\rightleftarrows$ reduced rock + O_2 (gas)

(2) carbonated rock $\rightleftarrows$ decarbonated rock + CO_2 (gas)

(3) hydrated rock $\rightleftarrows$ dehydrated rock + H_2O (gas)

It is obvious that in the case of the relatively cold planets, Mars and Earth, all three of these reactions are virtually suspended on the surfaces for kinetic reasons and that the quantities of gases in the atmosphere are governed instead by secondary reactions of the following type:

(4) organisms $\rightleftarrows$ O_2 (gas)

(5) organisms $\rightleftarrows$ CO_2 (gas)

(6) CO_2 (ice) $\rightleftarrows$ CO_2 (gas)

(7) H_2O (liquid) $\rightleftarrows$ H_2O (gas)

Even these reactions seldom approach equilibrium because of various dynamic and other perturbations. However, as is well known (4) and (5) play a dominant role in the CO_2 and O_2 economy of Earth and readily account for the great excess of O_2 in the atmosphere over that allowed by reaction (1). Similarly, (6) and (7) govern the appearance and disappearance of ice caps on Mars and Earth as previously discussed.

If we exclude Mercury, because of its tenuous atmosphere, only Venus appears hot enough for reaction (1), (2) and (3) to approach equilibrium. The result is that carbon on this planet is probably largely volatilized into the atmosphere as CO_2 whereas, on Earth, it abounds in the lithosphere and biosphere as carbonates and reduced carbon compounds. In fact, calculations show that if all known carbon compounds on Earth were volatilized into the atmosphere as CO_2, the pressure of this gas would be close to that observed on Venus. On the other hand, the small quantity of water on this planet tells us that either this compound

was in short supply from the start or was rapidly lost as is commensurate with the high temperatures of the lower atmosphere. We have already mentioned that the affinity of H_2O and O_2 for the lithospheric minerals is also great enough to account for their low partial pressures.

Finally, it should be emphasized that the interaction of planetary atmospheres and lithospheres is a two-way process. The gases are not simply lost from rock, by "degassing" which corresponds to a slow secular leakage from the interiors according to reactions (1), (2) and (3). Indeed, it may have happened that great quantities of certain constituents were absorbed from the primordial atmospheres by these reactions, as O_2 and H_2O apparently are today on Venus. Hopefully, future planetary probes will answer these and other questions relative to the origin and development of the Solar System.

THE EARTH

As usual, the study of the earth led other subjects in the field of Planetology in terms of reportage in the literature. Some of the more exceptional contributions will be discussed here.

The use and limitations of K-Ar and Rb-Sr mineral ages were the subject of several investigations. In a rather extensive study, Hanson and Gast (28) have studied the effects of thermal metamorphism on both K-Ar and Rb-Sr mineral ages in the vicinity of two well-defined igneous contacts. They concluded that the temperatures required to effect essentially complete radiogenic daughter loss from biotite (a favorite mineral for K-Ar dating) in a simple thermal event are in excess of 300° C, and that the relative stability of mineral ages in a contact metamorphic zone is hornblende K-Ar > muscovite Rb-Sr > muscovite K-Ar > biotite Rb-Sr > viotite K-Ar. This latter conclusion is shown in Figure 3, where C/Co is the concentration of the species under consideration at any time over the original concentration. Livingston et al. (29) have shown that plagioclase feldspars from plutonic and pegmatitic environments can contain excess Ar^{40} with respect to that contained by cogenetic micas. This excess component is believed to have been occluded within these minerals at the time of their crystallization from the liquid magma, with the amount of excess Ar^{40} probably reflecting the partial pressure of Ar^{40} in the lithospheric gases. The authors suggest that the use of several phases from the same rock body and their interpretation by graphical isochron diagrams are more informative than the simple calculation and comparison of K-Ar ages from the phases.

Peterman et al. (30) have determined Rb and Sr and Sr^{87}/Sr^{86} values for samples of eugeosynclinal sedimentary rocks, mostly graywackes. These data are compatible with the theory of anatexis of eugeosynclinal sedimentary rocks in orogenic belts to produce granitic magmas provided that the melting occurs within several hundreds of million years after sedimentation. The low initial Sr^{87}/Sr^{86} ratios of these eugeosynclinal sedimentary rocks are related to the significant amounts of volcanogenic detritus present which probably was originally derived from the mantle.

A study of the development of lead isotopic ratios in oceanic basalts, by Ulrych (31), yields an age for the earth that is independent of the knowledge of the ages of the samples studied. The age is calculated to be 4530 ± 40 million years, which is in excellent agreement with several recent ages also obtained by studies of lead isotopes. Ulrych presents arguments as to why the age of 4750 million years obtained by Tilton and Steiger is too great. Ulrych also states that although the source of the basalts studied is not generally homogeneous, the differentiation of this source from a closed system has occurred fairly recently, geologically. The oldest age for any sample was 1230 ± 350 million years for Mid-Atlantic tholeiites.

Using radiometric ages to study possible continental drift, Hurley et al. (32) found the distribution of age values obtained by K-Ar and whole rock Rb-Sr determinations to be almost the same for West African rocks and basement rocks at opposite locations in South America. When Africa and South America are "fitted together" the sharply defined boundary between the Eburnean (2000 m.y.)

and the Pan African (500 m.y.) age provinces in West Africa strikes directly toward the corresponding age boundary in northeast Brazil. There is a suggestion of another age boundary in Cameroun-Gabon matching with the corresponding part of the east coast of Brazil, but the data are as yet insufficient. The authors state that these data support the hypothesis of continental drift, and the close proximity of these continents as recently as 500 m.y.

Hakli and Wright (32) have studied the distribution of Ni between olivine, clinopyroxene and glass from the Makaopuli lava lake in Hawaii where the temperature of the crystallizing samples is measurable (1050 to 1160° C). The data strongly suggest that the distribution of Ni obeys thermodynamic partition law, and that the distribution coefficients permit the estimation of the crystallization temperature within an accuracy of 10-20° C. However, the authors point out that the application of these data to plutonic rocks and other volcanic rocks should be done with caution as the effect of pressure and changing composition of the phases on the distribution coefficients is not known quantitatively.

In a very interesting study of an application of geochemical data, Hahn-Weinheimer and Ackermann (34) have used the analyses of Ti, Zr, P, Sr, Ba, Rb, K, and Na in 142 samples from the Malsburg Granite and country rock to attempt to evaluate the intrusion mechanism and direction of differentiation. They have shown that this body crystallized from the margin to the core, and there was a continuous process of crystallization-differentiation.

In a study of the composition of ancient graywackes from Wyoming, Condie (35) has suggested that the Precambrian continental crust did not change appreciably

in composition from that of quartz diorite or granodiorite during the last 3.0 - 3.5 x 10^9 years. He suggests that pre-Cretaceous graywackes may represent a nearly unmodified sample of continental crust over the last 3.0 - 3.5 x 10^9 years, and that the original chemical composition of the graywackes appears not to have been greatly affected by diagenesis and metamorphism.

Orbital Photography of the Earth

Although the Gemini Program was finished in 1966, interpretation of the nearly 1100 terrain photographs taken by the astronauts was just beginning in 1967. Preliminary study immediately indicated the most promising areas of geological application, as summarized in a review by Lowman (36). After discussing the unique advantages and disadvantages of orbital photographs, he concluded that they would be most useful in studies of continental drift, structure of rift valleys, investigations of transcurrent faulting, and other regional geologic problems. In another paper based on the Gemini photography, Lowman and Tiedemann (37) reported on the use of orbital photographs in field mapping in northern Mexico. They found that despite the small scale and relatively low resolution, such photographs could be used directly in the field with or without supplemental maps and photographs. They pointed out, however, that the inherent advantage of orbital photography, namely the great areal coverage per picture, could not be fully utilized unless very fast field transportation was available. Helicopters were recommended.

Because of its geological importance, the Great Rift Valley of Africa, part of which is occupied by the Red Sea, was a high-priority target for terrain photography

during the Gemini flights. Abdel-Gawad (38) used several of the Gemini IV pictures of the northern Red Sea and adjacent parts of Egypt to construct a tectonic map of southeastern Egypt (fig. 4). He arrived at several conclusions about the regional geology, a major one being that many of the long depressions of the Western Desert are tectonically controlled. The parallel sand dune belts may also be controlled by the regional structure. Abdel-Gawad found granitic intrusives easy to delineate, and found it possible to trace gradations from metasedimentary granites into igneous granites. He concluded that the geologic value of the Gemini photographs had been clearly demonstrated.

Because of its great complexity and breadth, the problem of the origin of continents and ocean basins will probably not be solved (if it is solved) by a specific investigation directed to that end. The answers will come instead from many separate studies, some of which will probably appear at first to have no relation to the problem or even to geology. A number of papers published in 1967 illustrate this.

Although the chain of reasoning: the continents are essentially granitic; batholiths are essentially granitic; therefore the origin of batholiths is the origin of continents; is over-simplified and possibly fallacious, there is no doubt that batholith formation has major implications for continental growth. A major paper by Bateman and Eaton (39) on the Sierra Nevada batholith provides a clear picture of how continental accretion may take place. They present evidence indicating that the batholith and the associated geosynclinal sediments and volcanics are a net addition to North America at the expense of the Pacific basin.

The batholith itself, they propose, was formed by anatexis and related processes of the geosynclinal rocks, rather than coming from the mantle.

In a comprehensive review of the batholith problem, Hamilton and Meyers (40) showed that batholiths may arise not only in miogeosynclinal environments, but completely outside geosynclines. They explain the nevertheless common association of eugeosynclines and batholiths as reflecting a related origin of the geosynclinal volcanics and the batholiths: "Batholiths form wherever temperatures are high enough at depth to melt the needed magmas, and eugeosynclines are only one setting in which these conditions are met."

In his presidential address to the Geological Society of Australia, S. R. Taylor (41) attacked the problem of origin and growth of continents directly. Reviewing a wide range of geophysical, geochemical, and geological evidence, Taylor concluded that continent formation is essentially a process of multi-stage fractionation of the mantle. Specifically, growth is by addition of andesites in orogenic zones, followed by sedimentation, metamorphism, and eventual consolidation of the orogenic zone. The process stops when the underlying mantle has been depleted in the radioactive elements which are the chief heat sources. Taylor's mechanism operates over geologic time; however, it is non-uniformitarian to the extent that it involves an initial geochemical fractionation of the upper 1000 km of the mantle.

Because of its size and geologic importance, the Pacific Ocean basin must have a central role in any comprehensive theory of continent or ocean basin

formation. This was brought out forcibly in several papers presented at the Eleventh Pacific Science Congress in 1966, and published as one volume in 1967.

From a general point of view, perhaps the major relation emphasized by the various papers was the remarkable geologic unity of the Pacific basin, especially in the later geologic periods. The "ring of fire," applied to the chains of andesitic volcanoes surrounding the Pacific, is of course well known; what is not so well known, however, is the ring of blue-schist facies metamorphic rocks. This facies, recognized only a few years ago, represent high pressure and relatively low temperatures, and is characterized by such minerals as glaucophane, lawsonite, and aragonite. Blue-schist facies metamorphic rocks are found around the Pacific basin as widely separated localities including California, Japan, New Caledonia, and New Zealand. The circum-Pacific region is also characterized by major wrench faults, such as the San Andreas (California) and Alpine faults (New Zealand).

The papers presented at the Congress have a number of major implications for the origin of continents and ocean basins. Several papers specifically or implicitly contradicted the theory that continents grow by accretion of eugeosynclines, and that the circum-Pacific orogenic belt (much of which arose from former eugeosynclines) represents the newest addition to the various continents. In a major study of the Canadian Cordillera, Roddick, Wheeler, Gabrielse, and Souther (42) found that continental (sialic) crust has existed near the present continental margin since Early Paleozoic or possibly Precambrian time, and

concluded that there has been no appreciable westward accretion since the Paleozoic. The geology of Taiwan, as shown by Ho (43), although dominated during the Tertiary by eugeosynclinal deposition and subsequent orogeny, does not indicate ensimatic continental growth, since the eastern part of the island (the oceanward side) is underlain by pre-Tertiary metamorphics. Similarly, New Zealand is underlain by relatively old continental rocks, (Aronson, 44) with radiometric ages of 350-370 million years, and possibly much older ones, implied by the discovery of zircons with lead ages of 1270 and 1360 million years.

On the other hand, several authors, including Vassilkovsky (45) and Burgl (46) considered at least part of the circum-Pacific orogenic belt to be accretions to the continent.

Continental drift was a relatively minor topic at the Congress, in sharp contrast to meetings focused on the Atlantic Ocean. Hamilton (47) supported the existence of continental drift in eastern Asia and Alaska, but Fleming (48) found that the Mesozoic biogeography of the southwest Pacific could be interpreted either for or against drift.

The geologic history of the Pacific basin is of importance in planetology not only as the largest single tectonic feature of the earth, but in relation to the origin of the moon, since one version of Darwin's recently-revived theory that the moon was formed from the earth holds the Pacific basin to be the birth scar. Although there was no mention of this theory in any of the Circum-Pacific Orogenesis Symposium, it is possible to draw a few inferences about the Darwin theory. In particular, it is almost certain that the supposed formation of the

moon from what is now the Pacific basin could not have happened later than the beginning of the Paleozoic Era. This follows from a variety of evidence, the most important fact being the continuity and unity of circum-Pacific geologic history since the late Precambrian. In addition, there appears to be nothing especially strange about the Pacific basin from a geologic viewpoint; its main peculiarity is the blue-schist zone surrounding it, and this is far too recent to have any direct relation to the supposed formation of the moon. Perhaps the strongest evidence against the theory is subjective: the total omission of the theory from all the published papers. Although this omission could be interpreted as reflecting the conservatism of the authors, it is nevertheless striking that there is no major enigma which would appear to require a planetary catastrophe for its explanation.

The extremely interesting work of Lamar and Marifield clarified the origin of the Earth-Moon system (49). Using the models in Table 2 (from their paper). they find that the distance from Earth to Moon should have varied during geologic time as shown in Figure 5. When combined with information on the length of the day from data obtained by counting the growth rings of corals (Figure 6), they conclude that the age of the Earth-Moon system is 0.5 to 2 billion years.

They point out that origin by fission or close-capture at such a late date should have left obvious indications in the geologic record and evidence of this seems to be lacking. However, a non-catastrophic origin (Baldwin's capture-at-a-distance or MacDonald's aggregation of many smaller moons) would cause an abrupt increase in oceanic tidal action.

In the study of geomagnetism, Heinrich (55) has studied the natural remnant magnetism of sixty-one specimens of lava flows from a volcanic field on the eastern slope of the Sierra Nevada. The rocks are dated as pliocene-pleistocene in age. The values obtained for the magnetic vectors fell in two distinct groups (declination, 64°; inclination, -67° for one group and D = 20°, I = +46° for the other group). This indicated that the first group represents an intermediate direction of magnetization during a magnetic reversal. Magnetic studies on volcanic specimens from Oregon by Baksi, York and Watkins (56) similarly indicated a change from reversed to normal polarity in rocks which were dated by radioisotopes at 15.1 m.y. On the other hand, Gromme, Merrill and Verhoogen (57) determined the natural remnant magnetism of rocks dated at 142 to 129 m.y. from the Sierra Nevadas which indicate the same pole position as rocks as young as 84 m.y. They conclude that polar wandering has not occurred in this period but that apparent polar wandering determined in rocks from Australia and Africa is due to continental drift. Coe (58) studied the intensity of the paleo-geomagnetic field as preserved in volcanic rocks from the western U.S. A value of 0.2 times the intensity of the present field given by miocene rocks is evidence that the intensity of the geomagnetic field decreases during reversals. Other specimens bear evidence that the field may not have exceeded twice its present value during the past several million years.

In a recent paper, Cox and Dalrymple (59) have developed a new statistical method for determining the ages of the boundaries between geomagnetic polarity

epochs. Their best statistical estimates of the ages of the boundaries between epochs in Gilbert-Gauss boundary, 3.36 m.y.; Gauss-Matuyama boundary, 2.5 m.y.; Matuyama-Brunhes boundary, 0.70 m.y. The duration of polarity events is estimated to vary from 0.07 to 0.16 m.y., and the best estimate of the time required for the earth's field to undergo a complete change in polarity in 4600 years. The statistical analysis shows that if the geomagnetic polarity time scale is to be extended much beyond its present limit of 3.6 m.y. another method of dating the rocks, other than K-Ar, will probably have to be used; this is certainly true if information is desired on the detailed polarity structure.

In a related study Ozima et al. (60) have reported that the age difference between the lowermost flows of an upper normal polarity group and the upper portion of the adjacent reversed group is about 0.05 m.y., which they suggest is the maximum time for transition of the earth's magnetic field.

Sykes (61) has studied data from long-period seismographs on 17 earthquakes, solving for the mechanism of faulting. Ten of the earthquakes studied occurred on mid-oceanic ridges and, for these, the motion was predominantly strike-slip in character. The sense of the faulting was opposite to that expected for simple offset of the ridge crests along the fracture zones. The results of the study agree with the hypothesis of the growth of the sea-floor at the crest of the mid-oceanic ridge system. Hodgson (62) has determined the direction of faulting in 65 earthquakes. He finds that, of 75 earthquakes (10 were studied previously), all but eight are the result of strike-slip faulting. For the strike-slip faults, the strike direction within any one area appears to be random.

Hodgson points out that these results are incompatible with several theories on the mechanism for deep-focus earthquakes which require thrust or gravity faulting. These theories do not explain the appreciable amount of strike-slip faulting.

Hales and Doyle (63) have investigated the velocity of seismic-wave propagation and, in particular, the variations in the velocities of P and S waves in several regions of the U.S. The arrival times are relatively early in central and eastern U.S. and relatively late and late in the west (differences ranging to about three seconds for P waves and eight seconds for S). The differences imply a variation in Poisson's ratio between the two regions and best fit a model in which the shear modulus varies at constant compressibility. The major part of the deviations may be due to differences in temperature in the upper part of the mantle under these regions—the west being at a higher temperature than the mantle under the central and eastern U.S. Pollack (64) pointed out that the near equality of heat-flow measurements in continental and oceanic regions, giving rise to the implication that the temperature under the oceans are greater than those under the continents, would indicate thermal displacements and stresses. These would give rise to several tectonic features. Thus, the continents would be centers of relative contraction while the ocean basins would be centers of expansion. In this model, normal shearing occurs on the surface of the expanding ocean basin and reverse shearing occurs on the continents. The zone of normal shearing which dips beneath the continental margin compares with the loci of earthquakes in the circum-Pacific seismic belt.

Anderson (65) has re-examined the question of a phase-change as an explanation of seismic and density discontinuities in the mantle. He points out that the velocity transition may be best explained by two transition regions, each about 75 to 90 km thick and at about 365 and 620 km depth. Pressures at these depths and estimates of the temperatures agree very well with transition temperatures and pressures in the system Mg_2SiO_4 - Fe_2SiO_4. This transition from olivine to spinel would take place at 1500° C at 365 km and 1900° C at 620 km and indicates a possible increase in the fayalite content with depth.

Harris, Reay, and White (66) have found evidence that there is geographic heterogeneity of mantle material, in a study of inclusions of ultramafic rocks in extrusive rocks. If such ultramafic xenoliths do, in fact, represent fragments of mantle material, the pyroxene peridotite zone of the upper mantle ranges from 100% olivine to 65% olivine plus 35% pyroxene. The difference between this layer and a garnet peridotite layer which, by the mineralogical composition. should contain 55% olivine, may be real. The garnet peridotite xenoliths also contain less Ca and Al and have a higher Mg/Fe ratio.

Caner, Cannon and Livingston (67) have performed "geomagnetic depth sounding" investigations. GDS involves the comparison of the variation in the three components of the geomagnetic field in order to obtain information on the electrical conductivity of sub-surface layers. The authors recognized a highly conducting layer within 25-35 km of the surface in the Cordillera region of North America.

Ergin (68) has used seismic data to investigate the structure of the Earth's core. The results indicate a layer of decreased seismic wave velocity below 4015 km. Two other transitions in velocity are required at 4500 and 4685 km in order to explain the refraction and reflection branches of the seismic waves. In general, the results suggest a layered transition zone between 4015 and 5140 km below the surface within which the general level of velocity is lower than those obtained by extrapolation of the velocities in the outer part of the outer core. Sachs (69) has used seismic P-waves diffracted by the core-mantle boundary to determine the radius of the core (3537 ± 9 km) and the velocity of the waves in the lower mantle (13.64 ± 0.045 km/sec). Irregularities in the arrival times of these diffracted waves indicate either variations of the velocities in the lower mantle or small differences in the radius of the core.

In the discussion of the thermal gradients of planetary bodies and the processes which took place during the formational stages of the planets, the condition of thermal energy, largely by radiation, is one of the most significant factors. Experimental difficulties, however, have resulted in a pausity of data on this subject. Aronson et al. (70) have now determined the radiative thermal conductivity of several at temperatures up to 1500° K. Their results (Table 1) indicate considerable deviation from values based on room-temperature data. They point out that these values are more in keeping with those necessary to explain the thermal history of the earth.

Bullen and Haddon (71) have presented variations (B_1 and B_2) of an earth model (B) which was constructed some years ago. This revision is based on

new estimates of the moment of inertia of the earth; density distribution in the core and evidence from the free oscillation of the earth. The difference in the two models is based on the values assumed for the density of the lower core; 15 gm/cm^3 for B_1 and 13 gm/cm^3 for B_2. The other parameters of these models are illustrated in figures 7 and 8.

THE MOON

The year 1966 was marked by a number of "firsts" in lunar exploration, including the first soft-landing spacecraft and the first successful circumlunar orbital surveys. These programs were continued in 1967 with equal or greater success, with four more Surveyors placed on the moon and the remaining three Lunar Orbiters placed in orbit around it. In addition, an unusually large number of astronomical investigations and theoretical studies of the moon was published.

SPACECRAFT INVESTIGATIONS

Surveyor III

Following the unsuccessful Surveyor II flight, Surveyor III made a successful landing in Oceanus Procellarum at 2.94 degrees S, 23.34 degrees West, only 1.7 miles from the mid-course aiming point (Milwitzky and Dwornik, 72). The spacecraft actually made three distinct landings, the vernier engines continuing to fire after initial touchdown, an unexpected but valuable occurrence that gave additional information on the landing dynamics and consequently the strength of the lunar surface. The final landing site was on the inner slope of a 200 meter wide crater.

Perhaps the most important scientific finding of the Surveyor III mission was the demonstration that the inside of a subdued mare crater looks very much like the intercrater mare areas such as that on which Surveyor I landed (fig. 9). The surface is relatively smooth, with occasional blocks, and is evidently unconsolidated to a depth of at least a few feet. The cumulative grain size resembles

that of a surface repeatedly impacted. This, and the Surveyor III pictures which show various degrees of rounding for blocks in the field of view, suggests that the fragmental nature of the surface is the result of primary and secondary impacts. A related phenomenon first discovered by Surveyor III is that of downhill creep of the lunar soil, indicated by the piling up of material on the uphill side of partly buried blocks. The cause for this creep is not known: meteoritic impacts and the attendant ground shock, temperature changes, and perhaps seismic activity, together with gravity, probably combine to produce it.

Another characteristic, discovered first by Surveyor I and confirmed by Surveyor III, is that subsurface material brought up either by the footpads or the surface sampler is darker than the surface (fig. 10). This development had been a surprise, the pre-Surveyor belief being that the lunar surface darkens with time, probably as the result of sputtering. Shoemaker, et al. (73) have suggested that this "lunar varnish," analogous to desert varnish on earth, is the result of deposition of a dark substance by some unknown process, possibly gases from below or atoms knocked off by sputtering and redeposited just below the surface.

Perhaps the most interesting Surveyor III experiment was the surface sampler, (fig. 11) the remotely-controlled shovel carried for the first time on this flight (Scott, et al. 74). Although this was primarily an engineering test, the quantitative information it provided is of considerable scientific interest. The static bearing strength, for the conditions of the tests, was estimated to be between 2.5-3 psi. Furthermore, the material became noticably stronger and

denser at depths of about 3 inches, although there was no sign of changing grain size or other visible properties. The soil was slightly cohesive, and described by Scott, et al. (74) as similar to a fine-grained, granular terrestrial soil. The color of the soil, according to Rennilson, proved to be essentially gray, as shown by the filter wheel (fig. 12). Shoemaker suggested that this indicates the iron to be primarily in the reduced state, in contrast to the prevailing oxidized state responsible for the characteristic reds, browns, and yellows of terrestrial soils.

Another "first" for Surveyor III was the photography, in color, of an eclipse of the sun by the earth, which is expected to be of scientific interest in the study of atmospheric scattering of light. The Surveyor III camera also served astronomically in returning pictures of the crescent earth and of Venus.

To summarize, Surveyor III was a highly successful mission for a variety of reasons, perhaps the most important of which was the demonstration that the terrain photographed by Surveyor I was not an isolated, unusual occurrence, but typical of considerable areas. It also tended to confirm the generality of other characteristics and features found by Surveyor I, such as the relative darkness of subsurface material.

Surveyor V

On September 10, the most successful of any soft-landing spacecraft to that date touched down in a chain crater near the western border of Mare Tranquillitatis (fig. 13). Surveyor V was essentially similar to Surveyor III, with the addition of the first compositional experiments to be carried on a soft-landing

lunar probe: an alpha-scattering instrument and a magnet fastened to a footpad. All the experiments were remarkably successful; the major results of the mission were the following (Jaffe, et al. (75).

Like Surveyor III, the Surveyor V spacecraft landed on the inner slope of a small crater, 9 by 11 meters; this one was found from Lunar Orbiter V photographs to be a member of a string of subdued craters. The spacecraft landed just below the rim of the crater, and tilted 20° from the vertical, providing a good view of both the inside of the crater and the surrounding terrain in addition to views of the solar corona after sunset. The inside of the chain crater (possibly two coalescing craters) was generally similar to the Surveyor III crater, as shown by fig. 14. It had no rim, which, in conjunction with its alignment with the N45° W-trending Imbrian fracture system, led the experimenters to believe that it was formed by drainage into a tectonically-controlled fissure.

The close-up views of the ground around the spacecraft were extraordinarily clear, and provided new insights as to the nature of the mare material. A lucky accident enhanced the value of these pictures (fig. 15): the numbers 2 and 3 footpads had dug trenches as the spacecraft slid down the side of the crater after landing, permitting close examination of the subsurface material. This proved to be, as in the Surveyor I and III sites, fragmental debris with a wide range of grain sizes. Much of it appears to be aggregates, or clods, of finer-grained material. Some of the smaller pieces look very much like glassy impactites from Meteor Crater and similar impact craters. Most of the larger fragments were thought to be rock. The overall nature of this regolith to a depth

of a few meters, appears to be the result of repeated, superimposed impacts by meteorites and ejecta from other impact craters. This interpretation, if correct, has important implications for the alpha-scattering experiment. The latter analyses one spot on the surface, unless moved by some means, and hence the significance of the analysis is open to question. If, however, the spot analyzed is a mechanical composite of material from a considerable area, as implied by the impact interpretation, the results are much more significant.

Also noticed in the close-up television pictures was the now-familiar lightening of the surface (or darkening of the subsurface), both in footpad ejecta and in the trench dug by footpad 2. The albedo of the dark material was estimated to be about 5% lower than that of the undisturbed surface (which was about 12%).

An interesting engineering soil test was performed by firing the vernier engines, 53 hours after the landing, for about half a second each. Although it was not possible to view the engine firings as they happened, study of pictures taken before and after permitted a detailed analysis of the effects (Christensen, et al., (76). This analysis verified that the soil was somewhat cohesive, and consisted largely of particles in the 2 to 60 micron size range.

The major achievement of Surveyor V was, of course, the compositional experiments. The simpler of the two, the magnet fastened to footpad 2 (fig. 16), was intended to help decide between two extreme views of the nature of the lunar surface material: that it was formed wholly by meteoritic impact, or that it was formed wholly by internal (i.e., essentially, volcanic) processes (De Wys, 77). A prevailing impact origin would indicate that considerable meteoritic iron should

be found in the lunar soil, whereas a volcanic soil would not contain much more iron than volcanic rocks. The magnet, which was paired with a non-magnetic control bar of identical size and shape to eliminate confusion by non-magnetic adhesion, was dragged through the soil when the spacecraft landed. A small amount of material stuck to it which, from the clean condition of the control bar and the fact that it was not removed by the vernier firing, was inferred to be magnetic oxide. Comparison of the appearance (fig. 17) of the magnet on the television pictures with vacuum chambers tests of an identical magnet in a variety of rock powders, with varying amounts of added iron, indicated that the soil at the Surveyor V site contained not more than 1% by volume of metallic iron. This indicates, according to de Wys (77) that the mare material on which the spacecraft landed was not simply impact-pulverized non-volcanic rock, but more probably powdered volcanic rock such as basalt.

The experiment of greatest fundamental scientific importance on Surveyor V was the Alpha Scattering Experiment (fig. 18). The chemical composition of the moon has long been one of the most refractory scientific problems, most remote analytical methods applied to it having given information about physical structure rather than composition. The pioneering gamma-ray survey by Luna 10 in 1966 had indicated a basaltic composition, but had been very difficult to interpret because of the high background (Walter and Lowman, 78). Consequently, the results of the in-situ alpha scattering experiment were eagerly awaited.

The experiment, as described by Turkevich, et al., (79) depended on measurement of the energy spectra of alpha particles emitted by curium 242 sources and

reflected by the surface material, as well as on measurement of protons produced in the surface by the alpha particles. The upper limit of alpha particle energy is characteristic of elements in the atomic weight range 7 to 28, including oxygen, silicon, aluminum and other elements common in the earth's crust and in stony meteorites. To be interpreted, the energy spectra of a variety of materials had to be measured for comparison. During the mission, measurements were made of a standard sample of known composition carried on the spacecraft, and of the background in the lunar environment, before the instrument was lowered to the surface to begin the actual analysis.

The experiment was highly successful. The instrument was placed on fragmental material thrown out by the footpad, and thus analyzed a more representative sample than an undisturbed surface would be. Furthermore, the fragmental nature of the mare material in general implies that at any one spot, the composition is a composite of the surrounding area. Nevertheless, Turkevich, et al. (79) stressed the preliminary nature of the analysis and the fact that it was of only one site on the moon.

The results of the Alpha Scattering Experiment are shown in Table 4, and in graphic form in figs. 19 and 20. It is at once obvious that the composition of the material at this site is much more like that of the earth's crust than that of the sun's atmosphere, as would have been expected. More significant is the comparison with various rock types and with tektites. It appears that ultrabasic rocks and chondritic meteorites can definitely be ruled out, and granitic rocks can probably be also eliminated. The most plausible analogues are basalts and

basaltic achondrites, the latter having been previously suggested to come from the moon by Duke and Silver (80). In general, then, the mare material at this site has the chemical composition of basalt. This interpretation is plausible for a variety of independent reasons. First, the magnet experiment already described had results consistent with powdered basalt. Second, the general physiography and distribution of the mare material is similar to that of volcanic rocks, as is the fine structure if the fragmental nature can be accounted for.

This result indicates that the moon is a differentiated body, since the mean density is too high for it to be basalt all the way through. More generally, it supports the concept of the moon as a relatively warm, actively or recently evolving body—a school of thought that has been coming back into favor in the past few years (Walter and Lowman, 78).

Lunar Orbiters III, IV, and V

The last three of five planned Lunar Orbiter spacecraft were successfully placed in orbit around the moon during 1967, continuing the flood of new information begun by Lunar Orbiter I in 1966. The original program objective had been to obtain detailed photographs of potential Apollo landing sites; thanks to the success of the first three Orbiters, the last two were available chiefly for scientific photography of the front and back sides of the moon. Figs. 21, 22, 23, 24. The program was essentially completed in 1967, although study of the results will continue for some time; therefore, the scientific results of the program as a whole will be summarized here.

In an indirect sense, the achievement of Apollo landing site certification itself was—or will be—of great scientific importance. In addition to the expected scientific return from the manned landings, the Lunar Orbiter program further demonstrated the essential correctness of inferences made from earth-based observations and earlier lunar probes such as the Ranger series. One of the most encouraging discoveries made by all the precursor probes has been, in fact, the relative scarcity of totally unexpected discoveries that would affect the Apollo program.

Some of the most scientifically significant results of the Lunar Orbiter Program are in lunar geodesy, specifically in study of the moon's gravitational field by analysis of tracking data. Pre-Orbiter knowledge of the moon's mass distribution had been so unsatisfactory in some respects that it appeared the moon became less dense toward the center—i.e., was more like a hollow sphere than like the earth (MacDonald, 81). However, studies by Michael, et al. (82) indicated rather definitely that the moon is nearly homogeneous, with similar density throughout. This of course contrasts with the earth, but is much more believable geophysically. Another preliminary deduction from the tracking data is that the radius of the moon aimed toward the earth is one or two kilometers less than previous estimates, implying that the center of mass is displaced (toward the earth) from the center of figure. This may indicate that the moon is in isostatic equilibrium, as previously deduced by O'Keefe and Cameron (83) and, from the Lunar Orbiter I tracking data, by Kaula (84). This would be in agreement with the abundant evidence of widespread volcanic activity

uncovered by the Orbiters and other lunar probes, although, as Baldwin (85) pointed out, even non-isostasy would not preclude igneous activity.

The Lunar Orbiter spacecraft all carried micrometeoroid detectors of the "beer can" type, in which hits are detected by loss of pressure when a pressurized cylindrical container made of .001" thick copper is penetrated (Corliss, 86). As reported by Gurtler, each spacecraft carried twenty of these cells, with an exposed area of two square feet. Over the 14 months in which various members of the Lunar Orbiter fleet circled the moon, 18 of the 100 detectors were punctured. The punctures were randomly oriented, showing no directional flux. This rate is less than one-half the flux measured in the near-earth region by similar detectors on Explorers XVI and XXIII. Although the Lunar Orbiter micrometeoroid data are primarily of engineering value (providing, for instance, little knowledge of meteoroid mass or velocity), they are also of scientific interest.

Geology, which can be informally defined as what we see, in contrast to geophysics (what we don't see), obviously is the chief scientific beneficiary of the Lunar Orbiter program. Because of the high-quality of the Lunar Orbiter photographs, and because there is no successor currently planned, geological study of these pictures will continue for several years. However, the main implications appear clear.

The major geologic importance of the Orbiter results is the new insight they provide as to the extent and nature of lunar volcanic processes and mass

wasting. Although the controversy about the origin of craters continues, it is clear that volcanism has played a major role in the formation of lunar rocks and land forms. Specific evidence for this comes from Orbiter photographs of domes, craters, mare surfaces, and other features. Lunar domes, such as those of the Marius Hills (fig. 26), had long been considered to be of igneous origin (either shield volcanoes or laccoliths); as illustrated by McCauley (87), some of them closely resemble volcanoes when seen at high resolution. Several of the domes have a composite topography, consisting of relatively steep-sided upperparts superimposed on broad, gently-sloping bases; these have been tentatively interpreted by McCauley (87) as tholoids of intermediate to acidic lavas overlying basaltic shield volcanoes. The domes exhibit far more variety and complexity than had been evident in earth-based telescopic photographs. Another interesting characteristic of the domes is the apparent absence of bedrock exposures; like the maria, they appear to be covered to some depth by unconsolidated material, perhaps produced by mass wasting.

As a favorable landing sites, the maria were of course repeatedly photographed by the Orbiters. A number of pictures show details of the "tree-bark structure," on both mare and highland terrain. Taken in conjunction with the Surveyor pictures, which show apparent down-slope mass movement, the Orbiter pictures (fig. 27) suggest that this structure is the result of mass-wasting. A possible cause is the seismic disturbances set up by major impacts. Other mare features notable for their unexpected scarcity are flow fronts, finally photographed by the Orbiters. They tend to confirm the

Surveyor analyses indicating basalt as the mare material. The scarcity of flow fronts and other typical lava features is still not completely understood; the most favored explanation is that originally proposed by Shoemaker (88) for the Ranger 7 pictures of Mare Cognitum, namely that the original topography has been largely destroyed by repeated impacts of meteorites and ejecta from meteorite impacts. However, some geologists feel that the eruption of the mare lavas was followed by major ash falls, which blanketed the originally rough topography. These two explanations are not necessarily contradictory; a compromise model consisting of lava overlain by ash, and saturated with impact craters, appears plausible.

The origin of the moon's craters continues to be controversial, despite, or to a degree because of the many excellent crater pictures returned by the Orbiters, especially Lunar Orbiters IV and V. Of greatest interest are the vertical, high-resolution views of Tycho, Copernicus, and Aristarchus (figs. 28, 29, 30). The Tycho photographs will be discussed in some detail, since this crater, because of its relative youth, displays extremely well the topography common to all three. The most conspicuous feature is the rough floor of the crater, which has a striking resemblance to terrestrial lava flows. It appears certain that some sort of relatively viscous liquid at one time covered much of the crater floor, but since there is evidence of large quantities of former melt in some terrestrial structures of suspected impact origin, such as the Manicouaga structure in Canada, the lava explanation is by no means unarguable. Other features for which a volcanic origin has been proposed include the small

areas of what appear to be mare material, filling depressions in the outer flanks of Tycho. Here too, however, an impact origin—in this case from fallback as a "base surge"—is favored by some. The apparent flows on the outer flanks of the crater are of extreme interest since Surveyor VII landed on one of them, returning an analysis indicating the elemental composition of a low-iron basalt.

In summary, Tycho (and to different degrees, Copernicus and Aristarchus) exhibits a number of topographic features strikingly similar to those of volcanic terrains. This was rather unexpected, except by those who consider these craters to be large calderas, because these craters appeared, with telescopic resolution, to be relatively uncomplicated by possible volcanic activity, as are Archimedes and Plato (large, mare-material filled craters). There appears a very real possibility that, even if the initial craters are formed by meteoritic or cometary impact, there has been substantial post-impact volcanic activity.

Zond 3

Results from two experiments carried on the Russian lunar probe, Zond 3, which flew by the moon in 1965, were reported in 1966 at the Vienna COSPAR meeting by the investigators. Lebedinsky, Krasnopolsky et al. (89) described the ultraviolet spectrophotometer, and presented typical spectrograms (of a total of 15) obtained during the flight. The curves are similar to that of sunlight, although there are some differences. Another ultraviolet experiment carried by Zond 3 (Lebedinsky, Aleshin et al. 90) covered the 2850-2550 A region. This technique has potential value for compositional determinations, according to the authors, but only preliminary analysis had been conducted at the time the paper

was presented. A well-defined albedo vs. wavelength curve was derived, showing a decrease from 4 to 3% in the 3550-3400A range, a leveling off at 3%, then a rapid decrease from 3% to 1% in the 3100-2850A range.

Explorer 35

On July 22, 1967, a spacecraft of the interplanetary monitoring platform type (IMP) was placed in orbit about the moon and designated Explorer 35, or informally the "Anchored IMP." Although the primary objective of this satellite was to study the space environment of the moon and the interaction of the solar wind with the moon, the information returned permitted significant inferences about the moon itself. Preliminary results of the magnetic field experiment were reported by Ness, et al. (91).

Perhaps the major deduction from the magnetometer data was that the moon has no strong magnetic field. Specifically, no field was detected at the periselene altitude of 800 km, indicating, according to Ness, et al. that the intrinsic field at the surface is no more than 16 gammas. (For comparison, the interplanetary magnetic field during quiet sun conditions is about 5-10 gammas.) This result had, in general, been expected, although Gold (92) had suggested that the moon might accumulate the interplanetary magnetic field, and Dolginov (93) interpreted the Luna 10 results as indicating a field of 24-40 gammas near the moon.

An extremely interesting indirect deduction was also made by Ness, et al. about the interior of the moon from the magnetic data. Explorer 35 detected no evidence of a bow shock wave around the moon such as is formed by the interaction

of the earth's magnetic field with the solar wind. This indicates that the interplanetary magnetic field diffuses through the moon rapidly. From this diffusion time, Ness, et al. calculated that the interior electrical conductivity is no higher than 10^{-5} mho/meter. This in turn implied, assuming a temperature dependence of the conductivity similar to that of olivine ($(Fe, Mg)_2 Si_2 O_4$) and periclase (MgO), that the average temperature of the moon is less than 1000° K.

Whether this interpretation can be reconciled with the evidence of abundant past and present volcanic activity remains to be seen.

OPTICAL ASTRONOMY

Geological Mapping of the Moon

Despite the dramatic discoveries made by the Lunar Orbiters and Surveyors, telescopic mapping of the moon remains an important project. For several years, the U. S. Geological Survey, in cooperation with the N.A.S.A. and the Aeronautical Chart and Information Center, has conducted a 1:1,000,000 scale lunar mapping program based on relatively objective principles such as superposition and transecting relationships. Several new maps in this series were published in 1967, including the following.

The Copernicus Quadrangle was completed by H. H. Schmitt, N. J. Trask, and E. M. Shoemaker (94). This map (fig. 32) is of special interest since it shows what is probably the best-known and most thoroughly studied large crater on the moon. The Lunar Orbiter II oblique photographs were used in final revision of the map before publication. As a result of increasing experience and

study, as well as new telescopic and spacecraft photography, the Copernicus map is remarkably detailed compared with comparable maps proposed only a few years earlier. Probably one of the most important things brought out in it is the growing realization that lunar geologic evolution has been an extremely complex combination of internal and external processes. Although Copernicus itself, and similar craters such as Eratosthenes and Reinhold, are interpreted by Schmitt, et al. as impact craters, there are many features considered of internal origin, including the domes, sinuous rilles, dark-halo craters, and Eratosthenian chain craters. The mare material is as usual interpreted as volcanic, either pyroclastics or flows. The existence of craters such as Lansberg and Reinhold B which were clearly formed after the Imbrium Basin (since they are not cut by Imbrium sculpture or overlain by Imbrium ejecta), but before emplacement of the mare material, demonstrates that the mare material is not simply breccia from the impact formation of the mare basins—a misconception still encountered in some publications.

J. F. McCauley (95), completed the geologic map of the Helvelius region, which is on the western limb of the moon (fig. 23). The Helvelius quadrangle is of special interest for a number of reasons, a major one being the abundance of apparently volcanic land forms found there. In addition to the part of Oceanus Procellarum included in the map area, there is a large dome field west of the crater Marius, many sinuous rilles, chain craters, and dark-halo craters, all of which are interpreted by McCauley as volcanic.

The Hevelius map is notable for the number of new mapping units introduced. Oldest of these is the Hevelius Formation, a relatively smooth material becoming rougher toward Mare Orientale, which is outside the Helvelius quadrangle. It is interpreted by McCauley as ejecta from the impact believed to have formed the Orientale basin, and thus is analogous to the Fra Mauro Formation (around Mare Imbrium) and Vitello Formation (around Mare Humorum), as well as to the ejecta blankets of innumerable smaller craters. (McCauley discusses these interpretations in more detail elsewhere (McCauley, 96).) Another new unit is the Marius Group, divided into four subgroups on the basis of topography. It includes the material of the Marius dome field, which McCauley interprets as volcanic flows, volcanoes, tholoids, and elsewhere (McCauley, 96) as possibly laccoliths in some examples.

The Cavalerius Formation, a very dark unit of Copernican age, is also interpreted as volcanic, chiefly pyroclastics. Luna 9, the Russian probe launched in 1966 (Walter and Lowman, 78), is thought to have landed on the Cavalerius Formation, although the uncertainty is such that it may be located on hills composed of relatively recent (Copernican) slope debris. The last new unit, the Reiner Gamma Formation, was given to the light-toned tadpole-shaped feature on Oceanus Procellarum whose nature has been speculated on for many years. McCauley points out that this unit is unique on the earthward hemisphere and has no obvious terrestrial analogues; he suggests tentatively that it may be an ash flow deposit originating in the Marius hills area.

Lying just north of the Helvelius Quadrangle is the Seleucus Quadrangle, a map of which was published by Moore in 1967 (97). Although no new formations were introduced, the Seleucus map is of interest because of the large number of apparently volcanic features it shows. The most important of these is the Aristarchus Plateau, a large raised area over 200 km wide named from the crater Aristarchus on its east end. Part of the Plateau had been mapped earlier by Moore (Moore, 98); the Seleucus map shows the progress made in refining and subdividing the various rock-stratigraphic units. The most obvious difference is elimination of the Fra Mauro Formation (interpreted as Imbrium ejecta) except in cross-section; part of the Aristarchus Plateau which would have been formerly mapped as Fra Mauro is now shown as the Vallis Schroteri Formation. This is a five-member unit, generally dark and with a reddish color, typically exposed along Schroter's Valley (formally Vallis Schroteri), and including rock types and structures interpreted as volcanic flows, pyroclastics, maars, domes, and possibly laccoliths.

Another notable feature shown on the Seleucus map is the complex structure of the Aristarchus Plateau, which has apparently been cut by a large number of normal and reverse faults, which can be grouped, with other lineaments, in four main sets. Some of these are evidently relatively old, being related to the formation of the Imbrium basin, but some are younger than the Plateau. This suggests again that the moon is a tectonically active body - a concept in agreement with the well-known observations of present changes (the "red spots") near and in the

crater Aristarchus in 1963 by observers of the Aeronautical Chart and Information Center.

The area of Mare Humorum was mapped by Titley (99), who had previously mapped the adjoining Pitatus Quadrangle with Trask (Trask and Titley, 100). This map includes all of Mare Humorum and a considerable part of the surrounding highlands, which Titley mapped as Vitello Formation, interpreted as being ejecta from the mare basin. A new unit in the Humorum map is the Doppelmayer Formation, a very dark, smooth material blanketing the southwest part of Mare Humorum and adjacent craters. Ascribed by Titley to either the Imbrian or Eratosthenian system, it is interpreted as volcanic flows or pyroclastics or both. A number of craters are assigned to the Gassendi Group, including Gassendi itself, Doppelmayer, and Vitello. These are craters demonstrably later than the mare basin, but younger than the mare material, and thus analogous to Archimedes and Plato; they are of genetic interest in furnishing additional evidence that a significant interval elapsed between formation of the mare basins and emplacement or eruption of the mare material. This point is of some importance in view of the residual doubts that the mare material is internally generated.

Although the Surveyor I color wheel verified that the lunar surface would be rather colorless to the eye at close range, there is nevertheless significant permanent color variation over large areas of the moon. The most recent of many studies of lunar colors (excepting transient changes, which will be discussed separately) was reported by Evsyukov (101). Using the 200 mm refractor

of the Kharkov Observatory, Evsyukov photographed the moon, at various phase angles, in the ultraviolet at 3700 A and in the infrared at 1000 A. He derived a color index for about 170 lunar surface features indicating whether they were greener or redder than the average moon. Most features varied by no more than $0.^{M}25$ from the mean color index as measured by his equipment of $-0.^{M}97$. However, a few objects—in particular Aristarchus and Proclus—were much more strongly colored, which Evsyukov attributed to luminescence. He categorized a number of features, including individual craters, highland areas, and maria, as greenish or reddish compared to the average moon, and found his results agreeing with those of earlier workers such as Barabashov who had taken color photographs of the moon. The older formations seemed to be chiefly reddish and the younger greenish; this suggests that "cosmic factors" diminish color contrasts and make the color more reddish.

The problem of lunar colors is of course intertwined with that of changes on the moon. Rackham (102) reported the continuation of his earlier work on the problem. He performed a photometric analysis of lunar negatives taken on three nights during the quiet sun period of July, 1964, at two passbands centered at 5700 Å and 6700 Å. Two-hundred and five points were analyzed, lying chiefly in western Mare Imbrium, eastern Oceanus Procellarum, and adjoining areas. Analysis of the derived color indices showed evidence of considerable changes in color for a number of points during the period of observation, including Copernicus, Kepler, Gambart A, Diophantus B, and other craters. Aristarchus, interestingly, did not show much change in color. Rackham pointed out that much more

additional observational and interpretive work is needed to determine the cause of these color changes.

A major study of transient color changes was presented by McCord (103), who used the Mount Wilson 60-inch telescope and a grating spectrometer during six lunations in 1965 to study 24 points on the moon. The observation period included times of both modest solar activity and solar calm. McCord found no differences in line depth corresponding to changes in visible emission greater than about 5% of the reflected light, in contrast to earlier workers who had reported changes of 5 to 17%. He did, however, find significant temporal and spatial variations in the 0.5 to 2.0% range indicating visible emission occurring on or near the surface (i.e., non-solar). There was no obvious correlation of these changes with the changing observational parameters, preventing any unique conclusion as to the cause of the changes.

A retroactive search for changes on the moon was conducted by W. Cameron, (104), who collected more than 550 reports of lunar transient (LTP) phenomena extending back 400 years. This number included a series of lunar observations made by Bartlett (105) over the past 17 years. Cameron compared the occurrence of the LTP which included color changes, brightenings, obscurations, and similar effects, with the anomalistic period and with the distance from the terminator. She also plotted their location, finding them concentrated around mare edges. She found it difficult to arrive at firm conclusions as to the cause of the LTP; however, she found no strong evidence of tide-induced degassing,

first suggested by Green (106). Possibilities remaining open included reaction of surface materials and/or gases with sunlight, and luminescence caused by solar particles focused by the earth's magnetic field (Speiser, 107).

Cameron and Gilheany (108) presented preliminary results of a more direct approach to lunar transient phenomena, Operation Moon Blink. This project, originally conceived by James Edson, uses an analogue of the astronomical blink technique used to find motion of celestial objects; Tombaugh found the planet Pluto in 1930 with this method. The Moon Blink apparatus is designed to detect transient blue or red enhancements of as little as 2% greater than background. A confirmation network was set up to provide independent reports of any observed events. Twenty-five LTP were reported by Cameron and Gilheany, sixteen of which were red spots or glows, or star-like flashes in or near Aristarchus. (Site of the 1963 observations.) They found no good correlation between the sightings and either solar activity or the moon's distance from the earth. However, seven color events occurred during the 4.5 day period when the moon was passing through the earth's magnetic tail, tending to support Speiser's theory, previously mentioned, that the earth's magnetic field may focus solar particles on to the moon. Taking into account the historical survey of lunar transient phenomena by Burley and Middlehurst (109), Cameron and Gilheany felt that the tidal theory should also be retained as a working hypothesis. They pointed out the similarity of many of the phenomena—red glows and flashes—to ash flow eruptions, which might leave little observable change on the moon's surface, in contrast to eruptions of lava.

Some of the difficulty encountered by Cameron and others in correlating LTP with the moon's orbit may be explained by the work of Tamrayzan (110), who studied the problem of whether terrestrial earthquakes (specifically in Transcaucasia) can be triggered by the moon's gravity. Previous studies had found no simple correlation however, Tamrazyan found that it is necessary to take into account simultaneously the position of the moon with respect to the earth and the sun. Doing this, he discovered a significant increase in earthquakes at syzygy and the perigean third quarter of the moon's orbit. This correlation is chiefly applicable to earthquakes with foci shallower than 400 km. Tamrayzan's conclusion tends to strengthen the tidal theory of lunar degassing, since tectonic earthquakes are the result of movement along faults, and such movement in the moon would presumably increase the changes of gas leakage.

Further progress in a previous study of historical records of about 400 lunar transient phenomena was reported by Middlehurst and Moore (111). Using most of the same records collected by Burley and Middlehurst (109) and by Cameron (104), they found that the LTP tended to be concentrated around the edges of maria (in agreement with Cameron), in ray craters, and in mare-floored craters such as Plato. An interesting negative finding was the absence of anuthenticated reports of LTP in the southeastern highlands. Middlehurst and Moore concluded that the geographic distribution supported an internal cause, perhaps of volcanic nature.

The problem of correlating LTP was also attached by Chapman (112), using a different approach. Chapman restricted his investigation to the crater

Aristarchus, for which 27 sightings had been reported between 1963 and 1965, and attempted to find a correlation not only between the sightings and the moon's distance, but also with the librations. He found that Aristarchus events tended to occur on the same day as tidal-gravity maximums, and one day after the tidal-gravity minimums. Concluding that there was a strong and predictable correlation, he suggested that Aristarchus be monitored closely on favorable times in 1970, when it should be more active.

It is apparent that the internal origin of lunar transient phenomena has been somewhat reinforced in the past two years, not only by the investigations just cited but also by the demonstration by Nash (113) that proton excitation was too inefficient to produce the observed effects. However, Palm (114) proposed that the latter difficulty might be circumvented if solar particles created color centers in lunar surface materials, which might then produce either increased reflectance or photoluminescence.

Although not intended for that purpose, an investigation by Lipskii and Pospergelis (115) of lunar polarization throws possible light on the nature of LTP around Aristarchus. They used an electronic polarimeter to measure the Stokes parameters of polarization of various points on the moon. On the night of June 31, 1964, the plane of polarization was rotated 12° from the polarization direction of adjacent areas; this phenomenon was not noticed on the other 13 nights on which measurements were made. Lipskii and Pospergelis interpreted this as being caused by a cloud of some scattering medium over the crater, possibly of

volcanic origin. An interesting aspect of their method is that the discovery was made from only about 1% of the total light flux from the crater, which would not be possible with ordinary photometry.

A project of considerable potential value in determining the figure of the moon was reported by Mills (116), who, with his colleagues, determined the absolute coordinates of 960 well-defined small craters. They used the stereoscopic method, in which the apparent positions of the chosen points are determined at greatly different librations, in order to determine the geometric or true, figure of the moon. A contour map prepared with the data from this study shows a 2 kilometer bulge just southeast of Alphonsus, which, they suggest, agrees with preliminary determinations of the lunar gravity field from Lunar Orbiter I (although, Mills points out, there is no necessity for such agreement).

INFRARED, RADIO, AND RADAR ASTRONOMY

Since they permit inferences as to the subsurface structure infrared, radio, and radar investigations of the moon continue to be of considerable importance, even after the ultra-high resolution photographs returned by various lunar probes in 1966 and 1967.

A paper presented in 1966 at the Seventh International Space Science Symposium (COSPAR), but not published until 1967, describes infrared absorption studies by Markov and Khokhlova (117). They performed scans with the 125 cm Crimea telescope in the 0.8-13 micron region, much of which, however, is absorbed by the earth's atmosphere. The most prominent feature of the moon's absorption spectrum was a decided minimum at 3-4 microns (i.e., the albedo is at a maximum in this region). They also found no evidence of limb darkening in the 0.8-13 micron range, confirming evidence from other methods that the surface is rough ("dispersive") on this scale.

Saari and Shorthill (118) summarized the results of an extensive program in which they mapped the visible face of the moon in the far-infrared (10-12 micron) and visible (0.445 micron) regions. The mapping was done with a focal plane scanner, used with the 60-inch Mt. Wilson and 74-inch Helwan Observatory telescopes, at 23 phases through a lunation. The results are presented as a series of isophotic and isothermal contour maps. These maps demonstrate the now-familiar correlation of thermal anomalies and high-albedo features, the optically bright areas being generally cooler on the illuminated disk (the reverse is true on the dark disk).

The thermal behaviour of lunar surface features was further clarified by the 8-14 micron observations of Salisbury and Hunt (119) in the Tycho region. Using an infrared imaging system which permitted precise location of thermal anomalies, they demonstrated that the well-known thermal anomaly is confined to Tycho and the immediate surroundings. Furthermore, they found that the crater walls that had been facing the sun just before sunset stayed warmer than those that had been facing away, thus indicating that the anomaly is primarily solar rather than internal.

Another infrared reconnaissance in the 8-14 micron region, performed in 1964, was reported by Wildey, et al. (120). These investigators used a 24-inch telescope during July and August, 1964, although only a few nights permitted good observations. They presented a catalog of lunar nighttime thermal anomalies, all on the eastern half of the moon (which was in the third quarter). Two features stand out from their data, which were also used to construct an 8-14 micron brightness temperature map: an enhanced brightness for Mare Crisium, and an absence of brightness temperature between highlands and maria. Further interpretation of these results were to be published.

The well-known Russian radio astronomer, V. S. Troitskii, with his colleagues V. D. Krotikov and N. M. Tseitlin (121) presented results of their measurements of the moon in the 30-60 centimeter wavelengths. Earlier studies had indicated that the apparent temperature rises to a depth corresponding to the penetration, or depth of emission, of 30 cm radiation. These observations indicated that in the

30-60 cm band, the temperature is constant and independent of wavelength, and averages 225° K.

Lunar thermal radio emission can also be used to infer the electrical properties and roughness of the near-surface layer. This was done by Losovskii (122), who measured the polarization of 0.8 cm radio emission with a 22 meter radio telescope, finding a maximum polarization value of 4 ± 1%. Analysis of the data indicates a dielectric constant of 1.5 ± 0.2, and considerable diffuse scattering (caused by roughness) for waves shorter than 1 cm.

As pointed out by Eshelman (123) in a valuable review of radar astronomy, the problem of loss of echo strength with distance can be overcome by the bistatic technique, in which either the transmitter or receiver is carried on a spacecraft to the vicinity of the body under study, the complementary equipment being on earth. This was actually done for the first time on 12 October 1966, as reported by Tyler, et al. (124) with Lunar Orbiter I. The returned signal was difficult to explain in terms of slope, roughness, or shadowing; the investigators found instead that variation in reflectivity were probably responsible for the observed time-frequency variations. In physical terms, this may be the expression of patches of bare rock or dense soil. This result, while hardly surprising, demonstrates the potential value of bistatic radar for the mapping of planetary surfaces such as Venus.

The complex subject of interpretation and physical meaning of optical, thermal, radio, and radar observations of the moon was reviewed by Cook (125). This

report, which is extensively referenced, concludes that there are no unique interpretations of the available data, although some general conclusions can be reached.

INTERPRETIVE, EXPERIMENTAL, AND THEORETICAL STUDIES

It is axiomatic in many scientific fields that acquisition of information takes little time, compared to the time needed to interpret the information. Space science is a prime example of this; the 1964-5 Ranger probes sent back their pictures in a few minutes, but interpretation of these pictures was continuing in 1967. Comparable interpretive studies were carried out for the other lunar probes, both Russian and American.

Two comprehensive papers on the geologic significance of the pictures returned by the Ranger, Surveyor, Lunar Orbiter, and Luna spacecraft were presented. McCauley (87) covered much material that has already been summarized here, and which will therefore not be repeated. However, his review contains two significant new interpretations. First, he proposed that the Orientale Basin, first photographed from directly overhead by Lunar Orbiter IV, is the youngest of the circular mare basins, and was formed by the impact of an asteroid-sized body. The peculiar blanket of material surrounding the basin was, McCauley suggests, deposited by a base surge, analogous to the cloud of material that comes from the bottom of the cloud over an explosion crater. The concentric scarps, which are the most prominent feature of the Orientale Basin, were formed either by collaspe or slumping shortly after the crater was excavated. A second

contribution of McCauley's paper is also based on the Lunar Orbiter IV Mare Orientale photos (fig. 26). There are two craters, one about 55 km and the other about 35 km in diameter, on the floor of the inner Orientale Basin. The larger is essentially similar to Copernicus, Eratosthenes, and other ray craters generally considered to be of impact origin, possessing terraced inner walls, humocky ejecta blankets, and a halo of secondary craters. The smaller has a relatively smooth rim and none of the topographic features listed for the other crater, and is floored by mare material. McCauley points out that both are youthful post-Orientale features, and that the differences cannot therefore be explained by saying that the smaller crater is an eroded version of the larger. He suggests that the differences may reflect contrasting origins; the smaller crater may actually be volcanic. This interpretation, if correct, is extremely important for two reasons. First, this pair of craters would furnish a type locality for comparison of impact and volcanic craters (assuming, of course, that the larger one is an impact crater). Second, it implies that there are many more large volcanic craters than previously recognized. Until the Lunar Orbiter IV picture, it had been widely believed (Lowman, 126) that all large lunar craters were essentially similar to Copernicus, if allowance were made for subsequent mare flooding, isostatic uplift, impact erosion, and other post-crater events. McCauley's interpretation indicates that this may not be true.

Another paper summarizing results from the first three Lunar Orbiters, by Trask and Rowan (127), put more stress on mass wasting as a lunar geomorphic

process. They called particular attention to the parallel ridges noticed on many mare slopes, which appear to follow contour lines, proposing that these, and the convex terraces seen at the base of many slopes, are the result of downslope movement of loose debris.

The fragmental nature of the mare material has been inferred for some time, especially since the availability of high-resolution photographs of the maria. However, there has been considerable variation among estimates of the thickness of this fragmental layer. A major contribution to this problem was made by Oberbeck and Quaide (128), who estimated the thickness of the fragmental layer in Oceanus Procellarum. Their approach was the following. They produced experimental craters in a variety of target material, and demonstrated that the shape of the craters depends largely on whether the material is completely fragmental, or is underlain by a solid layer. Craters in fragmental material are simple holes; craters that just reach a solid layer have flat floors, and those that penetrate the solid layer have one or more concentric terraces (fig. 25). Quaide and Oberbeck tabulated the number of craters with different shapes in the parts of Oceanus Procellarum photographed by various lunar probes, and combining this tabulation with the experimental data, estimated the areal extent of fragmental layers of different thickness. They found that 85% of the area studied has a fragmental layer between 5 and 15 meters thick, with a modal thickness of 5-6 meters and an average thickness of 8-9 meters. Furthermore, they found craters with as many as three terraces, implying a mare structure with three alternating layers of hard rock and fragmental debris in the upper 100 meters.

These estimates are not only important for engineering purposes, but have interesting genetic implications. In particular, they indicate that there have been several periods of formation of mare material—a conclusion arrived at independently by geologists who have mapped the maria, such as Titley (99), whose Mare Humorum map has been discussed previously. Another implication, from the absence of concentric-terrace craters in the highlands, is that the highlands are underlain by a very thick fragmental layer or by none at all. The latter possibility seems unlikely, from the greater age of the highlands and from radar and infrared studies.

The Lunar Orbiter photographs, taken to find suitable Apollo landing sites, were not studied scientifically as rapidly as were the more science-oriented Ranger or Surveyor photographs, to which large teams of investigators were assigned. Consequently, geologic interpretation of the Orbiter photos has been attempted by a large number of individuals and organizations. One of the first such attempts published in 1967 was by O'Keefe, et al. (129), who studied the Lunar Orbiter I photographs of the Flamsteed Ring, (figs. 28, 29), or Von Karman crater as it has also been named. The Flamsteed Ring appears to be an extremely old, pre-mare crater, of which only a few remnants of the former rim remain. However, O'Keefe, et al. noticed that the rim material actually overlaps some mare craters, has a convex lower slope, and is remarkably crater-free compared to the adjacent mare areas. They therefore suggested that it is a post-mare extrusion of siliceous lava, such as andesite, dacite, or rhyolite. Fielder (130) published the same theory shortly after.

The theory that this apparently ancient crater is actually a young volcanic feature attracted some attention because of its novelty. Goles and Taylor (131) argued that the viscosity of the supposed lava could not reliably be used to infer its composition; Milton (132) suggested that the convex slope might be the result of seismic induced landslides. Hartmann (133) also differed with the lava interpretation pointing out that similar convex slopes were found on a number of other features whose volcanic nature seemed doubtful. (One of these, interestingly, was the crater Gambart, for which McCauley (136) proposed a possible volcanic origin because of its similarity to the 35 km crater in Mare Orientale previously discussed.) The theory proposed by O'Keefe, et al. may thus be in doubt; however, it demonstrates that resolution limits on earth-based observation may limit the accuracy of superposition determinations; previous studies of the Flamsteed Ring (Marshall, 134) had indicated that the mare material was later than the Ring material, which the Lunar Orbiter photographs demonstrated to be untrue, at least locally.

Fulmer and Roberts (135) arrived at a somewhat similar conclusion to that of O'Keefe, et al. in a study of Lunar Orbiter photographs. They were primarily concerned with surface lineaments, which they found to be remarkably widespread, even in unconsolidated material. However, they also concluded that some craters, such as Gambert, might be the extrusive expression of ring dikes.

Another interpretation of the Lunar Orbiter photographs was published by Rackham (136), who studied a dark halo crater located on the south flank of Copernicus. He suggested that the reason for the dark color of ejecta from the

crater was that the impact which presumably formed it penetrated the light-colored Copernicus ejecta to bring up dark-colored mare material. Extending this to other craters, he pointed out that a similar mechanism might be applied to the large ray craters such as Copernicus itself, which might have been formed in an area of shallow mare material, the light colored ejecta being in fact continental material excavated by the impact. Rackham also, in the same paper, called attention to the apparent stratum in the breached central peak of Copernicus.

A long-time advocate of lunar vulcanism as a crater forming process, J. Green, (137) published a survey of the evidence for this theory, with a discussion of the implications of lunar vulcanism for manned exploration of the moon. He presented a discussion of caldera-forming processes on the earth and pointed out how lunar conditions might affect them. Finally, he listed the economic advantages a primarily volcanic lunar terrain would have over an impact terrain, including the availability of extractable water, sulfur, and other materials, and perhaps of geothermal energy.

The famous controversy about lunar dust was somewhat muted by the confirmation that the surface material had substantial bearing strength, as shown by the behaviour of Luna 9 and Surveyor I. However, the main features of the dust theory (originally developed by Gold on the basis of radar returns and thermal data) were in fact proven by the early soft-landing probes, in that the lunar soil was found to consist of unconsolidated, slightly cohesive material, to a depth of at least a meter in some places. Hapke (138), in a series of experiments, tried to demonstrate that virtually all the small terrain characteristics shown by the

lunar probe photographs could be duplicated by explosions or impacts in fine-grained Portland cement powder. He produced a series of photographs with remarkable similarities to the lunar terrain, including the rock-like objects, which were compressed clots of dust. Furthermore, he pointed out that the optical, thermal, and radar properties of the moon are nearly universal (this excludes the known anomalies, such as Tycho), indicating that if the maria are largely dust, the highlands must also be largely covered with the same type of material. This implies an external origin; he favors specifically meteoritic impact.

The question of the structure and physical properties of the lunar soil, specifically of the maria, were also investigated by Jaffe (139), who was of course also chairman of the Surveyor Scientific Evaluation Advisory Team. Jaffe combined the pre-Surveyor data with those from Surveyor I to arrive at a composite mare surface model, with the following major features: a particulate nature, most particles being 100 microns or smaller; density ranging from 0.6-0.7 g/cm^3 at the surface to 2-3 g/cm^3 at depths of 1-10 meters; failure primarily by local shear; static bearing strength about 4×10^5 $dynes/cm^2$ for a 25 cm bearing diameter, increasing with depth; internal friction angle about 55°; and cohesion about 10^3 $dynes/cm^2$.

Jaffe's estimate for static bearing strength was roughly confirmed by a novel technique applied by Filice (140). Filice measured, on a Lunar Orbiter II photograph, the track length and width, and other pertinent quantities, of the trail left on the wall of the crater Sabine D by a 13 meter boulder that had rolled down the side of the crater. He found the effective bearing strength to be 4×10^6

dynex/cm^2, in rough agreement with the extrapolation of Jaffe's figure. This estimate is important because it applies to a distance of 650 meters, rather than just one spot, as do the estimates from Surveyor footpad behavior.

The question of the density of the upper layer of lunar soil was experimentally approached by Salisbury and Adler (141), who conducted a series of vacuum chamber simulations. They concluded that the uppermost, fine-grained surface layer probably has a density between about 0.3 and 1.5 g/cm^3, with grain shape having a major influence on the value.

B. G. Smith (142) studied the size-frequency distribution of boulders around the Luna 9 landing site, constructing a histogram to show the values derived. The diagram shows a sharp peak in the 2-5 cm range, differing somewhat from comparable Russian estimates.

The problem of the moon's chemical composition is a classic one, which had never been directly approached until the delivery of analytical instruments to the vicinity of the moon by Luna X and to the surface by Surveyor V. However, O'Keefe and Scott (143) developed a way to combine the radar reflectivity properties of the lunar surface with data on physical properties of soil, from Surveyors I and III, to set limits to the chemical composition. This was done by calculating soil porosity from the Surveyor data, and from this calculating the grain dielectric constant by means of the Böttcher formula relating bulk and grain dielectric constant for granular materials. The most likely value for the grain dielectric constant was 4.3, which is inconsistent with chondritic meteorites, but consistent with either vesicular basalt or acidic rocks.

The albedo and color of lunar rocks could be used to infer chemical composition, according to Adams (144), who made a series of optical measurements of various rock powders with Filice (Adams and Filice, 145). He concluded that the main albedo difference between maria and terrae might be due to grain size variations, there are probably compositional variations within the maria. He found a basic or ultrabasic composition to best satisfy the optical properties of the maria and probably the highlands as well. These findings were also applied to the soil distrubed by the Surveyor I landing pad by Filice (146), who found a basic or ultrabasic composition most likely for this spot. Filice further concluded that albedo differences, including the light mare surface previously discussed, were probably largely the result of grain size differences produced by micrometeorite bombardment.

Hartmann (47, 48, 49) published a series of papers presenting new studies of lunar and terrestrial craters. Crater counts in Alphonsus, from the Ranger IX photographs, suggested either accelerated crater destruction on the walls by mass-wasting, or an internal origin for some of those on the crater floor. Hartman found it difficult to decide which of these was correct, but cited considerable evidence favoring the second, i.e., indicating an internal origin for many of the floor craters. He also suggested that the central ridge is an old, partially flooded horst (up-faulted block). In a second crater count study, Hartmann found that the size-frequency slopes of the continental areas studied, the Alphonsus wall, and a mare area had the same slope. If the cratering rate has been constant, the maria would be 1/30 the age of the highlands, although

Hartmann had argued elsewhere that the early cratering rate was higher. In a third paper, Hartmann compared lunar craters with the Kapoho pumice cinder field in Hawaii that had been repeatedly impacted by volcanic ejecta during the 1960 Kileauea eruption. He found that fields of fragments from meteoritic volcanic ejecta impact would have about the same size-frequency distribution, and that close examination would be necessary to distinguish the meteoritic from volcanic blocks. He commented on the close similarity in appearance between the volcanic field and the lunar terrain photograph by spacecraft. Most of the impact craters at Kapoho were formed by solid blocks, rather than unconsolidated masses, but the blocks were frequently buried out of sight. Subsidence craters, formed by drainage of pumice into cavities, were numerous.

It has been believed for several years that the darkening of lunar rays is the result of sputtering, i.e., the selective removal of oxygen atoms by the protons and alpha particles of the solar wind. However, an illuminating series of experiments by Nash (150) throws considerable doubt on this theory. Nash bombarded silicate rock powders with 2 to 16 Kev protons, and found that the darkening was not only dose-dependent but also rate dependent. He further found that the cause of the darkening was not sputtering, but more probably either carbon from decomposed hydrocarbons (such as vacuum pump oil) or metal from the ion source. He concluded that earlier experiments indicating darkening by sputtering were affected by contamination. However, Nash pointed out that contamination darkening, either from lunar hydrocarbons or directly, from the carbon fraction of the solar wind, appeared quite possible, although he further stated

that, since the lunar photometric function has been shown to be not unique, solar wind darkening may not be effective at all.

Ken Knight, et al. (151) who had previously conducted extensive experiments to investigate the cause of lunar surface darkening, confirmed the probable importance of carbon and hydrocarbons in this phenomenon. On the other hand, they presented evidence that solar wind bombardment probably has had considerable effect on the optical properties of the lunar surface, in particular on the color, whose uniformity may be due to long distance flight and redeposition of sputtered atoms. They estimated the erosion rate due to sputtering as 0.1 to 0.2 A/year.

A third investigation of the sputtering problem was undertaken by Greer and Hapke (152). They confirmed that contamination of the bombarded powders by metal and carbon could occur; however, they found inconsistencies in the experimental results which they felt precluded dismissal of all reports of ion darkening as due to contamination. They stressed the danger of prematurely extrapolating experimental results to the moon.

The interaction of solar and cosmic particles with the lunar surface depends on the energy of the particles, among other things. Zeller and Ronca (153) simulated the bombardment of various minerals with protons and deuterons in the 1 Mev range (contrasted with the Kev range of the sputtering experiments just described). They demonstrated that nuclear particles with such energies might be absorbed in the target material, rather than bouncing off, as would happen in sputtering; i.e., high-energy particles are additive rather than subtractive. Since most solar wind particles are protons (hydrogen nuclei), the net result would be

hydration, or "space weathering." They suggest that chemical zonation similar to terrestrial soil horizons could thus be formed, with the degree of hydration decreasing downward. Its depth would be on the order of a few millimeters. The importance of the Zeller-Ronca study is emphasized by the findings of Ness, et al. (91) from Explorer 35 that the solar wind probably impacts the lunar surface directly because of the absence of a lunar magnetic field.

It has been hoped that ultraviolet spectral surveys of the moon, which would be possible outside the earth's atmosphere, would provide compositional information about lunar compositions. However, Greenman, et al. (154) conducted experiments to measure the ultraviolet reflectance of possible lunar rock types, and found little difference in the reflectance of different rocks. They concluded that compositional differences would have to be sought in the fine structure of the UV spectra if they exist.

Polarimetry of the moon, a classic area of study, is still a fruitful one, as shown by the experiments of Egan (155). He demonstrated, with measurements made by a large polarimetric device capable of registering the polarimetric response of samples up to 3.5 inches in diameter, that the polarimetric properties of the moon could be duplicated by volcanic ash coated with fine grains of the same material.

Since many geologic processes such as seismic activity, vulcanism, and perhaps internal convection currents, are driven by thermal energy, the study of a planetary body's thermal history is essentially a study of its internal geologic

history in general. Several papers on the moon's thermal history were published in 1967, including the following.

Fricker, Reynolds, and Summers (156) constructed several theoretical thermal models of the moon, based on their earlier work on the earth's thermal history. Previous studies, such as those of Urey, MacDonald, and Lowman, had considered the thermal regime of the moon to the beginning of melting; the work of Fricker, et al. took melting into account as well. Like the earlier studies, their calculations indicated that even if the moon had been initially cold, long-lived isotopes would raise the temperature to the melting point eventually. After partial melting, the thermal gradient would flatten and the radioactive materials would be segregated in the liquid fraction. The melting zone would gradually work its way outward, producing extensive volcanic activity peaking between 1 and 3 billion years ago. Their calculations indicate that the moon should be largely solid now.

Miyamoto (157) followed a different line of reasoning in studying the thermal evolution of the moon (and Mars). He interpreted the surface physiography of the moon as indicating mantle convection currents corresponding to harmonics of the second and higher orders, as has been done for the earth by Runcorn. The circular maria and mare-floored craters would be the locus of converging currents.

Two other Japanese scientists, Iriyama and Shimazu (158), approached the problem of the moon's thermal history, performing a series of numerical calculations with two different initial temperatures and a chondritic composition.

Their treatment is unique, however, in taking into account the heat liberated by formation of the moon's hypothetical core. From the calculations, they derive a series of curves showing variation of the surface heat flow through geologic time, for sudden and for gradual crust formation, as well as for different uranium concentrations.

Still another series of thermal calculations was carried out by Ornatskaya and Al'ber (159); following, in general, the methods and assumptions of earlier workers in this field, such as Levin, MacDonald, and Urey, they solved the thermal conductance equations for varying distributions of the radioactive elements in the moon. Their approach was somewhat similar to that of Fricker, et al. previously described, and some of their calculated thermal gradients are very similar. Ornatskaya and Al'ber found that the moon would have been almost entirely melted at an early stage if the radioactive element concentration had been high; with the lowest concentration, the moon would not have been molten closer to the surface than 4-600 kilometers. An interesting result of their calculations is that the greater the concentration of the radioactive heat-producing elements, the more the moon would have cooled at the present time. The reason for this is that with a high concentration of radioactive elements, the melting would begin very early, providing more cooling time.

The ultimate question to be answered about the moon is, of course, its origin. There has been an interesting tendency in recent years for theories of the moon's origin to diverge, in contrast to those for the origin of the solar system, most of which are in substantial agreement on major points (Lowman, 160).

The main disagreement about the moon centers on whether it has some close, genetic relation to the earth, or is a captured body from somewhere else in the solar system. The chief evidence favoring the capture theory is the apparent difference in bulk composition (inferred from the density difference) between the earth and the moon; the significance of this difference has been underlined by the growing body of evidence ruling out the phase-change theory first proposed by Ramsey for the formation of the earth's core.

Three papers published in 1967 all agree that the moon was formed somewhere in the earth's vicinity. Two of these (Fish, 161; Hartmann and Larson, 162) are based on the fact that the angular momentum of the earth-moon system appears to conform to the relationship between angular momentum and masses of the planets, pointed out by MacDonald (163).

The third paper (Ruskol, 164) is an extension of Ruskol's earlier work on the evolution of the earth-moon system. It is concluded that the primeval lunar orbit was much closer to the earth than is the present one, but always inclined to the earth's equator. The study finds no evidence, in the tidal variations of the lunar orbit, to support the capture theory, favoring instead an origin for the moon in the vicinity of the earth.

SUMMARY

The most spectacular scientific achievement in the study of the moon during 1967 was without much doubt the chemical analysis performed by the experiments

on Surveyor V. These are the first contact experiments of their kind ever performed, and as such are of historic significance.

From a broader viewpoint, it would seem that the greatest progress has been in clarifying the nature and extent of volcanic processes on the moon. It is generally (though not universally) agreed that the maria are at least partly basalt, but of volcanic origin whatever their bulk composition. Their volcanic nature is emphasized by the high-resolution photographs of many minor features, in particular the dome fields and sinuous rilles, which appear to have some connection with volcanic processes. The role of volcanism in formation of the large ray craters remains disputed, the dispute being heightened by the discovery of features that have almost certainly resulted from fluid flow (the ropy textures in the floor of Tycho are the best example).

On the other hand, the high-resolution views of Mare Orientale have tied together the mare basins and the ray craters, and many feel that an impact origin (with or without subsequent vulcanism) is most probable. The curious paradox that more and more impact structures are being found on the earth while more and more volcanic structures are found on the moon continues; it is to be hoped that the mean to which both schools of thought are trending is the truth.

IMPACT CRATERING AND METAMORPHISM

Considerable progress was made during 1967 in field and laboratory investigations of terrestrial craters. Interest in the study of meteorite impact craters and their associated shocked rocks continues to grow.

As in previous years, the most extensive studies have been carried out in Canada where to date some 16 probable impact craters are now recognized. In 1967, a report on Lac Couture (165) was issued by the Dominion Observatory in Ottawa. Drilling of 3 more holes at the Brent structure, under the supervision of M. Dence, provided additional core and subsurface data which add to the ranking of this crater as one of the most completely investigated impact sites in the world. Of particular interest was the K-Ar dating by J. Hartung of some highly shocked granite gneiss breccia fragments collected near the crater base. An age of 460 ±10 m.y. obtained by this method corresponds reasonably well with the estimate of an early Ordovician age for Brent on the basis of sedimentary rocks of this period within the crater. Currie and Shafiqulla (166) presented chemical and petrographic evidence of a direct relation between the Brent structure and rock types associated with carbonatites and claim therefore that Brent has a purely endogenetic origin. Work on the West Hawk Lake structure involving petrographic and instrumental analyses of drill core from the breccia and rupture zones was reported by Short (167). This structure, similar to Brent in size, shows in comparison somewhat lower and more varied shock damage owing to the presence of fine-grained quartz-mica schists and amphibole-rich rocks in the target material.

The field project to map and sample the Manicouagan structure in eastern Quebec, before it is partially inundated by backwaters from the world's third largest dam, was completed by the Quebec Geological Survey under the direction of J. Murtaugh. Although the question of origin is still hotly debated, Murtaugh and others now believe that this structure, the largest of its kind known on earth, is best explained as the consequence of a meteorite impact. A paleomagnetic study (168) of thermoremanent magnetization of flow units from the Manicouagan group indicates these to have formed in 10000 years or less—a result not inconsistent with an impact origin in that it suggests rapid post-impact intrusion following the event, as may be expected from sudden off-loading.

With the publication (169) of a paper by French describing shock effects in the Onaping tuff of the Sudbury (Ontario) structure, interest was greatly enlarged in the meteorite impact origin of this famous nickel-copper ore locality as first proposed by Dietz (170). Over 50 shatter cone localities (171) have now been found in and around the Sudbury basin. Local geologists there have discovered shock features in the "rim" units outside the irruptive. Because Sudbury is the first suspected impact structure to have major economic value, the search for further field evidence of shock and other features attributed to cratering is now being intensified as more geologists are beginning to seriously consider the impact hypothesis.

In the spring of 1967, a prospector reported finding some unusual rock fracturing in rocks along the St. Lawrence river. These were identified by

J. Murtaugh as shatter cones, marking thus the first time that these unique features, previously found only at presumed impact crater sites, were initially responsible for calling attention to another possible impact structure. The structure, called Malbaie after a town on the St. Lawrence some 110 km. northeast of Quebec City, was visited by B. Robertson and M. Dence of the Dominion Observatory. They collected samples of mixed breccia containing abundant evidence of shock damage. A diameter of 37 km. provisionally assigned to Malbaie makes this the third largest of the Canadian structures of the cryptoexplosion class (Robertson, (172)). It is now inferred to be an impact crater of the complex type that strongly resembles Manicouagan.

Following identification in 1966 of a buried structure (Steen River) in northwest Alberta as a probable astrobleme because of the occurrence of shocked rocks in drill core, Canadian oil companies and other sources have reported as many as 6 other structures which possess similar characteristics. Most were found by geophysical methods and several have been drilled. These structures are now undergoing further examination in search of shock criteria which would place them in the putative impact crater category.

In the United States, major field investigations by the U. S. Geological Survey of the Flynn Creek, Tenn. and Sierra Madera, Texas structures were completed in 1967. Six shallow drill holes were emplaced at Flynn Creek which helped to confirm the presence of a central peak and the occurrence of relict mixed breccias (Roddy, (173)). The map prepared by D. Roddy emphasizes the style of

deformation at Flynn Creek as one of intense folding and faulting that dies out abruptly with depth. Roddy attributes the formation of Flynn Creek to impact by a cometary body rather than a meteorite. At Sierra Madera, Wilshire et al. (174) have mapped the central uplift in great detail, demonstrating a stratigraphic uplift of some 6400 meters associated with steep to overturned, complexly faulted beds in the central zone. Within this central core, the Permian rocks appear to have moved both inward and upward to reach their present position. The uplift, now visible as rugged mountains, is surrounded by a depressed ring of down-dropped Cretaceous rocks and an outer zone of structurally higher rocks of similar age. The overall deformation rapidly dies out with depth, which fact, coupled with the presence of possible shock metamorphism in mixed breccias, leads Wilshire et al. to favor impact as the most likely mode of origin.

Three papers were presented in 1967 (175, 176, 177) by Seeger dealing with the Jeptha Knob structure, Kentucky. A magnetic survey showed that there is probably no basement counterpart to the surface feature and a gravity survey revealed a +1 mgal anomaly. The scant drilling information indicates that the deformation decreases with depth and is shallow. Multiple hypotheses were used to eliminate any endogenetic origin, leaving hypervelocity impact by a meteorite or comet as the most probable explanation.

A gravity survey (Bull, et al. (178)) at the 6 km. wide Serpent Mound area, Ohio indicates that density reductions are confined to the near surface and apparently do not extend into the basin or beyond the limits of the structural disturbance. In lieu

of drilling, this evidence provides a subsurface picture suggesting a breccia lens which, together with shatter cones and coesite found in surface samples, best fits the impact crater model.

The group under Prof. W. v. Engelhardt at the University of Tubingen published several important papers in 1967 describing various aspects of their continuing study of the Rieskessel structure in Bavaria. Forstner (179) reported results of a detailed examination of suevite recovered from two drill holes at the Ries. His description of variations in particle size distribution helps to characterize the mode of "sedimentation" associated with the fallback process. Stoffler (180) carefully documented shock-induced changes in plagioclase from breccia fragments derived from the crystalline basement rocks beneath the Ries. He concludes that isotropization of these minerals takes place within the 300-500 kb. pressure range whereas selective melting occurs between 500-650 kb and total melting results at higher pressures. W. v. Engelhardt et al. (181) presented evidence for distinguishing between diaplectic glasses (those developed by solid state isotropization) and glasses resulting from actual melting during the Ries cratering event. The diaplectic glasses will have higher densities and indices of refraction than normal glasses and may also preserve certain original or shock-induced internal structures. W. v. Engelhardt (182) also reported chemical analyses of glass bombs from the Ries and elsewhere and identifies the bombs as shock-melted granitic basement rocks whose textures vary with cooling rate, extent of transformation and degree of recrystallization. W. v. Engelhardt et al. (183) presented new evidence for a meteorite impact origin of

the Steinheim basin west of the Ries; this includes discovery of planar features and other signs of shock damage in minerals from breccia fragments in drill core. Johnson and Vand (184) reported an analysis of topographic features at the Ries using a computerized Fourier data smoothing technique which lead to a mathematical reconstruction of the original crater shape. Their results indicate that one or more secondary rims developed at the Ries. They also state that the method permits calculation of the location of the center of impact and the direction of meteorite entry.

In 1967, F. Kraut first informed other investigators of a structure in central France containing crystalline rocks which show shock damage effects very similar to those observed in the Rieskessel (185). Suevite-like breccias occur in outcrops near the towns of Rochechouart and Chassenon, southwest of Limoges. Neither the shape nor the diameter of the structure have been determined but known outcrops range up to 12 km. apart. Although the schists and granite gneisses in the structure are geographically near volcanic terrane (including the Auvergne), there is no evident interrelations and the structure appears to be an ancient astrobleme. Brecciation accompanied the movements which in the extreme led to blocks and plates being rotated and/or overturned. Drilling shows that this intense deformation diminishes with depth. Shatter cones abound at Gosses Bluff (186,187). A closely related feature there, called shatter fracturing, consists of sets of striated planar surface which intersect in near rhombohedral angles. The resulting rhombohedral blocks can grade into shatter cones.

S. R. Taylor reported (188) that glass collected from the Henbury (Australia) strewnfield has a chemical composition which, after iron due to meteorite contamination is removed, matches the composition of certain greywackes exposed within the largest of the Henbury craters.

Bunch and Cassidy (189) have found convincing evidence of a meteorite impact origin of the Monturaqui crater in Chile. Microprobe analysis confirms the presence of metallic nickel-iron in inclusions within the impactite glasses. Crystalline fragments in these glasses show planar features in quartz and feldspars and thetomorphs of these minerals have formed by shock.

In the last few years the subject of meteorite impact cratering has become closely entwined with that of the new field of shock metamorphism. Review articles on both topics appeared during 1967. Explosion craters, embracing both nuclear and impact craters, and astroblemes, i.e., eroded meteorite craters, were considered by Short (190, 191). A review article on shock processes in geology by the same author appeared in late 1966 (192). Two important articles on shock or impact metamorphism by E. C. T. Chao (193, 194) brought this subject to the attention of the general scientific community. R. Barringer (195) updated his earlier versions of a catalog of the world's meteorite craters.

Several significant papers dealing with experiments in cratering were published in 1967. Diehl and Jones (196) described their detailed study of the Snowball chemical explosion crater, a 500 ton surface burst over soil and clay sediments in the prairie terrain of Alberta, Canada. This produced a shallow

crater approximately 100 m. (apparent lip) in diameter. Of particular interest was the formation of a well-defined, strongly deformed central peak. Distinctive fracture patterns, consisting of circumferential and radial fractures, developed beyond the lip. A nuclear explosion, code-named Palanquin, which formed a crater by a gas-erosion mechanism, was investigated by Hansen (197). Its importance lies in its similarity—except for the rapid development—to certain types of volcanic maar craters with respect to general mode of origin.

Baeta and Ashbee (198) described certain fracture types in quartz produced by compression experiments at atmospheric pressure but at temperatures from 550-700°C. Currie (unpublished) reports that similar features form in plagioclase at somewhat higher temperatures. From inspection of photomicrographs of these specimens as seen in the petrographic microscope, it would appear that they resemble planar features commonly found in shocked rocks; however, definitive orientation data are lacking. Greenwood (199) described deformation lamellae parallel to $\{10\bar{1}3\}$ and (0001) planes in quartz—two frequent planes associated with features in shocked quartz—in rocks from the Belt series which have no apparent meteorite impact history. Bunch, Dence and Cohen (200) presented data on the characteristics of natural terrestrial maskelynite found in the presumed impact craters at Clearwater West and Manicouagan. Heating maskelynite at temperatures well below the melting point of the corresponding plagioclase causes a reversion to the crystalline state, indicating a degree of

structural disordering comparable to that of fused plagioclase glass has not occurred.

During 1967 students of terrestrial volcanic craters continued to examine calderas, maars, and vents and compared their morphology and associated surface features with certain lunar craters. Green (201, 202), using both calculations and direct studies of terrestrial volcanoes as analogs to certain lunar structures, presented a strong case for the origin of many lunar craters by endogenetic processes of volcanic nature. Katterfeld (203) analyzed morphological characteristics of many large terrestrial calderas, maars and ring dikes, showing thus that these bear many similarities in shape and profile to some of the larger lunar craters whose origin he attributes to comparable volcanic processes. Hartmann (204) noted that the craters formed by impacts of ejecta from explosive volcanic eruptions of Kilauea resemble on aerial photos many secondary craters visible in the probe photos of the lunar surface. Roddy (205) calculated the energy needed to form the Ubehebe maar crater near Death Valley, Calif., which is roughly 730 m. wide and 230 m deep, to be approximately 10^{22} ergs. He concludes that a volcanic eruption, operating by a similar gas escape mechanism, of this magnitude on the moon would produce a much deeper and somewhat wider crater. Ronca (206) examined the possible link between meteorite impact and induced volcanism in craters. He concluded that triggering or localizing by impact is possible but contends that very large impacts would be needed to remove sufficient overburden to activate melting; the crater size and

effective removal needed to initiate the process depends largely on the geothermal gradient in the region of impact.

Studies in crater morphology, distribution, and formational processes on the moon's surface were advanced in 1967 by new data from successful lunar probes, continuing telescopic mapping, model experiments, and theoretical analyses (207). Trask (208) classified craters seen in Ranger VIII and IX photos into four categories depending on relative sharpness of rim and depth-diameter ratio. Most craters at 100 meters are broad-rimmed and have smaller depth-diameter ratios than the more common sharper-rimmed craters visible down to the resolution limit near 1 meter. Trask interprets this result to indicate an episode of destruction—volcanic activity and/or intense bombardment by asteroid fragments and micrometeorites—which modified the 100 m. class of craters, obliterated most smaller ones, and produced a smoothed surface on which younger, sharper craters have formed.

Members of the staff of the U. S. Geological Survey's Branch of Astrogeology have proposed a model in which small craters will be degraded faster than larger ones, leading to the conclusion that smaller subdued craters could be contemporaneous with some larger sharp ones (209). They have proposed a scheme in which relative crater age can be tied to both crater diameter and a set of definitive morphological criteria (fig. 38). A family of crater types is thus defined, with relative age value specified by an index number. When superposition is evident, higher index craters are almost always superposed on lower

index craters. Certain modifying factors, e.g., mass-wasting effects on lunar slopes, can vary the relative rates of degradation.

Walker (210) analyzed crater distribution as a function of crater size and time of exposure to assumed fluxes of impacting bodies. Until the surface becomes saturated with craters, the distribution will correspond to the flux but from the time of saturation onward the surface no longer reflects the continuing flux. Secondaries contribute significantly to the surface up to ~ 100 meters but their effects on saturation are distinguishable.

Chapman and Haefner (211) objected to the cumulative diameter-frequency curves commonly used to summarize crater distribution. They provided improved plotting method which contains an adjustable exponent B in the crater equation $N = A\ D^B$ relating the number N of craters to size as diameter D.

Baldwin (212) has analyzed the energy requirements appropriate to the crater formed by the Ranger VIII impact on the Mare Tranquilitatis surface. He used a scaling law equation derived from cratering explosion experiments in soil-like materials to calculate the range of diameters expected for the energy involved in the Ranger impact at a speed below the hypervelocity limit (at 5 km/sec). When he applied the equation to the two fresh-looking craters close to the impact point which NASA cites as the most probable collision sites for Ranger VIII, he concluded that the smaller crater would represent the size expected in a low cohesion material if cube-root scaling is used. However, Baldwin contended that fourth-root scaling, which takes into account the energy

needed to overcome gravity effects in raising materials out of the crater, properly applies to those impacts on the Moon that result in larger craters of the size range that still does not extend through the local regolith or rubble mantle. He furthermore minimizes the effects of variations of gravity values (for different planetary masses) as a decisive factor in determining the actual diameter, as has been suggested by others from experimental work. Baldwin, therefore, selects the larger (13 meters) fresh crater as the more likely Ranger VIII impact site, because it closely approximates the size expected from his gravity scaling calculations.

Pike (213) noted major discrepancies in the values of "Schroeter's Rule," i.e., the ratio of crater rim volume to true crater volume, normally supposed to be 1:1, for both terrestrial and lunar craters. This, he explained, results from one or more modifying processes, such as erosion, partial burial by extrusive products, and isostatic adjustments. Scott (214) carried out a mathematical analysis of viscous flow of large craters which supports the role of isostasy in raising the central region and lowering the rim.

Walker (215) presented evidence from experimental hypervelocity impacts into materials whose strengths vary in terms of target density and cohesion, which indicates that rock or metal projectiles produce relatively deep craters in hard (solid) targets and shallow craters in granular, low cohesion targets. From this he infers that smaller lunar craters are mostly emplaced in weak, soil-like layers. Overbeck and Quaide (216) used a similar approach to estimate

the thickness of the surface regolith on the Moon. They note a systematic change in crater morphology as diameters increase. Flat-bottomed and ringed craters result wherever a solid "bedrock" layer is penetrated by a crater surface. Relative thickness of the fragmental cover can be estimated from ratios of crater diameter to layer thickness derived experimentally from laboratory impacts into sand layers of varying thickness overlying bonded material. Ratio boundaries are correlated with the different crater geometries so that, for craters normalized to constant diameter, it is possible to estimate the thickness of a cratered area on the basis of distribution and frequency of the several morphological types. As applied to parts of Oceanus Procellarum visible in Orbiter I photos, the thickness of 85% of the areas investigated ranges between 5 and 15 meters.

IRON METEORITES

Isotope Analyses

Rare gases in meteorites are divided into three types; primordial, radiogenic, and spallogenic. The primordial gases were formed after accumulation of the isotopes and are used to determine gas retention ages, and the spallogenic gases were formed after cosmic ray exposure and are used to determine cosmic ray exposure ages. Lammerzahl (217) has recently reviewed the method and results of rare gas isotope studies on meteorites.

It has been shown that ^{3}H in irons and the iron phases of stones is low. Two explanations have been offered; diffusion of ^{3}H out of the iron phase during

terrestrial descent or residence and solar heating of the meteorites in space. Fisher (218) showed experimentally that the temperature—time history during atmospheric descent is not sufficient, but that long times on the surface of the earth, aided by grain boundary diffusion, is sufficient for ^{3}H loss. Hintenberger, et al. (219) measured He and Ne contents in 40 irons. The hexahedrites investigated (12) showed a definite loss of spallogenic ^{3}He. They conclude that this indicates that these irons were always in the vicinity of the Earth or even closer to the Sun; i.e. that tritium loss occurs by solar heating in space. Schultz (220) in a study of ^{3}H losses found a correlation between iron meteorites of low cosmic ray exposure ages, amount of spallogenic ^{3}He, and the low spallogenic tritum content in freshly fallen iron meteorites. Therefore, he concluded that solar heating of meteorites in space causes the tritium loss in iron meteorites.

The isotopic composition and abundance of Li was measured by Krankowsky and Müller (221) on several chondrites as well as silicate and trilite inclusions in the Odessa octahedrite. The $Li^{7}:Li^{6}$ ratio of the meteorite samples as well as that of terrestrial diabase W-1 and granite G-1 agree to within ±2%. Therefore, all of these materials were exposed to the same proton flux even though they probably came from different regions of the solar system. Burnett and Manuel (222) investigated the origin of noble gas anomalies in the Canyon Diablo graphite. Using the measured ^{129}I-^{129}Xe ratios, they were able to date the formation interval, the time between nucleosynthesis and the temperature

at which Xe^{129} is retained in graphite, as 131 million years. The stone meteorites have formation intervals between 127 and 300 million years and show no appreciable differences from the Canyon Diablo (iron) meteorite.

Several other studies of spallogenic rare gas isotopes were also carried out. Spallogenic isotopes of helium, neon and argon were measured in 36 irons (Schultz and Hintenberger (223)), and concentration of ratios of ^{3}He, ^{4}He, ^{21}Ne and ^{38}Ar were determined, Munk, 1967 (224) determined Ne, A, K and Xe in the iron Castilla Peak. He found a cosmic ray exposure age between 400 and 640 million years and a I-Xe formation interval of 230 m.y. In an attempt to see if the Campo del Cielo strewn field and the North Chilean hexahedrites are related, Nyquist, Huneke, and Signer (225) measured the rare gases in the El Taco (Campo del Cielo) meteorite. Based on differences of terrestrial ages they concluded that the two groups were not from the same body.

Cosmic ray exposure ages (the time between break-up of the parent body and capture by the earth) of 60 iron meteorites were determined by Voshage (226, 227) using the $^{41}K/^{40}K$ method. A histogram showing all the exposure age data is given in Figure 39. Exposure age data for the several structural and chemical groupings, Og + H (coarse octahedrite + hexahedrites), Om + Of (medium and fine octahedrites), Of IVa (fine octahedrites of chemical group IVa), and D (ataxites) are also included. Medium and fine octahedrites of chemical group III are found in a peak at 550-750 m.y., and fine octahedrites of group IVa in a peak at 400 m.y. Presumably each of these groups were produced in a major

collision. The correlation between structure, Ga-Ge chemical grouping and cosmic ray exposure ages for Groups III and IVa suggest that each of these meteorites groups come from the same parent bodies. Hexahedrites, coarse octahedrites of the chemical group I, and ataxites have age distributions which are continuous. Voshage suggests that these three groups of meteorites are fragments of a multiplicity of nickel-iron inclusions within the surface layers of the Moon, Mars and the asteroids respectively.

The cosmic ray exposure ages of stone meteorites are clustered between 1 and 30 million years, over one order of magnitude lower than the data for the irons. To determine the effect of space erosion on the relative exposure rates of irons and stones, Comerford (228) investigated the effect of small particle bombardment. He found that mass loss is much greater with brittle material (chondrites) but no quantitative data could be obtained as to rates of erosion.

Radiogenic gases (K/Ar) have been measured in order to obtain the formation or solidification age of iron meteorites. Recent K/Ar age data have indicated ages of from about 7 to 10×10^9 years whereas the age of the solar system is generally well accepted at about 4.7×10^9 years. Rancitelli et al. (229) measured a K/Ar age of about 10^{10} years in the Weekeroo Station meteorites. This disagrees with the Sr/Rb age of 4.7×10^9 years from silicate inclusions of the same sample. The authors conclude that the potassium: argon dating technique as applied to iron meteorites gives unreliable results. Recently Rancitelli and Fisher (230, 231) showed that perferential teaching of K relative to Ar in irons

by terrestrial weathering processes is a mechanism that may account for the old "ages" determined by the K/Ar age method. Bogard et al. (232) measured the rare gases, He, Ne, Ar as well as K in silicate inclusions of several iron meteorites. The K-Ar age of the silicate from Weekeroo Station is less than the Sr/Rb age of the same silicate fraction and does not agree with the high K/Ar ages measured by other investigators for this and other iron meteorites.

Rb-Sr measurements have been made by Burnett and Wasserburg (233) on different types of silicate inclusions extracted from 7 iron meteorites. Four Corners and Pine River have irregular patches of silicates, Toluca, Odessa and Linwood have silicates as minor constituents of troilite or graphite nodules and Colomera and Weekeroo Station have drop-like silicate inclusions. Six of seven of these meteorites give $4.6 \pm 0.2 \times 10^9$ year isochrons, compatible with chondrite-achondrite ages. The strontium evolution diagram for 4 of these meteorites are given in figure 40. Toluca and Odessa are typical octahedrites showing a well developed Widmanstatten pattern.

Chemical Analyses of Irons

Chemical analyses have been performed on iron meteorites for hundreds of years. Only within the last 20 years, however, has the analyst possessed the necessary apparatus for performing analyses for both major elements Fe, Ni, Co and the minor element (P, S, C). Recently measurements of trace elements (Ga, Ge, Pt, Lr, Cr, Cu etc.) in irons using techniques of emission spectroscopy, neutron activation etc, are being actively performed (234). These measurements may

ultimately be more useful than major element analyses since they help to differentiate several groups of irons from each other.

With respect to trace elements, Tanner and Kohman (235) have determined the Hg and Bi abundances in 20 iron meteorites. They found Hg contents in the range of 0.03-13 ppm and Bi contents in the range of 0.04-0.10 ppm. Rao (236) spectrographically determined the siderophilic elements Os in 3 iron meteorites and the results agree with those of neutron activation. In measurements of the abundance and distribution of Cl in iron meteorites by neutron activation. Berkey and Fisher (237) found that terrestrial processes have, through weathering, locally raised the Cl abundances in some meteorites. The Cl content ranged in value from < 0.005 ppm to 10^4 ppm, and was segregated mainly at grain boundaries, cleanages and Neuman bands.

Since the initial discoveries of the "quantization" of Ga in iron meteorites by Goldberg, et al. (238) and the correlation of Ga-Ge by Lovering et al. (239) several investigators have proposed that members of Ga-Ge groups are related genetically. The authors of four papers (Cobb, (240), Smales et al. (241), Wasson, (242), and Kimberlin, (243)), have all attempted, by measurements of various combinations of trace elements, to further define these chemical groups.

Cobb (240) has measured Co, Cu, As, Ga, Ir, and Au in 33 iron meteorites by neutron activation. The trace element values were compared for meteorites within each of the structural groups of iron meteorites: hexahedrites; coarse medium and fine octahedrites and ataxites. He found a good correlation between

Au, Ir and Ga and the structural groups Hexahedrites, coarse octahedrites, and medium octahedrites. The complexity of trace element distribution between structural groups is proposed as an argument for a number of parent bodies. For the hexahedrites, and coarse octahedrite, the trace-element composition of the melt and conditions of crystallization were similar. Cobb also postulates a melt of different trace element compositions for the medium and fine octahedrites. The lack of trace element uniformity in the ataxites could be due to any individual ataxite being a late-stage portion of any one of the starting melts. Due to the small number of meteorites studied, further refinement of the groups was not possible.

Smales, Mapper and Fouche (241) measured Ge, As, Sb, Gu, Cr, Mo, Ag, In, Zn, and Pd by neutron activation on 67 iron meteorites. The authors found that Sb, Zn and Cu were associated with troilite inclusions and Cr was associated with inclusions. The elements Ge, Zn, Ga, As, Sb, Ag, In are more concentrated in the coarse octahedrites; Cr is least concentrated and Mo and Cu are not correlated with the structure of the Irons. They point out that $\sim 40\%$ of the meteorites studied do not belong to the Ga-Ge groups as set out by Lovering (239) and that a correlation between two trace elements is not sufficient to define a chemical group. By considering possible correlations between trace elements, they found that Ge-Zn, As-Sb and As-Pd were strongly correlated. They also found chemical groupings between some of the members within each of the broadly defined Ga-Ge groups.

Wasson (242) has measured Ga and Ge in 34 iron meteorites by neutron activation and Wasson and Kimberlin (243) measured Ga-Ge and Ir by neutron activation and Ni by atomic absorption in 69 additional irons and eight pallasites. They define chemical groups when the differences in trace element composition is smaller than for meteorites as a whole, the major and trace elements vary coherently with each other and the member meteorites have similar textures. Results for five resolved groups, are given in the following table (Table 5).

Group	Ni variation Wt%	Ga(ppm)	Ge(ppm)	Ir(ppm)	Correlation with Ni, as Ni Increases		
Group IIIa	8.65-7.53	22-17-	47-33	0.4-13	inc.	inc.	dec.
IIIb	9.3-10.7	20-16	38-28	— —	dec.	dec.	---
IVa	7.4-9.2	1.6-2.2	.09-.135	1.9-2.8	inc.	inc.	---
IVb	16.2-18.2	0.18-.31	.03-.06	— —	inc.	inc.	---
P	8.8-12.3	26-13	72-11	.1-.25	dec.	dec.	---

The Group IIIa may be resolvable into smaller groups and groups IIIa and IIIb may come from the same parent body. A plot of the Ge-Ni and Ga-Ge variation for all the meteorites studied is shown in figure 41. Many meteorites are not members of chemical groups. The fractionation processes which may be responsible for the formation of the Ni-Ga-Ge-Ir correlations are discussed briefly.

Since so much importance has been placed on the importance of Ge abundances several studies have been conducted to see if Ge is distributed, as has

been assumed, totally within the metallic phases. Goldstein (244) studied the Ge distributions in 10 iron meteorites with bulk Ge contents between 8 and 2000 ppm using the electron probe. He found that Ge is not detectable (< 20 ppm) in either schreibersite, troilite, or cohenite and is concentrated in the metallic phases. During the formation of the Widmanstatten pattern the Ge was redistributed preferentially to the parent taenite phase. Wai, et al. (245) performed laboratory studies on the equilibrium distribution of trace amounts of Ge between iron-silicate and Fe-FeS at controlled temperature, pressure and oxygen fugacity. In both experiments Ge was observed to be strongly siderophile, being found in the iron phase. From these results it seems that a one-stage oxidation reduction process is unlikely to cause the extremely low Ge content in some iron meteorites.

Trace element concentrations have also been used to establish whether separate meteorites fell to earth in the same shower. In one study, Wasson (246) showed that the Boxhole, Henbury and Wolfcreek meteorites are unique in composition and each associated crater was caused by a unique event. Wasson and Goldstein (247) using Ni, Ga, Ge and Ir results along with microprobe and structural studies, showed that the North Chilean Hexahedrites have not resulted from a single shower, but rather from a minimum of four falls. There appears to be no connection between these hexahedrites and the Campo del Cielo irons. In a study of the Ni, Ga and Ge contents in a series of Canyon Diablo and Odessa meteorite specimens, Wasson (248) found that Canyon Diablo and Odessa are members of the same chemical group but are not likely to be from the same fall.

In order to determine the possible differences between Canyon Diablo rim and plains specimens, Moore, Birrell and Lewis (249) analyzed Ni and C in a large number of separate iron specimens and determined the volume percent of various phases. They found more taenite and less oxide in the rim specimens than in the plains specimens. The C content was also significantly higher, 0.33 wt%, for the rim specimens than the plains specimens, 0.11 wt%. They were not able to tell whether the differences between iron + plains specimens are gradual or sharp. Total sulfur for 100 iron meteorites was determined by Moore et al. (250) using an oxygen combustion technique. The valves ranged from 0.001 to 0.063 weight % S with the majority of samples containing less than 0.0075 wt%S.

MINERALOGY

Non-Metallic Minerals

Many non-metallic minerals have been found in iron meteorites. The composition and oxidation state of each mineral as well as its relation to other surrounding minerals provide independent data on the conditions under which the iron meteorites formed.

Reed (251) has recently reviewed the evidence from iron meteorites which bears on the nature of meteorite parent bodies. His paper reviews work up to 1966. Olsen (252) found amphibole (richterite) as a primary mineral enclosed in a graphite module in the Wichita County iron. Terrestrially, this mineral indicates formation temperatures between 300 and 800°C, water pressures between 100 and 300 atmospheres. Olsen and Fuchs (253) estimated the

oxidation states of two iron meteorites (Mt Stirling, Odessa) which contain chlorapatite-silicate-schribersite assemblages. Although many thermodynamic uncertainties were present, they concluded that phosphate-bearing metallic meteorites represent approximately the same range of oxidation as the ordinary chondrites. Most iron meteorites represent more reduced regions in a parent body. Two new phosphate minerals were discovered in the Dayton meteorite (Fuchs, et al. (254)). The authors estimated the oxidation state of this iron and found that it also has an oxidation state similar to ordinary chondrites. El Goresy (255) analyzed coexisting sphalerite, daubreelite and troilite in the Odessa iron meteorite with the electron microprobe. He found that the minerals had variable compositions and formed under non-equilibrium conditions. Therefore, the FeS-ZnS system which has been used as a geological thermometer could not be used. El Goresy (256) also found K-Feldspar gains in graphite-trailite modules in Odessa. Bence and Burnett (257) have studied the compositions of silicate inclusions in 2 irons, Four Corners and Kodaikanal, with the electron microprobe. Four Corners silicate represents more typical silicate with homogeneous minerals and two species of pyroxene with lesser amounts of olivine and feldspar. Kodaikanal silicates are predominantly alkalifeldspars which are non-homogeneous and have excess SiO_2.

Mason (258) describes a general classification for silicates commonly found in iron meteorites. Except for the rounded drop-like silicate inclusions in Colomera, Kodaikanal and Weekeroo Station, these inclusions are similar to

those of chondritic meteorites. This suggests that chondritic material was incorporated into the metal and recrystallized during slow cooling. Possibly these meteorites represent a border zone between a metallic core and a silicate mantle in one or more asteroids. Brett and Henderson (259) found two types of troilite (1) narrow, long inclusions and (2) elongated bodies. The Widmanstatten pattern is non-continuous across the narrow-long inclusions but is continuous across the elongated bodies. Evidence is presented to show that the long-narrow lamellae form from this liquid and that octahedrites containing elongated bodies of troilite have faster cooling rates.

Up until a few years ago, the presence of diamonds in several meteorites and the presence of cohenite, which is instable at low pressures, was evidence for the formation of iron meteorites at high pressures. However, recent studies have shown that diamond can be produced by shock. The following papers present different types of evidence all bearing on the formation of diamonds and cohenite in iron meteorites. Lipschutz (260) has observed that cohenite grains in Canyon Diablo show evidence of shock-induced alterations. The nature and extent of these were determined by X-ray diffraction and eight Odessa iron shock standards. Marvin (261) has also observed by X-ray diffraction analysis that grains of ureyite and sphalerite from small, diamond-bearing specimens of Canyon Diablo also show evidence of shock transformation. Hexagonal diamond, a new polymorph of carbon, was discovered by Hanneman, Strong and Bundy (262) in the Canyon Diablo meteorite. Their results provide strong evidence that these

hexagonal diamonds were produced by intense shock pressures acting on crystalline graphite inclusions present within the meteorite before impact rather than by disintegration of large statically-grown diamonds. Brett (263) has presented a rather thorough study of cohenite, its occurrence and origin. If cohenite was stabilized at high pressures, then it should be present in all meteorites with sufficiently high C contents. In fact Brett finds that cohenite is present almost entirely in iron meteorites with Ni contents between 6-8 wt% Ni. On the basis of phase diagrams and kinetic data it is proposed that temperatures were too low for cohenite to form in meteorites over 8 wt% Ni and that any cohenite which formed in meteorites having Ni contents lower than 6 wt% Ni decomposed because of the high temperature during cooling of the meteorite. The absence of cohenite in meteorites containing both metal and graphite requires low pressures during cooling. These meteorites cooled in parent bodies of asteroidal size or near the surface of large bodies. Brett and Higgins (264) studied the formation of Cliftonite in iron meteorites. Some investigators have considered cliftonite to be a pseudomorph after diamond and have used the diamond ancestry of cliftonite as evidence of a high pressure origin for iron meteorites. The authors synthesized cliftonite as a decomposition product of Fe_3C (cohenite) in evacuated tubes at 550°C. Cliftonite was only produced at low oxygen fugacities and in the presence of Ni. Cliftonite has not been found in meteorites with more than 8 wt% Ni since no cohenite is present. They suggest that meteorites containing cliftonite formed at low pressures.

Metallic Minerals

Metallographic examination of iron meteorites yields information on structural relationships and the heat treatment of the samples. In a study of the Goose Lake meteorite and the Goose Lake fragments Axon and Rieche (265) found, by metallographic techniques, that the structure of the fragments was consistent with that of the main mass. Buchwald (266) studied six iron meteorites which had been reheated to varying degrees by metallographic techniques. Axon and Faulkner (267) have investigated hot working or thermal-mechanical in the parent taenite of iron meteorites. Annealing twins were found in Lawrens County, Toluca and Gibem. Non-octahedral kamacite, was also found in Gibean (Axon and Faulkner (268), Frost (268)) which predates the formation of the Widmanstatten pattern. The non-octahedral kamacite was caused by slip deformation on the cube plane at high temperatures.

Two papers discussed the structure of plessite formed by the decomposition of taenite at low temperature. Duerr and Ogilvie (269) investigated the formation of plessite in the octahedrite Carbo. They determined the orientation of the martensite in taenite and attributed the morphology of plessite to the presence of carbon. Goldstein (270) used the scanning electron microscope to look at plessite structures at high magnifications. Three regions and types of plessite were delineated and the mechanisms for each of these were outlined. In an attempt to see whether shock pressures up to 228 kb changed the Ni contents of kamacite-taenite interfaces Axon and Boustead (271) examined both cohenite-rich, cohenite-poor and cohenite-free, artifically shocked meteorites with the

electron probe. They found that the interface relations were not altered by shock. Jaeger and Lipschutz (272) investigated shock effects by metallographic and X-ray diffraction techniques in five octahedrites. All but one was shocked by metallographic and X-ray diffraction techniques in five octahedrites. All but one was shocked by preterrestrial collisions to at least 130 kilobars. In a much more complete study the same authors, Jaeger and Lipschutz (273) investigated 65 octahedrites. Most of the shocked (> 130kb) meteorites are in Ga-Ge Group III defined by Lovering (239), Figure 42.

These shocked meteorites also cluster around a 650 ± 60 million year exposure age and may be from the same parent body. Since the majority of the hypersthene chondrites have a 520 my exposure age, the authors postulate that the parent bodies which contained the hyperstheme chondrites and the Group III irons were involved in a collision and provide the majority of the iron meteorites.

Development of the Widmanstatten Pattern in Iron Meteorites

Since the advent of the electron microanalyzer we found that the growth of the Widmanstatten pattern in meteorites is incomplete and large Ni and Fe gradients along with models for the growth of the Widmanstatten pattern have enabled investigators to estimate the rate at which irons have cooled within their parent bodies. Investigations on major and minor element redistribution in the metal phase and on cooling rate distributions have been continued.

Axon and Yardley (274) examined the Ni distribution at phase interfaces in the Brenham County Pallasite. They found that the Ni distribution in taenite is

identical whether the taenite is in contact with olivine or with kamacite. The results also suggest the possibility of enhanced nickel diffusion along phase interfaces. The effect of P on the development of the Widmanstatten pattern is not well known. Reed (275) measured the P distribution in the Mt. Edith Octahedrite with the electron microprobe. He found that kamacite contains 0.09-0.10 wt% P and taenite contains 0.02-0.03 wt% P. The P and Ni gradients in kamacite near schreibeirite inclusions are consistent with the formation of schreibersite as a solid-state precipitation.

Goldstein and Short (276) have determined cooling rates for 27 iron and stony-iron meteorites. The cooling rates were obtained by comparing measured Ni gradients in kamacite-taenite areas with those gradients calculated by a theoretical growth analysis. A wide range of cooling rates was found (0.4-40°C/my). Three groupings were found: 1) fine octahedrites, (chemical group IVa), 9-40°C/my; 2) fine and medium octahedrites, 1-5°C/my and 3) pallasites, 0.4-1°C/my. These groups of meteorites developed their Widmanstatten pattern in different thermal environments and under conditions of low pressure.

Short and Goldstein (277) developed two rapid and simple methods for the determination of approximate cooling rates of iron phases in meteorites without the need for extensive computer calculations. One of these methods was used by Goldstein and Short (278) to determine the approximate cooling rates of 193 iron meteorites. About two thirds of the meteorites cooled between 1 and 10°C/my although the total variation in cooling rates is 0.4-500°C/my. These variations

indicate that meteorites formed in more than one body, and the Widmanstatten pattern formed at low pressures. Evidence was given that meteorites within each chemical (Ga-Ge) group are further correlated by bandwidth, plessite structure and cooling rate. The variation in cooling rate and Ni content for meteorites in the five of the chemical groups is shown in figure 43.

The cooling rate variations in both groups I and IIIb are small (2-3°C/my and 1-2°C/my respectively) and independent of chemical composition. These meteorites probably formed in the cores of their parent bodies. The cooling rate variations in both groups IIIa and IVa are large (1.5-10°C/my and 7-90°C/my, respectively) and vary with the Ni content, descreasing as the Ni content increases. These meteorites probably formed in isolated regions spread throughout their parent bodies.

MINERALOGY

Stony Irons

The stony iron meteorites including the pallasites and mesosiderites, constitute less than 5% of the number of meteorites. However, their unusual mineralogy and their possible link between the two major groups of meteorites makes them important. The petrology and chemistry of eucrites, howardites (Ca rich achondrites) and mesosiderites was described by Duke and Silver (279). They concluded that the principal mineralogical and textural properties are due to original magmatic crystallization followed by complex fragmentation and recrystallization episodes. The authors suggest that these meteorites come from the moon, probably as surficial material. Preliminary Surveyor data tend to confirm in part this suggestion. Powell and Weiblen (280) examined microscopically 10 mesosiderites. They also analyzed most of these with the electron microprobe to determine the major element compositions of all major phases and of certain accessories. A large variety of structures was observed, and that individual mesosiderites have had dissimilar histories.

Several investigations on the pallasites were also published. Stanofieldite, a new phosphate mineral was found by Fuchs (281) in one mesosiderite and 6 pallasites. A new pallasite, Marburg, was also described chemically and mineralogically (Buseck, et al. (282)). Buseck and Goldstein (283) examined the olivine and metal phases with the electron microprobe in over 75% of the known pallasites. The olivine compositions and homogeneity data indicate that the

pallasites were derived from a limited number of parent bodies. The cooling rate data indicate that pallasites formed in a site more termally insulated than were the iron meteorites. Wasson and Kimberlin (243) determined Ni, Ga, Ge and Ir in 6 pallasites. They conclude that the pallasites are all members of a single genetic group. However, their data are only marginally consistent with the previously observed correlation that the fayalite content of the pallasitic olivine increases with increasing Ni content of the metal.

In a discussion section of a paper on the Bununu meteorite and in a review article on meteorites, Mason (284, 285) proposes that most of the stony-iron meteorites and achondrites, other than the enstatite achondrites, can be derived by melting and fractional crystalization of one or more parent bodies with overall composition of the chondrites. In this way a continuum of structures and meteorite types develop from the core of the parent body to the surface. Pallasites are then found in the center of the body and are surrounded by howardites and then eucrites. The mesosiderites are close to the surface and are breccias of the eucrites and howardites.

STONE METEORITES

As in previous years, the researches on stony meteorites centered around the search for those types which represent the most primary material and, thus will yield the most significant data concerning the origin of the elements, the solar system and meteorites.

A new classification scheme for chondritic meteorites was proposed by Van Schmus and Wood (286) which depends on essentially two parameters; the chemistry and the petrologic type. On the basis of chemistry (the Fe/SiO_2 ; MgO/SiO_2 ratios in the bulk analyses and the ratio of FeO/FeO + MgO in olivines and pyroxenes) the meteorites are categorized into Enstatite, Carbonaceous, High (-iron), Low (-iron) and Low-low (-iron) groups. Each of these is further divided by petrographic type as shown in Table 6. The use of this classification has, in a short time, gained wide acceptance and, as will be noted here, can be correlated with many of the results of analyses on chondritic meteorites. The existence of the distinctive features (which result in types 1 through 6 in Table 6) is, for the most part, unquestioned. On the other hand, their origin is the subject of some controversy. These authors attribute them to metamorphism which increases in grade from 1 to 6. This, they feel, is consistent with increasing homogeneity of the silicates in the higher groups, the disappearance of glass and the disappearance of low-calcium clinopyroxene. Dundon and Walter (287) have likewise correlated the higher petrologic type with an increased ordering of the Fe and Mg between two dissimilar cation sites in pyroxenes from these meteorites. This is indicative of a lower equilibration temperature for these meteorites. Van Schmus and Koffman (288) used the constant of equilibration K, for the distribution of Fe and Mg between high-calcium (clino-) pyroxenes and low-calcium (ortho-)pyroxenes to determine the approximate

temperature of equilibration. The use of K, where:

$$K = \frac{X_{Fe_{clinopyx}} \cdot X_{Mg_{orthopyx}}}{X_{Fe_{orthopyx}} \cdot X_{Mg_{clinopyx}}}$$

assumes ideal mixing for which there is some evidence. The authors found, from previous microprobe analyses, that, for the equilibrate ordinary chondrites (those in types 5 and 6), K varied between 0.55 and 0.65. Using the curve shown in fig. 44 which is based on thermodynamic data, they derived a value of 820 ± 20°C. for the equilibration temperature.

In a general survey of the unequilibrated ordinary chondrites, Dodd, van Schmus and Koffman (289) presented evidence (fig. 45) that, as the heterogeneity of the olivine of a chondrite decreases, the average FeO content of the olivine increases. (The heterogeneity is determined by the point-to-point variation in the microprobe analysis of many olivine grains of the various chondrites and is presented as the % Mean Deviation of these analyses. The authors maintain that this parameter is inversely correlated with the degree of metamorphism.) Thus, they conclude, the High-, Low- and Low,Low-iron groups represent three distinct metamorphic series which involve a general increase in the oxidation state. Wood (290), on the other hand, finds that, in Type II Carbonaceous Chondrites, the average FeO content of the olivine decreases as heterogeneity decreases. He proposes metamorphism of these meteorites as taking place in a reducing atmosphere of modified solar composition.

Dodd et al. (289) tabulated the analyses of water, carbon and Ar^{36} in unequilibrated ordinary chondrites (Table 7). These are seen to decrease with increasing "metamorphic grade" and decreasing % Mean Deviation. Suess and Wänke (291), however, point out that the argon/xenon ratio does not change with degree of metamorphism, although argon would diffuse much more rapidly than xenon. In response to this argument, Wood (292) suggested that xenon might be, in effect, walled into the crystalline structures to the extent that iron and magnesium could be redistributed during metamorphism without affecting the xenon. Otting and Zahringer (293), however, show that, while there are no reports of primordial Xe^{132} in H6 chondrites, there is a steady decrease in primordial Ar^{36} from the H3 to the H6 types. This decrease holds true for both primordial Xe^{132} and Ar^{36} in L-group chondrites. Finally, Heymann and Mazor (294) have shown that the noble gases are strongly fractionated in the unequilibrated chondrites relative to their cosmic abundances. However, the more unequilibrated the chondrite, the greater the primordial component of solar gas. They conclude that the original rare-gas content of even the most unequilibrated chondrites is probably not entirely primordial, indicating that even these chondrites have been heated to some degree. This is in agreement with the absence of primordial neon component which, presumably was lost during this mild heating.

Wood (295) was also forced to propose a heating period for the unequilibrated chondrites. In a study of diffusion at the boundaries between taenite and kamacite metal grains in chondrites, he found that equilibrated meteorites have apparently

cooled through the temperature of 500°C. at a greater rate than the unequilibrated chondrites (2-10°C per million years for the former; .2-2°C per million years for the latter). The temperature for partial equilibration of Ni in the metal phase (500°C) is substantially lower than the temperatures below which mobilization in the silicate phase ends (800°, approx) so that reheating to a temperature between these would permit retention of the disequilibrium silicate phases in the unequilibrated chondrites. Slow cooling in these would cause equilibration of the metal phase while fast cooling in the equilibrated (in terms of the silicate phase) chondrites would result in disequilibrium (in the metal phase). Binns (296) differentiated between "primitive" and "transitional" groups and noted that, in the latter, the striated structure of the orthopyroxene was evidence that it had formed by inversion from clinopyroxene. This supports the contention that the more metamorphosed (transitional) chondrites were reheated. In a study of chromite in ordinary chondrites, Bunch et al. (297) found definite variations in the trace-element content of this mineral as a function of petrologic type (fig. 46) as well as chemical group. They were unable to conclude, on the basis of their study, whether these systematic variations were the result of primary crystallization or metamorphism.

Kurat (298) re-emphasized the possibility that the homogeneous distribution of olivine and pyroxene compositions in the equilibrated chondrites might be the natural result of a fast quench of a silicate liquid, so that crystallization took place at temperatures below the solidus. The unequilibrated meteorites, on the

other hand, may have cooled more slowly, having time to develop compositional heterogeneity as crystals slowly separated from the melt. He points out that many of the mineral phases in "equilibrated" meteorites are in disequilibrium.

Reid and Fredriksson (299) point out that, in order to derive an equilibrated from an unequilibrated chondrite, considerable redistribution of iron must take place, especially since the average FeO content of pyroxenes in unequilibrated chondrites is substantially lower than that of equilibrated types. The chondrite Bjurböle, which bears low-calcium clinopyroxene but homogeneous silicates, has chondrules which are quite distinct and could not have withstood the migration of iron. In addition, since the matrix of Bjurböle consists of ground-up chondrules and that of an unequilibrated chondrite, Chainpur is of fine-grained carbonaceous material, the latter could not be a simple precursor of the former by metamorphism. They also question how glass in the Bjurböle chondrite could have been preserved during metamorphism. The temperature of equilibration, as determined by the composition of coexisting ortho- and clino-pyroxenes is higher than the crystallization temperature of gabbro (according to the same data used by van Schmus and Koffman, (288)) and raise the question as to how such temperatures might have prevailed without causing extensive remelting in the meteorite.

The Shaw meteorite, according to Fredriksson and Mason (300), has coexisting ortho- and clino-pyroxenes which indicates a temperature of crystallization of 1100°C. It has no chondritic structure but contains equilibrated olivine and

pyroxene which characterize the chondrite as L-group. The total iron, however, is low so that it might be classified as LL-group. They propose that the iron content was high originally but that iron sulphide drained away during the melting process.

There have been several interesting studies on meteorites which exhibit shock effects and brecciation. Van Schmus (301) presented a petrographic description of the unequilibrated ordinary chondrite, Mesö-Maderas, and, in particular, described several breccia inclusions which occur in that meteorite. Glass in the chondrules is close to albite ($NaAlSi_3O_8$) in composition but does contain some iron and magnesium. It lies close in composition to the eutectic composition in the phase systems forsterite-silica-nepheline and fayalite-albite. It is, therefore, the result of quenching rather than shock-produced glass. One inclusion he describes resembles the Murray Type II carbonaceous chondrite, bearing olivine and pyroxene of variable composition. Another, and more common, inclusion has homogeneous olivines and pyroxenes and contains distinct chondrules. A third type has less distinct chondrules and glass which contains appreciable FeO, MgO and CaO, indicating a relatively high temperature of formation. This type of inclusion contains globular sulphides. The petrography of the Mesö-Maderas chondrite, he concludes, indicates the following sequence of events: deposition of unequilibrated chondrules; regions of the parent body heated to 800-1200°C causing local homogenization and partial melting; breakup; reaccumulation.

Binns (302) describes inclusions of cristobalite in the Farmington meteorite. These are surrounded by rims of diopsidic pyroxene. The meteorite also has cavities into which globular metal particles project. Experimental heating of the Parnallee meteorite caused melting and the production of blackened voids similar to those in Farmington. He believes that the heat which caused melting in Farmington was probably not due to shock since this would have destroyed the voids. Ortho-clino-pyroxene equilibration temperatures indicate that the chondrite was heated to 1000°C. The origin of the calcium which forms the diopside surrounding the cristobalite is unknown—however, the cristobalite is definitely foreign and injected into the meteorite.

Buseck (303) discussed the post-formational history of the hypersthene chondrite, Beenham which, according to petrographic study, has been subjected to strong shock effects. He presents the following chronology for this chondrite: formation of metal-free chondrules (this agrees with Wood's model); crystallization of metal; formation of kamacite from taenite in the metal phase; formation of sulphides (which selectively replace kamacite); shock event and the formation of Neumann bands; shock melting.

Metallographic studies by Heymann (304) indicate that the blackened hypersthene chondrites have been strongly shocked (from a few hundred to over a thousand kilobars shock pressure). At this stage, these meteorites experienced helium loss to varying degrees. He^3 and He^4, when corrected, give an isochron for this event at 520 ± 60 million years. The concordance of many K-Ar dates of

the hypersthene chondrites with this value indicates that approximately one-third of these meteorites were involved in that event.

Tanenbaum (305), however, made a statistical study analyses of cosmic-ray induced activities of chondrites and concludes that the clustering of cosmic ray exposure ages of hypersthene chondrites may well be random although clustering of these ages for bronzite chondrites at 4 million years is probably statistically significant.

The Rb-Sr age method has been useful in defining the time of crystallization of meteorites. However, in the majority of previous investigations, it has been necessary to assume that at least two meteorites are genetically related in order to calculate an age. If different portions of one meteorite can be found to contain different Rb/Sr ratios, it is possible to determine when the different portions became closed systems (crystallization, metamorphism?), without assuming any relationship between meteorites. In the past several years, the techniques of Rb/Sr dating have been improved to the point where very small samples may be analyzed so that the analysis of the component parts of meteorites is feasible. During 1967 three important papers have reported work of this type. The "internally determined" ages for three chondrites (306), an achondrite (307), and silicate inclusions in six iron meteorites (308) are all compatible with the generally accepted ages of meteorites, as determined by assuming genetic relations between meteorites—about 4.5×10^9 years.

Hohenberg et al. (309) irradiate samples of several meteorites and determined the release of xenon as a function of temperature. They found that, although xenon has been lost from the low-temperature sites in meteorites to varying degrees, the high-temperature sites have retained their xenon, giving an original I^{129}/I^{127} ratio of 10^{-4}.

Morgan and Lovering (310) determined uranium and thorium abundances in carbonaceous chondrites by neutron activation analysis. The type I carbonaceous chondrites were found to be quite variable in uranium concentration, even for separate samples from the same meteorite. The mean Th/U ratios for Type I and II carbonaceous chondrites were found to be 3.2 ± 0.7 and 3.5 ± 0.5 respectively. The abundances are considerably lower than predicted by nucleosynthetic theory which could mean either that the carbonaceous chondrites are not primary or that nucleosynthetic theory must be revised.

On the other hand, Tanner and Ehmann (311) have analyzed antimony in a number of meteorites, including two type I carbonaceous chondrites, and on the basis of these later two analyses suggest a cosmic abundance for Sb of 0.40 ($Si = 10^6$). This value is considerably higher than is predicted by current theories of nucleosynthesis. They point out that the recent experimental abundances in the Type I carbonaceous chondrites for the mass region bracketing the isotopes of Sb are generally two to six times the calculated values (see figure 47), but they point out the atomic abundance curve for the Type I carbonaceous chondrites matches, in a relative sense, the calculated cosmic

abundance curve of Clayton and Fowler much better than the curve for the Type II carbonaceous chondrites. They suggest that the theories of nucleosynthesis should be re-examined to reconcile the approximately four-fold greater experimental abundances in this mass region.

Other studies reported during the past year which bear on the questions of cosmic abundances of the elements and fractionation of the elements among the various types of meteorites include studies on I, U, Te (312); Rb, Pd, Os, Ir, Pt, and Au (313); Cl, Br, and I (314); Li (315); Re and Os (316); Fe, Ni, Co, Ca, Cr, and Mu (317); and Si (318).

The isotopic composition of tin in a variety of meteoritic and terrestrial samples have been studied by DeLaeter and Jeffery (319). They found no evidence of significant variations resulting from inhomogeneities in Galactic or Solar System processes. Tin was chosen specifically as each of its various isotopes is produced by one of the major synthesizing processes: r, s, and p. From the lack of isotopic anomalies in tin, the authors question the validity of the Fowler, Greenstein and Hoyle model of nucleosynthesis. From a study of the lithium isotopic composition in meteoritic matter, Krankowsky and Muller have reached a similar conclusion concerning inhomogeneities; that is, if the FGH model is correct, the postulated proton flux must have been constant over several A.U., or that large scale mixing processes occurred over the same distances.

Greenland (320) has analyzed many specimens of all types of chondritic meteorites for several trace elements. He found that fractionation of these elements cannot be explained on the basis of a one-step separation. Several of the elements (Cd, Bi, Pb and Tl) were separated from the chondrites independently of each other and the other fractionated elements while there is evidence for fractionation of groups of other elements. The former fractionation type might be explained as due to sulphide extraction which was proposed earlier. The latter may be due to the mixture of a high-temperature fraction with a low-temperature fraction of cosmic (primordial) composition. This view is consistent with the idea that Type I carbonaceous chondrites and certain types of enstatite chondrites are the most primitive.

Mueller and Olsen (321) have compared the amount of normative olivine in chondrites of types H, L and LL with the oxidation states of the meteorites. They find that these factors are related in adherence to a corollary of Prior's rule—that the olivine content increases as the oxidation state increases. The same relationship holds for all these types indicating that they are quite homogeneous. This factor must be taken into account in theories of meteorite origin.

Ahrens (322), on the other hand, has found significant fractionation of calcium (relative to silicon) between carbonaceous chondrites (Ca/Si = 10.1) and ordinary chondrites (Ca/Si = 15.5), representing a fractionation of 54% between the two groups. The ratios Si/Mg and Si/Al vary by 10 and 27% between these groups.

Larimer (323) has made a study of the thermodynamics of condensation of material from a gas of solar composition. His results are summarized in figure 48 and are given for fast condensation and slow (equilibrium) condensation. In both cases, metallic iron precipitates at the highest temperatures (after the precipitation of several minor compounds). This relative sequence may not conform to several petrographic studies but relative fractionation of volatiles can be used to explain the extreme depletion of Pb, Bi, In and Tl in ordinary chondrites. The evidence, Larimer concludes, supports the hypothesis of a mixture of two fractions: volatile and involatile. Larimer and Anders (324) point out that, in the sequence: Carbonaceous Chondrites Type I; II; III and Enstatite Chondrites, Type I, 31 volatile elements decrease by the factors: 1:0.6:0.3:0.7. The volatile contents of the meteorites when applied to the data of Larimer (323) indicate that Carbonaceous Chondrites condensed at temperatures below 400°K; Enstatite Chondrites (Type I) between 400-480°K; ordinary and Type II Enstatite Chondrites between 530-650°K and unequilibrated ordinary chondrites above 530°K. They point out that these temperatures are higher than the blackbody temperature of objects in the asteroid belt. These temperatures and the proportion of volatile (A) and non-volatile (B) fractions in various meteorite types and the earth as determined by their trace element investigations are presented in Table 9.

Blander and Katz (325) also discuss a model for the condensation of primordial gas of solar composition to form the chondrules taking into account the

difficulties such a slowly condensing gas has in finding nucleation sites. Their mechanism of disequilibrium condensation seems to explain several perplexing aspects of the formation of chondrules. (Equilibrium condensation of a low-density solar gas takes place at temperatures at which crystalline silicates are stable. Thus, in order to form chondrules which have obviously been molten, a re-heating stage is required.) This paper points out that, in disequilibrium condensation, liquids can form metasably below the solidus of the system, enabling liquid chondrules to condense directly from the solar gas. Furthermore, it may be more difficult for iron to start nucleation sites so that, while under equilibrium conditions, iron would precipitate at high temperatures (Larimer (323)), it begins to come out only after most silicates. This would agree with the petrographic evidence (Buseck (303)) and, because it would result in the increase in the activity of FeO in the gas, it would also explain the high and variable FeO content of primative meteorites (the FeO content being higher than predicted by the oxygen pressure of the solar gas).

Urey (326) also has discussed the origin of chondrules, pointing out that their accretion to form meteorites must have taken place in a gravitational field of appreciable strength. He proposes that chondrules are formed by the collision of objects in space (one of them, probably, the moon) and that the temperature of these objects was, at the time, close to their melting points. Repeated collisions with the parent body result in a surface covered with chondrules and matrix (ground-up chondrules). Since the starting material for the formation of

chondrules consists essentially of two phases, olivine and pyroxene, the droplets, being a small sample of this material, cool to form the same homogeneous minerals in varying proportions (explaining the mineralogical homogeneity and chemical heterogeneity of chondrules). The material at the surface absorbs inert gases of solar composition as it cools. The metal (which may have been derived from the colliding, smaller, objects) undergoes the transition from taenite to kamacite. The theory has one major advantage—it explains the accretion of the chondrules. As the author points out, collision between two asteroids might form droplets such as chondrules, but would result in the scattering of these droplets throughout space.

TEKTITES

Several interesting discoveries were made concerning tektites during the year. Of major importance was the discovery of microtektites—glass particles in the size range of 50-100 microns with the shapes and indices of refraction of tektites—by Glass (327). These particles were found in core samples from the ocean floor around Australia and were dated at about 700,000 years by their proximity to a geomagnetic reversal. This age agrees, essentially, with the potassium—argon age for the southeast asian tektite strewnfield. Extrapolation of the mass involved to form the density of microtektites as well as tektites has greatly increased the mass of material required to form the strewnfield. In addition, the size of the object or objects striking the earth and the association with the magnetic reversal suggested to Glass and Heezen (328) that the reversal

occurred because the shock caused alterations in the currents which cause the magnetic field. Periodic changes in the direction of the field indicate that, energetically, the vector is not very stable. Thus, a huge impact, such as that which produced the southeast Asian field, may have imparted sufficient energy to the earth to reverse the field.

Nininger and Huss (329) discovered several tektite specimens (figure 49) which indicate that they were partially molten at the time of landing. Others (figure 50) show fractures in, what must have been, a hardened skin, and the formation of a meniscus in what was a molten interior at the time of impact. If the flattening and fractures occurred by impact with the earth's surface, the tektites could not have come to the earth as individual fragments because, in that case, they would have been hardened throughout at the time of impact. These tektites do indicate that the surface sculpturing of tektites is the result of aerodynamic ablation rather than weathering since the meniscus surfaces (figure 50) are smooth relative to the rest of the surface of these specimens.

Gentner, Kleinman and Wagner (330) have compiled new fission—track age determinations together with older age determination of tektites and impact-crater glasses. The results, given in Table 10, show a very good correlation between the ages of moldavites and the Ries crater on one hand and Ivory Coast tektites and the Bosumtwi crater on the other. This evidence lends strong support to a terrestrial origin for these tektites. Kolbe et al. (331) determined the Sr/Rb age of the country rock around the Bosumtwi crater and found it to be

2110 million years—in general agreement with that age for both the Bosumtwi crater glass and the Ivory Coast tektites. This, again, relates the Ivory Coast tektites to the impact event at the Bosumtwi crater.

Finally, Walter (332) reported the results of the vapor fractionation of silicate melts at high temperatures. In this work, material of the composition of the most siliceous tektites was subjected to high temperatures (2800°C) in a solar furnace. The residual glass was then analyzed by microprobe and the variation of other oxides was plotted against silica content (figure 51). The resulting trends are quite similar to trends for the analyses of tektites within strewn fields such as the North American tektites (figure 52). This is strong evidence that all tektites (except, perhaps those from the Ivory Coast) were derived from an extremely siliceous starting material through a high-temperature vaporization process.

Table 1. Results of measurements made by Soviet Venera 4 as it approached planet Venus

Height	T	Pressure	Per cent by volume			
in km	°K	atm	CO_2	H_2O	O_2	N_2
26	313 ± 10	0.684	90-95	0.1-0.7	0.4-0.8	<7
23	353 ± 10	1.98	same	same	same	same
near Surface	543 ± 7	20 ± 2	same	same	same	same

Table 2. Dissipation Models and Torque Values

	Value of Torque	
	Modern	Ancient
	3.9×10^{23}	5.3×10^{23}
Model	dyne-cm	dyne-cm
All Body Tides (Eq. 3)	A	B
All Tidal Currents (Eq. 8)	C	D
Divided Equally between Body Tides and Tidal Currents (Eq. 9)	E	F

Table 3. Mean Values from Various Analyses of the Earth's Topography*

	Kossinna (1933)	Prey (1921)	Bruins (Private Communication)	Munk and MacDonald (1960)	Paper (1966)
Oceanic area, %	70.80	(70.8)	(70.8)	71.43	70.92
Continental area, %	29.20	(29.2)	(29.2)	28.57	29.08
Mean world elevation, meters	-2430	-2456	-2367		-2300
Mean land elevation, meters	875	771	801		756
Mean ocean depth, meters	-3800	-3787	-3674		-3554

*Values in parentheses are assumed.

Table 4. Chemical Composition of the Lunar Surface at Surveyor 5 site.

(Preliminary Results)

Element	Percent of Atoms
Carbon	< 3
Oxygen	58 ± 5
Sodium	< 2
Magnesium	3 ± 3
Aluminum	6.5 ± 2
Silicon	18.5 ± 3
Sulfur → nickel*	13 ± 3
Heavier than nickel	< 0.5
*Iron, Cobalt and Nickel	> 3

Table 5. Five resolved groups of iron meteorites by trace element analysis.

Group/	Ni variation Wt%	Ga(ppm)	Ge(ppm)	Ir(ppm)	Correlation with Ni, as Ni Increases		
Group							
IIIa	8.65-7.53	22-17	47-33	0.4-13	inc.	inc.	dec.
IIIb	9.3-10.7	20-16	38-28	-- --	dec.	dec.	---
IVa	7.4-9.2	1.6-2.2	.09-.135	1.9-2.8	inc.	inc.	---
IVb	16.2--18.2	0.18-.31	.03-.06	-- --	inc.	inc.	---
P	8.8-12.3	26-13	72-11	.1-.25	dec.	dec.	---

Table 6. Summary of petrologic types*

	Petrologic types					
	1	2	3	4	5	6
(i) Homogeneity of olivine and pyroxene compositions	---	Greater than 5% mean deviations		Less than 5% mean deviations to uniform	Uniform	
(ii) Structural state of low-Ca pyroxene	---	Predominately monoclinic		Abundant monoclinic crystals	Orthorhombic	
(iii) Degree of development of secondary feldspar	---	Absent		Predominately as micro-crystalline aggregates		Clear, interstitial grains
(iv) Igneous glass	---	Clear and isotropic primary glass; variable abundance		Turbid if present	Absent	
(v) Metallic minerals (maximum Ni content)	---	(<20%) Taenite absent or very minor	kamacite and taenite present (>20%)			

*See text for discussion of criteria.

Table 6—Continued

	Petrologic types					
	1	2	3	4	5	6
(vi) Sulfide minerals (average Ni content)	---	>0.5%	<0.5%			
(vii) Overall texture	No chrondrules	Very sharply defined chondrules		Well-defined chondrules	Chondrules readily delineated	Poorly defined chondrules
(viii) Texture of matrix	All fine-grained, opaque	Much opaque matrix	Opaque matrix	Transparent micro-crystalline matrix	Recrystallized matrix	
(ix) Bulk carbon content	~2.8%	0.6-2.8%	0.2-1.0%	<0.2%		
(x) Bulk water content	~20%	4-18%	<2%			

Table 7. Water, carbon and primordial argon in unequilibrated ordinary chondrites

Chondrite	Olivine (%MD)	H_2O (wt.%)	C (wt.%)	(Ar^{36}) primordial $(10^{-8}$ cc)
H-Group				
Tieschitz	45	0.88	0.25	22
Sharps	37	2.03	0.95	
Bremervorde	15	0.23	0.22	
Prairie Dog Creek	6.9		0.35	
Clovis No. 1	5.6		0.22	
Castalia	3.6	0.43	0.27	
Geidam	*	0.57		
Sindhri	*			
Weston	*	0.98	0.28	
L-Group				
Krymka	45		0.27	52
Bishunpur	39	1.10	0.53	55
Hallingeberg	38	0.95	0.26	
Manych	26			12
Mezö-Madaras	21		0.45	51
Khohar	18	1.16	0.32	
Carraweena	6.0		0.09	3.0

Table 7—Continued

Chondrite	Olivine (%MD)	H_2O (wt.%)	C (wt.%)	(Ar^{36}) primordial $(10^{-8}$ cc)
Ioka	5.8		0.12	
Barratta	4.2		0.09	5.6
Goodland	2.6		0.07	6.7
Cynthiana	*		0.10	
Tennasilm	*	0.51	0.10	
Bjurböle	*			2.5
Lua	*		0.11	
Modoo	*		0.16	
LL-Group				
Ngawi	40	1.40	0.39	
Semarkona	37	1.22	0.57	
Chainpur	32	1.00	0.44	5.0
Parnallee	19		0.10	1.5
Hamlet	3.5	0.04	0.16	9.5

Table 8. Number and Percentage of Solar-Type Rare Gas Containing H-Group Chondrites

Petrologic Group	Total Number of Meteorites	Number Analyzed	Meteorites with Solar Gases	%
H-3	8	6	1	17
H-4	33	21	3	14
H-5	74	45	6	13
H-6	44	25	0	0

Table 9. Formation conditions of meteorites and the Earth

Class	% Fraction A*	Features diagnostic of: Fraction A — H_2O	Fraction A — T1, Bi, In in "normal" abundance?	Fraction B — Na, K, Rb lost?	Inferred condensation or accretion temperature (°K) — Fract. A	Inferred condensation or accretion temperature (°K) — Fract. B
Carbonaceous I	≥80†	Yes	Yes	?†	≤315	?†
Carbonaceous II	55	Yes	Yes	Yes	≤315	>1300
Carbonaceous III	32	Yes	Yes	Yes	≤400	>1300
Enstatite I	66	No	Yes	No	400-470	~1200
Enstatite II	48	No	No	Yes	530-650	>1300
Ordinary	27	No	No	No	530-650	~1200
Eucrites, Howardites	<10		No?	Yes	>530?	>1300
Irons I, II	50-100		No		>530	≥1100
Irons III	20		No		>530	≥1100
Irons IV	2		No		>530	≥1100
Earth (surface)	~10	Yes	Yes	Yes	≤400	>1300

*Inferred from abundance of normally depleted elements.

†Type I carbonaceous chondrites seem to contain most elements, including alkalis, in their cosmic proportions. The simplest interpretation would be that they consist of pure fraction A. However, the data are not accurate enough to preclude the possibility of a slight (≤20%) depletion, and consequently a minor admixture of fraction B

Table 10. K/Ar and Fission Track Ages of Impact Glasses and Tektites from Gentner et al. (33)

Material	Number	Age Type	Age	Range
Mold.	5	Fis. Tr.	14.1 ± 0.6	13.4 - 14.5 m.y.
Mold.		K/Ar	14.7 ± 0.7	
Ries	5	Fis. Tr.	14.0 ± 0.6	13.7 - 14.6
Ries		K/Ar	14.8 ± 0.7	
I.C.	15	Fis. Tr.	1.02 ± 0.1	
I.C.	15	K/Ar	1.1 ± 0.1	
I=C=		Fis. Tr.	1.04 ± 0.2	
I.C.		K/Ar	1.3 ± 0.3	

REFERENCES

1. Barker, E. S., A Determination of the Martian CO_2 Abundance, Astrophys. J., Vol. 147, pp. 379-381, (1967).
2. Schorn, R. A. and Gary, L. D., The Martian Surface Pressure, Astrophys. J., Vol. 148, pp. 663-1767, (1967).
3. Wells, R. A., Some Comments on Martian White Clouds, Astrophys. J., Vol. 147, pp. 1181-1183, (1967).
4. de Vaucouleurs, G., A Low-Resolution Photometric Map of Mars, Icarus, Vol. 7, pp. 310-349, (1967).
5. Sinton, W. M., On the Composition of Martian Surface Materials, Icarus, Vol. 6, pp. 222-228, (1967).
6. Miyamoto, S., Lunar and Martian Crust and Mantle Convection, Icarus Vol. 6, pp. 50-55, (1967).
7. O'Leary, B. J. and Rea, D. G., On the Polarimetric Evidence for an Atmosphere on Mercury, Astrophys. J., Vol. 148, pp. 249-253, (1967).
8. Kliore, A., Levy, G. S., Cain, D. L., Fjeldbo, G. and Rasool, S. I., Atmosphere and ionosphere of Venus from the Mariner V S-band radio occultation measurement, Science, Vol. 158, pp. 1683-1688, (1967).
9. Tass, Izvestia, 31 October 1967.
10. Tass, Pravda, 22 October 1967.
11. Reese, D. E. and Swan, P. R., Venera 4 probes atmosphere of Venus, Science, Vol. 159, pp. 1228-1230, (1968).

12. Van Allen, J. A., Kringis, S. M., Frank, L. A. and Armstrong, J. P., Venus: an upper limit on intrinsic magnetic dipole moment based on absence of a radiation belt, Science, Vol. 158, pp. 1671-1675, (1967).

13. Barth, C. A., Pearce, J. B., Kelly, K. K., Wallace, L., and Fastie, W. G., Ultraviolet emissions observed near Venus from Mariner 5, Science, Vol. 158, pp. 1675-1678, (1967).

14. Mariner Stanford Group, Venus: ionosphere and atmosphere as measured by dual-frequency radio occultation of Mariner 5, Science, Vol. 158, pp. 1678-1683, (1967).

15. Connes, P., Connes, V., Benedict, W. S. and Kaplan, L. D., Traces of HCl and HF in the atmosphere on Venus, Ap. J., Vol. 147, p. 1230-1237, (1967).

16. Adamcik, J. A. and Draper, A. L., The temperature dependence of the Urey equilibrium and the problem of the carbon dioxide content of the atmosphere of Venus, Planetary Space Sci., Vol. 11, pp. 1303-1307, (1963).

17. Mueller, R. F., A chemical model for the lower atmosphere of Venus, Icarus, Vol. 3, pp. 285-298, (1964).

18. Lippincott, E. R., Eck, R. V., Dayhoff, M. O. and Sagan, C., Thermodynamic equilibrium in planetary atmospheres, Ap. J., Vol. 147, pp. 753-763, (1967).

19. Goldreich, P., and Peale, S., Spin-orbit coupling in the Solar System, II. The resonant rotation of Venus, Astronomical Journal, Vol. 72, pp. 662-668, (1967).

20. Saslow, W. C. and Wildey, R. L., On the chemistry of Jupiters upper atmosphere, Icarus, Vol. 7, pp. 85-93, (1967).

21. Trafton, L. M., Model atmospheres of the major planets, Ap. J., Vol. 147, pp. 765-781, (1967).

22. Dulk, G. A., Apparent changes in the rotation rate of Jupiter, Icarus, Vol. 7, pp. 173-182, (1967).

23. Marcus, A. H., Formation of planets by accretion of planetesimals. Some statistical problems. Icarus, Vol. 7, pp. 283-296, (1967).

24. Harris, P. G. and Tozer, D. C., Fractionation of iron in the solar system, Nature, Vol. 215, pp. 1449-1451, (1967).

25. Shimazu, Y. Thermodynamical aspects of formation processes of the terrestrial planets and meteorites. Icarus, Vol. 6, pp. 143-174, (1967).

26. Hartmann, W. K. and Larson, S. M., Angular momentum of planetary bodies, Icarus, Vol. 7, pp. 257-260, (1967).

27. Alfvén, H., On the formation of celestial bodies. Icarus, Vol. 3, pp. 57-62, (1964).

28. Hanson, G. H. and Gast, P. W.; Kinetic Studies in Contact Metamorphic Zones. Geochim. et Cosmochim. Acta., Vol. 31, pp. 1119-1153, (1967).

29. Livingston, D. E., Damon, P. E., Manger, R. L., Bennett, R. and Laughlin, A. W., Ar^{40} in Cognetic Feldspar—Mica Mineral Assemblages. J. Geophys. Res. Vol. 72, pp. 1361-1375, (1967).

30. Peterman, Z. E., Hedge, C. E., Coleman, R. G., and Snavely, P. D. Jr., Sr^{87}/Sr^{86} Ratios in Some Engosynclinal Sedimentary Rocks and their bearing on the origin of Granitic Magma in orogenic belts. Earth and Planet. Sci. Letters, Vol. 2, pp. 433-439, (1967).

31. Ulrych, T. D., Oceanic Basalt Leads: A new interpretation and an independent age for the Earth, Science, Vol. 158, pp. 252-256, (1967).

32. Hurley, P. M., De Almeida, F.F.M., Melcher, G. C, Cordani, V. G., Rand, J. R., Kawashita, K., Vandoras, P., Pinson, W. H. and Fairkairn, H. W., Test of the Continental drift by Comparison of Radioactive Ages, Science, Vol. 157, pp. 495-500, (1967).

33. Hakli, T. A. and Wright, T. L. The fractionation of Hi between Olivine and Argite as a geothermometer, Geochim. et Cosmochim. Acta, Vol. 31, pp. 877-884, (1967).

34. Hahn-Weinheimer, P. and Ackermann, H., Geochemical Investigation of Differentiated Granite Plutons of the Southern Black Forest-II, The zoning of the Malsberg Granite Pluton as indicated by the Elements, Titanium, Zirconium, Phosphorus, Strontium, Barium, Rubidium, Potassium and Sodium. Geochim. et Cosmochim. Acta, Vol. 31, pp. 2197-2218, (1967).

35. Condie, K. C., Composition of the Ancient North American Crust, Science, Vol. 155, pp. 1013-1015, (1967).

36. Lowman, P. D., Jr., Geologic Applications of Orbital Photography, NASA Technical Note D-4155, Washington, D.C., (1967).

37. Lowman, P. D., Jr., and H. A. Tiedemann, Field Mapping from Orbital Photographs (Abstract), paper presented at the 1967 Annual Meeting of the Geological Society of America, New Oreleans, Louisiana, Nov. 20-22.

38. Abdel-Gawad, M., Geologic exploration and mapping from space, presented at the meeting of the American Astronautical Society, 1967.

39. Bateman, P. C., and J. P. Eaton, Sierra Nevada Batholith, Science, Vol. 158, No. 3807, pp. 1407-1417; 15 Dec. 1967.

40. Hamilton, W., and W. B. Meyers, The nature of batholiths, in Shorter Contributions to General Geology, pp. 61-630 in Geological Survey Professional Paper 554-C, U.S. Government Printing Office; 1967.

41. Taylor, S. R., "The origin and growth of continents," Tectonophysics, Vol. 4, No. 1, pp. 17-34; 1967.

42. Roddick, J. A., J. O. Wheeler, H. Gabrielse, and J. G. Souther, "Age and Nature of the Canadian Part of the Circum-Pacific Orogenic Belt," Tectonophysics; Vol. 4, 4-6, pp. 319-337; 1967.

43. Ho, O. S., Structural evolution of Taiwan, Tectonophysics, Vol. 4, No. 4-6, pp. 367-378, 1967.

44. Aronson, J. L., Absolute ages of the plutonic and metamorphic rocks of New Zealand, (Abstract) Tectonophysics, Vol. 4, No. 4-6, pp. 499, 1967.

45. Vassilkovsky, N. P., On the geological nature of the Pacific mobile belt, Tectonophysics, Vol. 4, No. 4-6, pp. 583-593, 1967.

46. Burgl, H., The orogenesis in the Andean system of Colombia, Tectonophysics, Vol. 4, No. 4-6, pp. 429-443, 1967.

47. Hamilton, W., Continental drift in eastern Asia and Alaska, (Abstract), Tectonophysics, Vol. 4, No. 4-6, p. 569, 1967.

48. Fleming, C. A., Biogeographic change related to Mesozoic orogenic history in the southwest Pacific, Tectonophysics, Vol. 4, No. 4-6, pp. 419-427, 1967.

49. Lamar, D. L., P. M. Merifield, Cambrian fossils and Origin of Earth-Moon System, Geological Society of America Bulletin. Vol. 78, pp. 1359-1368.

50. Paddack, Stephen, On the Angular Momentum of the Solid Earth. J. Geophys. Res. Vol. 72, pp. 5760-5766, Nov. 1967.

51. Gold, T., Radio Method for the Precise Measurement of the Rotation Period of the Earth. Science, Vol. 157, pp. 302-304.

52. MacDonald, Gordon, Implications for Geophysics of the Precise Measurement of the Earth's Rotation. Science, Vol. 157, pp. 304-305.

53. Alley, C. O., P. L. Bender, R. H. Dicke, J. E. Fallor, P. A. Franken, H. H. Plotkin and D. T. Wilkinson. Optical Radar Using a Corner Reflector on the Moon. J. Geophys. Science, Vol. 70, pp. 2267, (1965).

54. Lee, H. K., and W. M. Kaula, A Spherical Harmonic Analysis of the Earth's Topography, J. Geophys.Res., Vol. 72, pp. 753-758.

55. Heinrich, D., Poleomagnetism of the Plio-Pleistocene Lousetown Formation, Virginia City, Nevada, J. Geophys. Res., Vol. 72, pp. 3277.

56. Baksi, A., York, D. and Watkins, N. D. Age of Steens Mountain Geomagnetic Polarity Transition. J. Geophys. Res. Vol. 72, pp. 6299-

57. Grommé, C. S., Merrill, R. T. and Verhoogen, J. Paleomagnetism of Jurassic and Cretaceous Plutonic Rocks in the Sierra Nevada, California, and it's significance for Polar Wandering and Continental Drift. J. Geophys. Res., Vol. 72, pp. 5661-

58. Coe, R. S., Paleo, Intensities of the Earth's magnetic field determined from Tertiary and Quaternary Rocks. J. Geophys. Res., Vol. 72, p. 3247.

59. Cox, A. and Dalrymple, G. B., Statistical Analysis of Geomagnetic Reversal Data and the Precision of K-Ar Dating. J. Geophys. Res., Vol. 72, pp. 2603-2621, (1967).

60. Ozima, M., Kono, M., Kaneoka, I., Kinoshita, H., Kobuyashi, K., Nagata, T., Larson, E. E. and Strongway, D.: Paleomagnetism and K-Ar ages of Some Volcanic Rocks from the Rio Grande Gorge, New Mexico, J. Geophys. Res., Vol. 72, pp. 2615-2621, (1967).

61. Sykes, L., Mechanism of Earthquakes and Nature of Faulting on Mid-Oceanic Ridges. J. Geophys. Res., Vol. 72, p. 2131-

62. Hodgson, John, Nature of Faulting in large Earthquakes—Bulletin of the Geological Society of America, Vol. 68, pp. 611-644.

63. Hales, A. L., Doyle, H. A., P. and S Travel time Anomalies and their interpretation, Geophys. J. R. Astr. Soc., Vol. 13, pp. 403-415.

64. Pollack, H. H., Tectonic Implication of a Thermal Contrast between Continents and Oceans. J. Geophys. Res., Vol. 72, p. 5043.

65. Anderson, D. L., Phase Changes in the Upper Mantle. Science—September 8, 1967, pp. 1171.

66. Harris, P. G., Reay, A. and White, I., Chemical Composition of the upper Mantle. J. Geophys. Res., Vol. 72, pp. 6359.

67. Caner, B., Cannon, W. H., Livingstone, C. E., Geomagnetic Depth Sounding and Upper Mantle Structure in the Cordilleree Region of Western North America, J. Geophys. Res., Vol. 72, pp. 6335.

68. Ergin, Kazim, Seismic Evidence for a New Layered Structure of the Earth's Core. J. Geophys. Res., Vol. 72, pp. 3669.

69. Sacks, I., Diffracted P-wave, Studies of the Earth's Core. J. Geophys. Res., Vol. 72, pp. 2589-2594.

70. Aronson, J. R., Eckroad, S. W., Ernslie, A. G., Radiative Thermal Conductivity in Planetary interiors. Nature, Vol. 216, pp. 1096-1097.

71. Bullen, K. E. and Haddon, R. A., Earth Models based on Compressibility Theory. Phys. Earth Planet Interiors, Vol. 1, pp. 1-13.

72. Milwitzky, B., and Dwornik, S. E., Introduction, Chap. 2 in Surveyor III, A Preliminary Report, NASA SP-146, June, 1967.

73. Shoemaker, E. M., R. M. Batson, H. E. Holt, E. C. Morris, J. J. Rennilson, and E. A. Whitaker, Chap. 3 in Surveyor III, A Preliminary Report, NASA SP-146, June 1967.

74. Scott, R. R., E. I. Roberson, and M. C. Clary, Chap. 4 in Surveyor III, A Preliminary Report, NASA SP-146, June 1967.

75. Jaffe, L. D., S. A. Batterson, W. E. Brown, Jr., E. M. Christensen, S. E. Dwornik, D. E. Gault, J. W. Lucas, R. H. Norton, R. F. Scott, E. M. Shoemaker, G. H. Sutton, and A. L. Turkevich, Chap. 1 in Surveyor V, A Preliminary Report, NASA SP-163, Dec. 1967.

76. Christensen, E. M., S. A. Batterson, H. E. Benson, R. Choate, R. E. Hutton, L. D. Jaffe, R. H. Jones, H. Y. Ko, F. N. Schmidt, R. F. Scott, R. L. Spencer, and G. H. Sutton, Chap. 4 in Surveyor V, A Preliminary Report, NASA SP-163, Dec. 1967.

77. de Wys, J. Negus, Chap. 8, in Surveyor V, A Preliminary Report, NASA SP-163, Dec. 1967.

78. Walter, L. S., and P. D. Lowman, Jr., Planetology, in Significant Achievements in Space Science, 1966, NASA SP-155, 1967.

79. Turkevich, A. L., E. J. Franzgrote, and J. H. Patterson, Chemical analysis of the moon at the Surveyor V landing site, Science, Vol. 158, No. 3801, pp. 635-637, 3 November 1967.

80. Duke, M. B., and Silver, L. T., Petrology of eucrites, howardites, and mesodiderites, Geochimica et Cosmochimic Acta, Vol. 31, pp. 1637-1665, (1967).

81. MacDonald, G. J. F., Interior of the moon, Science, Vol. 133, No. 3458, pp. 1045-1050, 7 April 1961.

82. Michael, W. H., Tolson, R. H., and Gapcynski, V. P., Lunar Orbiter: Tracking Data Indicate Properties of the Moon's Gravitational Field, Science, Vol. 153, pp. 1102-1103, 1966.

83. O'Keefe, J. A., and Cameron, W. S., Evidence From the Moon's Surface for the Production of Lunar Granites. Icarus, Vol. 1, No. 3, pp. 271-284, 1962.

84. Kaula, W., The geometric and dynamical figures of the moon, Paper presented at the American Astronautical Symposium, (Washington, D.C.), Dec. 29, 1966, Am. Astronautical Society preprint 66-189.

85. Baldwin, R. B., The Measure of the Moon, U. of Chicago Press, Chicago, 1963.

86. Corliss, W. R. Scientific Satellites, NASA SP-133, 1967.

87. McCauley, J. F., The nature of the lunar surface as determined by systematic geologic mapping, Chap. 8 in Mantles of the Earth and Terrestrial Planets, Ed. by S. K. Runcorn, Interscience Publishers, New York, 1967.

88. Shoemaker, E. M., Chap. 4 in Ranger VII, Part II, Experimenters' Analyses and Interpretation, Heacock, R. L., G. P. Kuiper, E. M. Shoemaker, H. C. Urey, and E. A. Whitaker, Technical Report No. 38-700.

89. Lebedinsky, A. I., V. A. Krasnopolsky, and A. A. Krysko, The spectrophotometric measurements of the moon in the 1900-2750 A range from the Zond 3 automatic spare probe, pp. 59-64 in Moon and Planets, etc., Dollfuss.

90. Lebedinsky, A. I., G. M. Aleshin, V. A. Iozenas, V. A. Krasnopolsky, A. S. Selivanov, and V. V. Zasetsky, The lunar ultraviolet spectrum in the range of 2850-3550A according to the data obtained from the Zond 3 automatic space probe, in Moon and Planets, etc., Dollfuss.

91. Ness, N. F., K. W. Behannon, C. S. Scearce, and S. C. Cantarano, Early results from the magnetic field experiment on Lunar Explorer 35, J. Geophys. Res., Vol. 72, No. 23, pp. 5769-5778, 1 Dec. 1967.

92. Gold, T., The magnetosphere of the moon, in the Solar Wind, ed. by R. J. Mackin, Jr., and N. Neugebauer, pp. 381-392, Pergamon Press, New York, 1966.

93. Dolginov, Sh. Sh., Ye. G. Yeroshenko, L. N. Zhuzgov, and I. A. Zhulin, Possible interpretation of the results of measurements in the near lunar satellite AMS Luna 10, Geomagnetizm i Aeronomiya, 7, 436-441, 1967. (Russian)

94. Schmitt, H. H., N. J. Trask, and E. M. Shoemaker, Geologic Map of the Copernicus Quadrangle of the Moon, Map I-515 (LAC-58). U. S. Geological Survey, Washington, D. C., 1967.

95. McCauley, J. F., Geologic Map of the Helvelius Region of the Moon, Map I-491 (LAC-56), U. S. Geological Survey, Washington, D. C.

96. McCauley, J. F., Geologic results from the lunar precursor probes, AIAA Paper No. 67-862, presented at the AIAA 4th Annual Meeting, Anaheim, California, October 23-27, 1967. (8 pages)

97. Moore, H. J., Geologic Map of the Seleucus Quadrangle of the Moon, Map I-527 (LAC-38), U. S. Geological Survey, Washington, D. C., 1967.

98. Moore, H. J., Geologic Map of the Aristarchus Region of the Moon, Map I-465 (LAC-39), U. S. Geological Survey, Washington, D. C., 1965.

99. Titley, S. R., Geologic Map of the Mare Humorum Region of the Moon, Map I-495 (LAC-93), U. S. Geological Survey, Washington, D. C., 1967.

100. Trask, N. J., and S. R. Tiley, Geologic Map of the Moon, Map I-485, (LAC-94), U. S. Geological Survey, Washington, D. C., 1966.

101. Evsyukov, N. N., Color contrasts on the lunar surface, in Soviet Astronomy - AJ - Vol. 10, No. 5, 840-843, March-April, 1967.

102. Rackham, T. W., Color on the moon, Icarus, Vol. 7, No. 3, pp. 297-309, Nov. 1967.

103. McCord, T. B., Observational study of lunar visible emission, J. Geophys. Res., Vol. 72, No. 8, pp. 2087-2097, 15 April 1967.

104. Cameron, W. S., Observations of changes on the moon, paper presented at the Fifth Annual Meeting, Working Group on Extraterrestrial Resources, March 1, 2, & 3, 1967, Marshall Space Flight Center. Huntsville, Alabama, pp. 47-56 in proceedings, published by National Aeronautics & Space Administration.

105. Bartlett, J. C., Jr., Aristarchus: the violet glare, The Strolling Astronomer, Vol. 20, No. 1-2, pp. 20-28, Jan-Feb. 1966.

106. Green, J., Tidal and gravity effects intensifying lunar defluidization and volcanism, An. N.Y. Academy Sciences, Vol. 123, Art. 2, pp. 403-469, July 15, 1965.

107. Speiser, T. W., Particle Trajectories in Model Current Sheets 2. Analytical and Numerical Applications to Auroras using a Geomagnetic Tail Model, NASA (GSFC) X-Document 641-65-451, Goddard Space Flight Center, Greenbelt, Maryland, 1965.

108. Cameron, W. S., and Gilheany, J. J., Operation Moon Blink and report of observations of lunar transient phenomena, Icarus, Vol. 7, No. 1, pp. 29-41, July, 1967.

109. Burley, J. M., and B. M. Middlehurst, Apparent Lunar Activity, Historical Review, Proc. Nat. Acad. Sci., U. S., Vol. 55, No. 5, May 1966, pp. 1007-1011.

110. Tamrazyan, G. P., Tide-forming forces and earthquakes, Icarus, Vol. 7, No. 1, pp. 59-65, July, 1967.

111. Middlehurst, B. M., and Moore, P. A., Lunar transient phenomena: topographical distribution, Science, Vol. 155, No. 3761, pp. 449-451, 27 January 1967.

112. Chapman, W. B., Tidal influences at the lunar crater Aristarchus, J. Geophys. Res., Vol. 72, No. 24, pp. 6293-6298, December 15, 1967.

113. Nash, D. B., Proton-irradiation darkening of rock powders: Contamination and temperature effects, and applications to solar-wind darkening of the moon, J. Geophys. Res., Vol. 72, No. 12, pp. 3089-3104, June 15, 1967.

114. Palm, A., Enhanced luminance of the moon, Icarus, Vol. 7, No. 2, pp. 188-192, September, 1967.

115. Lipskii, P. K., and M. M. Pospergelis, Some results of the total Stokes vector for details of the lunar surface, Soviet Astronomy - AJ, Vol. 11, No. 2, September-October, 1967, pp. 324-326.

116. Mills, G. A., Absolute coordinates of lunar features, Icarus, Vol. 7, No. 2, pp. 193-220, Sept., 1967.

117. Markov, M. N., and V. L. Khokhlova, The lunar surface absorption spectrum in the range of 0.8 to 13 microns, pp. 53-58 in Moon and Planets, A Session of the Seventh International Space Science Symposium, Vienna, 10-18, ed. by A. Dollfuss, North-Holland Publishing Company, Amsterdam, 1967.

118. Saari, J. M., and Shorthill, R. W., Isothermal and isophotic atlas of the moon; contours through a lunation, NASA Contractor Report CR-855, NASA, Washington, D. C., Sept. 1967.

119. Salisbury, J. W., and G. R. Hunt, Infrared images of Tycho on dark moon, Science, Vol. 155, No. 3766, pp. 1098-1100, March 3, 1967.

120. Wildey, R. L., B. C. Murray, and J. A. Westphal, Reconnaissance of infrared emission from the lunar nighttime surface, J. Geophys. Res., Vol. 72, No. 14, pp. 3743-3749, July 15, 1967.

121. Troitskii, V. S., V. D. Krotikov, and N. M. Tseitlin, Measurement of radio emission from the moon in the 30-60 cm band, Soviet Astronomy-AJ, Vol. 11, No. 2, pp. 327-328, Sept.-Oct. 1967.

122. Losovskii, B. Ya., Observations of polarization of lunar radio emission at 0.8 cm with high resolution Soviet Astronomy-AJ, Vol. 11, No. 2, pp. 329-331, Sept.-October, 1967.

123. Eshelman, V. R., Radar Astronomy, Science, Vol. 158, No. 3801, pp. 585-597, 3 Nov. 67.

124. Tyler, G. L., V. R. Eshelman, G. Fjeldbo, H. T. Howard, and A. M. Peterson, Bistatic-Radar detection of lunar scattering centers with Lunar Orbiter I, Science, Vol. 157, No. 3785, pp. 193-195, 14 July 1967.

125. Cook, J. J., A survey of lunar geology, Earth Resources Survey Program Technical Letter NASA-95, Manned Spacecraft Center, Houston, Texas, November, 1967.

126. Lowman, P. D., Jr., Lunar Impact Craters, in The Encyclopedia of Atmospheric Sciences and Astrogeology, Encyclopedia of Earth Sciences Series, V. II, Ed. by R. W. Fairbridge, Reinhold Publishing Co., New York, 1967; Origin of the Moon, ibid.

127. Trask, N.J., and L. C. Rowan, Lunar Orbiter photographs: Some fundamental observations, Science, Vol. 158, No. 3808, pp. 1529-1535, 22 Dec. 1967.

128. Oberbeck, V. R., and W. L. Quaide, Estimated thickness of a fragmental surface layer on Oceanus Procellarum, J. Geophys. Res., Vol. 72, No. 18, pp. 4697-4704, Sept. 15, 1967.

129. O'Keefe, J. A., P. D. Lowman, Jr., and W. S. Cameron, Lunar ring dikes from Lunar Orbiter I, Science, Vol. 155, No. 3758, pp. 77-79, 6 January, 1967.

130. Fielder, G., Volcanic rings on the moon, Nature, Vol. 213, No. 5074, pp. 333-336, 28 January, 1967.

131. Goles, G., and S. R. Taylor, Properties of lunar surface rocks, Science, pp. 1134-1135, Vol. 156, No. May 26, 1967.

132. Milton, D. J., Slopes on the moon, Science, Vol. 156, No. , p. 1135, May 26, 1967.

133. Hartmann, W. K., Slopes on the moon, Science, Vol. 156, No. , p. 1134, May 26, 1967.

134. Marshall, C. H., Geologic map and sections of the Letronne region of the moon, Map I-385 (LAC-75) U. S. Geological Survey, Washington, D. C., 1963.

135. Fulmer, C. V., and Roberts, W. A., Surface lineaments displayed on Lunar Orbiter pictures, Icarus, Vol. 7, No. 3, pp. 394-406, Nov., 1967.

136. Rackham, T. W., Lunar Orbiter photography, Icarus, Vol. 7, No. 2, pp. 263-267, September, 1967.

137. Green, J., Calderas as related to lunar exploration, U. S. Bureau of Mines Contract P. O. Minn. 788-67, Advanced Research Laboratories, McDonnell Douglas Corporation, Huntington Beach, California, 20 April 1967.

138. Hapke, B., Surveyor I and Luna IX pictures and the lunar soil, Icarus, Vol. 6, No. 2, pp. 354-269, 1967.

139. Jaffe, L. D., Surface structure and mechanical properties of the lunar maria, J. Geophys. Res., Vol. 72, No. 6, pp. 1727-1731, March 15, 1967.

140. Filice, A. L., Lunar surface strength estimate from Orbiter II photograph, Science, Vol. 156, No. 3781, pp. 1486, 16 June 1967.

141. Salisbury, J. W., and Adler, J.E.M., Density of the lunar soil, Nature, Vol. 214, No. 5084, pp. 156-158, April 8, 1967.

142. Smith, B. G., Boulder distribution analysis of the Luna 9 photographs, J. Geophys. Res., Vol. 72, No. 4, pp. 1398-1399, 15 February 1967.

143. O'Keefe, J. A., and R. F. Scott, Chondritic meteorites and the lunar surface, Science. Vol. 158, No. 3805, pp. 1174-1176, 1 December 1967.

144. Adams, J. B., Lunar surface composition and particle size: Implications from laboratory and lunar spectral reflectance data, J. Geophys. Res., Vol. 72, No. 22, pp. 5717-5720, Nov. 15, 1967.

145. Adams, J. B., and A. L. Filice, Spectral reflectance 0.4 to 2.0 microns of silicate rock powders (sic-PDL), J. Geophys. Res., Vol. 72, No. 22, pp. 5705-5714, Nov. 15, 1967.

146. Filice, A. L., Observations on the lunar surface disturbed by the footpads of Surveyor I, J. Geophys. Res., Vol. 72, No. 22, pp. 5721-5728, Nov. 15, 1967.

147. Hartmann, W. K., Lunar Crater Counts. I. Alphonsus, Communications of the Lunar & Planetary Laboratory, University of Arizona, Tucson, Arizona, No. 80, pp. 31-38, March 20, 1967.

148. Hartmann, W. K., Lunar Crater Counts. II: Three lunar surface type-areas, ibid, No. 81, April 5, 1967, pp. 39-41.

149. Hartmann, W. K., Secondary volcanic impact craters at Kapoho, Hawaii, and comparisons with the lunar surface, Icarus, Vol. 7, No. 1, pp. 66-75, July, 1967.

150. Nash, Douglas B., Proton Irradiation Darkening of Rock Powders: Contamination and Temperature Effects, and Applications to Solar Wind Darkening of the Moon, J. Geophys. Res., Vol. 72, No. 12, pp. 3089-3104, 1967.

151. KenKnight, C. E., D. L. Rosenberg, and G. K. Wehner, Parameters of the optical properties of the lunar surface powder in relation to solar-wind bombardment, J. Geophys. Research, Vol. 72, No. 12, pp. 3105-3129, June 15, 1967.

152. Greer, R. T., and B. W. Hapke, Electron microprobe analyses of powders darkened by simulated solar-wind irradiation, J. Geophys. Res., Vol. 72, No. 12, pp. 3131-3133, June 15, 1967.

153. Zeller, E. J., and L. B. Ronca, Space weathering of lunar and asteroidal surfaces, Icarus, Vol. 7, No. 3, pp. 372-379, November, 1967.

154. Greenman, N. N., V. W. Burkig, and J. F. Young, Ultraviolet reflectance measurements of possible lunar silicates, J. Geophys. Res., Vol. 72, No. 4, pp. 1355-1359, Feb. 15, 1967.

155. Egan, W. G., Polarimetric measurements of simulated lunar surfaces, J. Geophys. Res., Vol. 72, No. 12, pp. 3233-3245, June 15, 1967.

156. Fricker, P. E., R. T. Reynolds, and A. L. Summers, On the thermal history of the moon, J. Geophys. Res., Vol. 72, No. 10, pp. 2649- , 15 May, 1967.

157. Miyamoto, S., Lunar and Martian crusts and mantle convection, Icarus, Vol. 6, No. 1, pp. 50-55, Jan. 1967.

158. Iriyama, J., and Y. Shimazu, A note on the thermal history of the moon, Icarus, Vol. 6, No. 3, pp. 453-457, May, 1967.

159. Ornatskaya, O. I., and Ya. I. Al'ber, Thermal history of the moon, Soviet Astronomy-AJ, Vol. 11, No. 1, January-February, 1967, pp. 122-127.

160. Lowman, P. D., Jr., Origin of the Moon, ibid.

161. Fish, F. F., Jr., Angular momenta of the planets, Icarus, Vol. 7, No. 2, pp. 251-256, Sept. 1967.

162. Hartmann, W. K., and S. M. Larson, Angular momenta of planetary bodies, Icarus, Vol. 7, No. 2, pp. 257-260, Sept. 1967.

163. MacDonald, G.J.F., The internal constitutions of the inner planets and the moon, Space Sci. Rev., 2, pp. 473-557, 1963.

164. Ruskol, E. I., The tidal history and origin of the earth-moon system, Soviet Astronomy-AJ, Vol. 10, No. 4, pp. 659-665, Jan.-Feb., 1967.

165. Beals, C. S., Dence, M. R., & Cohen, A. J., Evidence for the Impact Origin of Lac Couture, Publ. Dominion Observatory, Vol. 31, No. 10, 1967.

166. Currie, K. L. & M. Shafiqulla, Carbonatite and Alkaline Igneous Rocks in the Brent Crater, Ontario, Nature, (Lond.), Vol. 215, pp. 725-726, 1967.

167. Short, N. M., The anatomy of a Meteorite Impact Crater - West Hawk Lake, Manitoba, Canada, abst., 30th Ann. Mtg. of the Meteoritical Society, 1967.

168. Larochelle, A. & Currie, K. L., Paleomagnetic Study of Igneous Rocks from the Manicouagan Structure, Quebec, J. Geophys. Res., Vol. 72, No. 16, pp. 4163-4169, 1967.

169. French, B. M., Sudbury Structure, Ontario: Some Petrographic Evidence for Origin by Meteorite Impact, Science, Vol. 156, No. 3778, pp. 1094-1098, 1967.

170. Dietz, R. S., Sudbury Structure as an Astrobleme, J. of Geology, Vol. 72, No. 4, pp. 412-434, 1964.

171. Bray, J. G., & Staff, Shatter Cones at Sudbury, J. of Geology, Vol. 74, No. 2, pp. 243-245, 1966.

172. Robertson, P. B., The Malbaie Structure, Quebec—An Ancient Meteorite Impact Site, abst. 30th Ann. Mtg of the Meteoritical Society, 1967.

173. Roddy, D., in Part B, Crater Investigations, Astrogeologic Studies, Ann. Progress Rpt., U.S. Geol. Survey, July 1, 1966-Oct. 1, 1967, pp. 28-30, 1967.

174. Wilshire, H. G., Cummings, D., Offield, T. W., & Howard, K. A., Geology of the Sierra Madera Cryptoexplosion Structure, abst., Ann. Mtg., Geol. Society of America, New Oreleans, p. 239, 1967.

175. Seeger, C. R., The Jeptha Knob Structure, Kentucky, I. Subsurface Structure, abst., 48th Ann. Mtg., Amer. Geophys. Union, Trans. A.G.U., Vol. 48, No. 1, p. 147, 1967.

176. Seeger, C. R., The Jeptha Knob Structure, II. Rock Deformation, abst., 30th Ann. Mtg., of the Meteoritical Society, 1967.

177. Seeger, C. R., The Jeptha Knob Structure, III. Origin, Ann. Mtg., Geol. Society of America, New Oreleans, p. 199, 1967.

178. Bull, C., Corbato, C. E., & Zahn, J. C., Gravity Survey of the Serpent Mound Area, Southern Ohio, The Ohio J. of Science, Vol. 67, No. 6, pp. 359-371, 1967.

179. Forstner, U., Petrographische Utersuchungen des Suevit aus den Bohrungen Deiningen und Wornitzostheim in Ries von Nordlingen, Contrib. Mineral. u. Petrol., Vol. 15, pp. 281-308, 1967.

180. Stoffler, D., Deformation und Umwandlung von Plagioklas Durch Stosswellen in den Gesteinen des Nordlinger Ries, Contrib. Mineral. u. Petrol., Vol. 16, pp. 51-83, 1967.

181. Engelhardt, W. v., Arndt, J., Stoffler, D., Muller, W. F., Jeziorkowski, H., & Gubser, R. A., Diaplektische Glaser in den Breccien des Ries von Nordlingen als Anzeichen fur Stosswellenmetamorphose, Contrib. Mineral. u. Petrol., Vol. 15, pp. 93-102, 1967.

182. Engelhardt, W. v., Chemical Composition of Ries Glass Bombs, Geochim, et. Cosmochim. Acta, Vol. 31, pp. 1677-1689, 1967.

183. Engelhardt, W. v., Bertsch, W., Stoffler, D., Groschopf, P., & Reiff, W., Anzeichen fur den meteoritischen Ursprung des Beckens von Steinheim, Die Naturwissenschaften, Vol. 8., pp. 198-199, 1967.

184. Johnson, G. G. & Vand, V., Application of a Fourier Data Smoothing Technique to the Meteoritic Crater Ries Kessel, J. Geophys. Res., Vol. 72, No. 6, pp. 1741-1750, 1967.

185. Kraut, F., Sur l' origin des clivages du quartz dans les breches "volcaniques" de la region de Rochechouart, C.R. Acad. Sci. Paris, 264, pp. 2609-2612, 1967.

186. Milton, D. & Brett, R., in Part B, Crater Investigations, Astrogeologic Studies, Ann. Progress Rpt., U.S. Geol. Survey, July 1, 1966-Oct. 1, 1967, pp. 31-35, 1967.

187. Dietz, R. S., Shatter Cone Orientation at Gosses Bluff Astrobleme, Nature, Vol. 216, No. 5120, pp. 1082-1084, 1967.

188. Taylor, S. R., Composition of Meteorite Impact Glass across the Henbury Strewnfield, Geochim. et Cosmochim. Acta, Vol. 31, pp. 961-968, 1967.

189. Bunch, T. E. & Cassidy, W. A., Petrographic & Electron Microprobe Study of the Monturaqui Impactite, abst. 30th Ann. Mtg. of the Meteoritical Society, 1967.

190. Short, N. M., Explosion Craters, in Encyclo. of Atmospheric Sciences & Astrogeology, (R. Fairbridge, editor), Reinhold Publ. Corp., N.Y., pp. 373-378, 1967.

191. Short, N. M., Astroblemes and Meteorite Craters, in Encyclo. of Atmospheric Sciences & Astrogeology, (R. Fairbridge, editor), Reinhold Publ. Corp. N.Y., pp. 40-43, 1967.

192. Short, N. M., Shock Processes in Geology, J. of Geological Education, Vol. 14, No. 4, pp. 149-166, 1966.

193. Chao, E.C.T., Shock Effects in Certain Rock-forming Minerals, Science, Vol. 156, No. 3772, pp. 192-202, 1967.

194. Chao, E.C.T., Impact Metamorphism, in Researches in Geochemistry (P. Abelson, editor), Vol. 2., J. Wiley & Sons, N.Y., pp. 204-233, 1967.

195. Barringer, R., World's Meteorite Craters, Meteoritics, Vol. 3, No. 3, pp. 151-158, 1967.

196. Diehl, C.H.H. & Jones, G.H.S., The Snowball Crater: I. General Background Information, II. Profile & Ejecta Pattern, Suffield Tech. Notes No. 187 & 188, 1967.

197. Hansen, S. M., A Nuclear Crater formed by a Gas-Erosion Mechanism, abst., 30th Ann. Mtg. of the Meteoritical Society, 1967.

198. Baeta, R. D. & Ashbee, K.H.G., Plastic Deformation & Fracture of Quartz at Atmospheric Pressure, Philosophical Mag., pp. 931-938, 1967.

199. Greenwood, W., Deformation Lamellae Parallel to (1013) & (0001) in Quartz of the Coeur d'Alene District, Idaho, Science, Vol. 158, pp. 1180, 1967.

200. Bunch, T. E., Dence, M. R., & Cohen, A. J., Natural Terrestrial Maskelynite, Amer. Mineralogist, Vol. 52, pp. 244-253, 1967.

201. Green, J., Moon - Lunar Volcanism, in Encyclo. of Atmospheric Sciences & Astrogeology, (R. Fairbridge, editor), Reinhold Publ. Corp., N.Y., pp. 651-658, 1967.

202. Green, J., Moon - Lunar Geology, in Encyclo. of Atmospheric Sciences & Astrogeology, (R. Fairbridge, editor), Reinhold Publ. Corp., N.Y., pp. 623-629, 1967.

203. Katterfeld, G. N., Types, Ages & Origins of Lunar Ring Structures - Statistical & Comparative Geological Approach, Icarus, Vol. 6, pp. 360-380, 1967.

204. Hartmann, W. K., Secondary Volcanic Impact Craters at Kapoho, Hawaii and Comparisons with the Lunar Surface, Icarus, Vol. 7, pp. 66-75, 1967.

205. Roddy, D., Minimum Energy of Formation of Ubehebe Crater, Death Valley, California, Ann. Mtg. Geol. Society of America, New Orleans, p. 187, 1967.

206. Ronca, L. B., Meteorite Impact & Volcanism, Icarus, Vol. 5, pp. 515-520, 1967.

207. Lowman, P. B., Moon - Lunar Impact Craters, in Encyclo. of Atmospheric Sciences & Astrogeology (R. Fairbridge, editor), Reinhold Publ. Corp., N.Y., pp. 629-633, 1967.

208. Trask, N. J., Distribution of Lunar Craters According to Morphology from Ranger VIII & IX Photographs, Icarus, Vol. 6, pp. 270-276, 1967.

209. Staff, in Part A, Lunar & Planetary Investigations, Astrogeologic Studies, Ann. Progress Rpt., U.S. Geol. Survey, July 1, 1966-Oct. 1, 1967, pp. 21-24, 1967.

210. Walker, E. H., Statistics of Impact Crater Accumulation on the Lunar Surface Exposed to a Distribution of Impacting Bodies, Icarus, Vol. 7, pp. 233-242, 1967.

211. Chapman, C. R. & Haefner, R., A Critique of Methods for Analysis of the Diameter-Frequency Relation for Craters with Special Application to the Moon, J. Geophys. Res., Vol. 72, No. 2, pp. 549-558, 1967.

212. Baldwin, R., Ranger VIII and Gravity Scaling of Lunar Craters, Science, Vol. 157, pp. 546-548, 1967.

213. Pike, R., Schroeter's Rule & the Modification of Lunar Crater Impact Morphology, J. Geophys. Res., Vol. 72, No. 8, pp. 2099-2106, 1967.

214. Scott, R. F., Viscous Flow of Craters, Icarus, Vol. 7, pp. 139-148, 1967.

215. Walker, E. H., The Structure of the Lunar Surface as Indicated by the Geometry of Impact Craters, Icarus, Vol. 7, pp. 183-187, 1967.

216. Overbeck, V. R. & Quaide, W. L., Estimated Thickness of a Fragmental Surface Layer of Oceanus Procellarum, J. Geophys. Res., Vol. 72, No. 18, pp. 4697-4704, 1967.

217. Lammerzahl, P., Rare-Gas Isotope Studies on Meteorites, Mantles of the Earth and Terrestrial Planets, ed. S. K. Runcorn, 1967.

218. Fisher, D. E., Cosmogenic Tritium Problem in Iron Meteorites, JGR, Vol. 72, pp. 1351-1354, 1967.

219. Hintenberger, H., Schultz, L., Wanke, H., Weber, H., Helium-und neonisotope in Eisenmeteoriten und der Tritium verlust in Hexaedriten, Zeitschrift fur Nuturforschung, 22a, pp. 780-787, 1967.

220. Schultz, L., Tritium Loss in Iron Meteorites, Earth & Planetary Science Letters, Vol. 2, pp. 87-89, 1967.

221. Krankowsky, D., Mueller, Isotopic Composition + Abundance of Li in Meteoritic Matter, G+CA, Vol. 31, pp. 1833-1842, 1967.

222. Burnett, J. H., Manuel, O. K., On the Origin of Noble Gas Anomalies in Canyon Diablo Graphite, Earth & Planetary Science Letters, 3, pp. 95-100, (1967).

223. Schultz, L., Hintenberger, H., Edelgasmessungen on Eisen meteoriten, Zeitschrift fur Naturforschung, 22a., pp. 773-779, (1967).

224. Munk, M., Spallation Ne, A, K, and Xe in an Iron Meteorite, Earth and Planetary Science Letters, 2, pp. 301-309, (1967).

225. Nyquist, L. E., Huneke, J. C., Signer, P., Spallogenic Rare Gases in the El Taco Meteorite, Earth & Planetary Science Letters 2, pp. 241-248, (1967).

226. Voshage, H., Bestrahlungsalter und Herkunft der Eisenmeteorite, pp. 477-506, (1967).

227. Voshage, H., Cosmic Ray Exposure Ages and Origin of Iron Meteorites, Radioactive Dating and Methods of Low-Level Counting, IAEA, pp. 281-295, (1967).

228. Comerford, M. F., Comparative Erosion Rates of Stone and Iron Meteorites under Small-particle Bombardment, G+Ca, pp. 1457, (1967).

229. Rancitelli, L., Fisher, D. E., Funkhouser, J., Schaeffer, O. A., Potassium: Argon Dating of Iron Meteorites, Science, 158, pp. 999-1000, 1967.

230. Rancitelli, L., Fisher, Problems in the K/Ar Dating of Iron Met., 30th Annual Meeting, Met. Soc.

231. Rancitelli, L. A., Fisher, D. E., K-Ar Ages of Iron Meteorites, "67 AGU Meeting, 48th Annual Meeting.

232. Bogard, D. D., Burnett, D. S., Eberhardt, P., Fanale, F., Wasserburg, G. J., K-Ar Ages and Rare Gas Contents of Silicate Inclusions in Iron Meteorites, '67 AGU Meeting, 48th.

233. Burnett, D. S., Wasserburg, G. J., ^{87}Rb-^{87}Sr Ages of Silicate Inclusions in Iron Meteorites, Earth and Planetary Science Letters, 2, pp. 397-408, (1967).

234. Kornblum, J. J., Neutron Produced Isotopes in Iron Meteorites, 30th Annual Meeting - Met. Soc. - Ames.

235. Tanner, J. T., Kohman, T. P., Determination of Hg and Bi in iron met. by Neutron Activation, 30th Annual Meeting - Met. Soc.

236. Rao, M. N., Osmium in 3 Iron Meteorites, JGR, Vol. 72, pp. 5758-5759, (1967).

237. Berkey, E. Fisher, D. E., The Abundance + Distribution of C1 in Iron Met. G+CA, Vol. 31, 1543-1558, (1967).

238. Goldberg, E., Uchiyama, A., Brown. Geochim et Cosmochim Acta, Vol. 2, pp. 1-25, (1951).

239. Lovering, J. F., Nichiporuk, W., Chodos, A., Brown, H. - Geochim et Cosmochim Acta, Vol. 11, pp. 263-278, (1957).

240. Cobb, J. C., A. Trace-Element Study of Iron Meteorites, JGR, Vol. 72, pp. 1329-1341, (1967).

241. Smales, A. A., Mapper, D., Fouche, K. F., The Distribution of Some Trace Elements in Fe Meteorites, as determined by neutron activation G+CA, pp. 673-720, (1967).

242. Wasson, J. T., The Chemical Classification of Iron Meteorites: I. A Study of Iron Meteorites with Low Conc. of Ga + Fe, G+CA, pp. 161-180, (1967).

243. Wasson, J. T., Kimberlin, J., The Chemical Classification of Iron Meteorities - II. Irons and Pallasites with Ge Conc. Bet. 8 and 100 ppm, G+CA, Vol. 31, pp. 2065-2093, (1967).

244. Goldstein, J. I., Distribution of Ge in the Metallic Phases of Some Iron Meteorites, JGR, Vol. 72, pp. 4687, (1967).

245. Wai, C. M., Wetherill, G. W., Ernest, W. G., Wasson, J. T., The Distribution of Trace Quantites of Ge bet. Fe, Silicate and Sulfide Phases, 30th Annual Meeting - Met. Soc.

246. Wasson, J. T., Differences of Composition Among Australian Iron Meteorites, Nature Vol. 216, pp. 880, (1967).

247. Wasson, J. T., Goldstein, J. I., The NiChilean Hexahedrites: Variations in Composition + Structure, 30th Annual Meeting - Met. Soc.

248. Wasson, J. T., Concentrations of Ni, Ga and Ge in a Series of Canyon Diablo + Odessa Meteorite Specimens, JGR, Vol. 72, pp. 721-730, (1967).

249. Moore, C. B., Birrell, P. J., Lewis, C. F., Variations in the Chemical and Mineralogical Comp. of Rim and Plains Specimens of the Canyon Diablo Meteorite, G+CA, Vol. 31, pp. 1885-1892, (1967).

250. Moore, C. B., Lewis, C. F., Gans, M., Total S Content of Iron Meteorites 30th Annual Meeting - Met. Soc.

251. Reed, S. J. B., Chemical and Mineralogical Evidence from Iron Meteorites on the Nature of the Parent Body, Mantles of the Earth and Terrestrial Planets, Ed. S. K. Runcorn Inter Science, 1967.

252. Olsen, E., Amphibole: First Occurrence in a Meteorite, Science 156, pp. 61-62, (1967).

253. Olsen, E., Fuchs, L. H., The State of Oxidation of Some Iron Meteorites, Icarus 6, 242-253, (1967).

254. Fuchs, L. H., Olsen, E., Henderson, E. P., On the Occurrence of Brionite and Panethite, 2 New Phosphate Minerals from the Dayton Meteorite. G+CA, Vol. 31, pp. 1711-1719, (1967).

255. El Goresy, Ahmed, Quantitative Electron Microprobe Analyses of Coexisting Sphalerite, Daubreelite and Troilite in the Odessa Iron Meteorite and Their Genetic Implications, G+CA, Vol. 31, pp. 1667-1676, (1967).

256. El Goresy, A., Quantitative Electron Microprobe Analyses of K-Feldspar Grains from the Odessa Iron Meteorite, 30th Annual Meeting - Met. Soc. - Ames.

257. Bence, A. E., Burnett, D. S., The Compositions of Silicate Inclusions in Iron Meteorites, 30th Annual Meeting Met. Soc. - Ames.

258. Mason, B., The Woodbine Meteorite, with Notes on Silicates in Iron Meteorites, Min. Mag., Vol. 36, pp. 120-126, (1967).

259. Brett, R., Henderson, E. P., The Occurrence and Origin of Lamellar Troilite in Iron Meteorites, pp. 721-731, G+CA, (1967).

260. Lipschutz, M. E., X ray Diffraction Analysis of Cohenite from Iron Meteorites, G+Ca, pp. 621-634, Vol. 31, (1967).

261. Marvin, U. B., Shocked Xtals of Ureyite and Sphalerite in the Canyon Diablo Iron Meteorite, '67 AGU Meeting, 48th.

262. Hanneman, R. E., Strong, H. M., Bundy, F. P., Hexagonal Diamonds in Meteorites: Implications, Science, Vol. 155, pp. 995-997, (1967).

263. Brett, R., Cohenite: Its Occurrence and a Proposed Origin, G+CA, pp. 143-160, (1967).

264. Brett, R., Higgins, G. T., Cliftonite in Meteorites: A Proposed Origin, Science, 156, pp. 819-820, (1967).

265. Axon, H. J., Rieche, R., The Goose Lake Meteorite and the Goose Lake Fragments, Nature, Vol. 215, pp. 379-380, (1967).

266. Buchwald, U. F., "Study of Six Iron Meteorites" - Analecta Geologica #2, Minerologist Museum Københaun, (1967).

267. Axon, H. J., Faulkner, D., Hot Working Effects in the Parent Alpha-Phase of Iron Meteorites, G+CA, Vol. 31, pp. 1539-1542, (1967).

268. Frost, M. J., Oriented Lamellae in the Gibeon Meteorite, Nature, pp. 607-613, (1967).

269. Duerr, J. S., Ogilvie, R. E., Martensitic Transformation Studies in Meteorites, 30th Annual Meeting - Met. Soc. Ames.

270. Goldstein, J. I., Scanning Electron Microscope Studies, of Plessite in Iron Met., 30th Annual Meeting - Met. Soc. - Ames.

271. Axon, H. J., Boustead, J., Kamacite-Taenite Relationships in Iron Meteorites, Nature, pp. 166-167, (1967).

272. Jaeger, R. R., Lipschutz, M. E., Pressure History of Some Iron Meteorites Nature, 1967, pp. 975-977.

273. Jaeger, R. R., Lipschutz, M. E., Implications of Shock Effects in Iron Meteorites, G+CA, Vol. 31, pp. 1811-1832, (1967).

274. Axon, H. J., Yardley, E. D., The distribution of Ni at Phase Interfaces in the Brenham County Pallasite, 30th Annual Meeting - Met. Soc. Ames.

275. Reed, S. J. B., The Distribution of P in the Mt. Edith Octahedrite, G+CA, Vol. 31, pp. 1969-1974, (1967).

276. Goldstein, J. I., Short, J. M., Cooling Rates of 27 Fe and Stony-Fe Meteorites, G+CA, pp. 1001-1024, (1967).

277. Short, J. M., Goldstein, J. I., Rapid Methods of Determining Cooling Rate of Iron and Stony Iron Meteorites, Science, Vol. 156, pp. 59-61, (1967).

278. Goldstein, J. I., Short, J. M., The Iron Meteorites, Their Thermal History and Parent Bodies. G+CA, Vol. 31, pp. 1733-1770, (1967).

279. Duke, M. B., Silver, L. T., Petrology of Eucrites, Howardites, and Mesosiderites, G+CA, Vol. 31, pp. 1637-1665, (1967).

280. Powell, B. N., Weibler, P. W., On the Petrology of Mesosiderites, 30th Annual Meeting - Met. Soc.

281. Fuchs, L. H., Stanfieldite: A New Phosphate Mineral from Stony-Iron Meteorites, Science, Vol. 158, pp. 910, (1967).

282. Buseck, P. R., Moore, C. B., Goldstein, J. I., Marburg - A New Pallasite G+CA, Vol. 31, pp. 1589-1593, (1967).

283. Buseck, P. R., Goldstein, J. I., Olivine Compositions and C. R. of Pallasitic Meteorites, Abstract AGU meeting 48th Annual Meeting.

284. Mason, B., The Bununo Meteorite, and a Discussion of the Pyroxene-plagioclose Achondrites, G+CA, Vol. 31, pp. 107-115, (1967).

285. Mason, B., Meteorites, Amer. Sci., Vol. 55, pp. 429, (1967).

286. Van Schmus, W. R. and Wood, J. A., A Chemical Petological Classification for the Chondrite Meteorites. Geochima et Cosmochim Acta - Vol. 31, 5, pp. 747-766, (1967).

287. Dundon, Robt. W. and Walter, L. S., Ferrous Ion Order-Disorder in Meteoritic Pyroxenes and the Metamorphic History of Chondrites, Earth and Planetary Science Letters 2 (1967) 372-376.

288. Van Schmus, W. R. and Koffman, D. M., Equilibration of Iron and Magnesium in Chondritic Meteorites - Science, Vol. 155, pp. 1009.

289. Dodd, R. T., Jr., W. R. Van Schmus and D. M. Koffman. "A Survey of Unequilibrated Ordinary Chondrites. Geochima et Cosmochima Acta, Vol. 31, pp. 921-951, (1967).

290. Wood, John A., Olivine and Pyrexen Composition in Type II Carbonaceous Chondrite. Geochima et Cosmochima Acta - Vol. 31, pp. 2095-2108, (1967).

291. Suess, Hans E., and Heinrich Wänke. "Metamorphosis and Equilibration in Chondrites. J. Geophys. Res. Vol. 72, No. 14, pp. 3609.

292. Wood, John A., Criticism of Paper by Suess & Wänke, "Metamorphosis and Equilibration in Meteorites. - J. Geophys. Res., Vol. 72, No. 24, pp. 63-79.

293. Otting, W. and J. Zahringer - Total Carbon Content and Primordial rare gases in Chondrites. Geochim. et Cosmochim. Acta, Vol. 31, pp. 1949-1960.

294. Heymann, D. and E. Mazor - Primordial rare gases in unequilibrated ordinary Chondrites. Science, Vol. 155, pp. 701.

295. Wood, J. A., 1967, "Chondrite: Their Metallic Minerals, Thermal Histories and Parent Bodies. Icarus, Vol. 6, pp. 1-49.

296. Binns, R. A., Structure and Evolution of Non-Carbonaceous Chondrite Meteorites. Earth and Planetary Science Letters, Vol. 2, pp. 23-28, (1967).

297. Bunch, T. E., Klaus Keel, and K. G. Snetsinger, Chromite Composition in Relation to Chemistry and Texture of Ordinary Chondrites. - Geochim. et Cosmochim Acta, Vol. 31, pp. 1569-1582.

298. Kurat, G., Zur Enstehung der Chondren, Geochim. et Cosmochim. Acta, Vol. 31, pp. 491-502.

299. Reid, A. M. and K. Fredriksson, "Chondrules and Chondrites. Research in Geochemistry", Vol. 2, John Wiley & Sons, New York, (1967).

300. Fredriksson, Kurt and Brian Mason, The Shaw Meteorite. Geochim. et Cosmochim.Acta, Vol. 31, pp. 1705-1709.

301. Van Schmus, W. R., - Polymect Structure of the Mezo-Maderas Chondrite. Geochim.et Cosmochim. Acta, Vol. 31, pp. 2027-2042.

302. Binns, R. A., "Farmington Meteorite: Cristobalite Xenoliths and Blockening - Science, Vol. 156, pp. 1222, (1967).

303. Buseck, Peter R., The Post - Formational History of Hypersthene Chondrite-Beenham. Geochim et Cosmochim Acta, Vol. 31, pp. 1583-1587.

304. Heymann, Dieter, On the Origin of Hypersthene Chondrites: Ages and shock effects of Black Chondrites. Icarus, Vol. 6, pp. 189-221, (1967).

305. Tanenbaum, Andrew S., Clustering of the Cosmic Ray ages of Stone Meteorites. Earth and Planetary Science Letters, Vol. 2, pp. 33-35, (1967).

306. Shima, M. and Honda, M.: Determination of Rb - Sr Age of Chondrites Using their Separated Components - Earth Planet - Sci. Letters. Vol. 2, pp. 337-343, (1967).

307. Bogard, D. P., Burnett, D. S., Eberhardt, P., and Wasserberg, G. J.: Rb^{87}-Sr^{87} J so chron and K-^{40}-Ar^{40} Ages of the Norton County Achondrite. Earth Planet, Sci. Letters, Vol. 3, pp. 178-189, (1967).

308. Burnett, D. S. and Wasserberg, G. J., Rb^{87}-Sr^{87} Ages of Silicate inclusions in Iron Meteorites - Earth Planet Sci. Letters, Vol. 2, pp. 397-409, (1967).

309. Hohenberg, L. M., F. A. Podosek and J. H. Reynolds. Xenon-iodine dating; Sharp isochronism in chondrites. Science, Vol. 156, pp. 223-236, (1967).

310. Morgan, J. W. and J. F. Lovering, Uranium and Thoruem abundances in Carbonaceous Chondrites. Nature, Vol. 213, pp. 873-875.

311. Tanner, J. T. and Ehmann, W. D.: The Abundance of Antimony in Meteorites, Tektites and Rocks by Neutron Activation Analysis. Geochim. et Cosmochim. Acta, Vol. 31, pp. 2007-2026.

312. Clark, R. S., Rowe, M. W., Ganapathy, R. G. and Kurada, P. K.: Iodine, Uranium and Tellurium Contents in Meteorites Geochim. et Cosmochim. Acta, Vol. 31, pp. 1605-1614, (1967).

313. Crockett, J. H, Keays, R. R. and Hsieh, S., Precious Metal Abundances in some Carbonaceous and enstatele Chondrites. Geochim. et Cosmochim. Acta, Vol. 31, pp. 1615-1624.

314. Gales, G. G., Greenland, L. P., Jerome, D. Y., Abundances of Chlorine, bromine, and iodine in Meteorites. Geochim. et Cosmochim. Acta, Vol. 31, pp. 1771-1778, (1967).

315. Krankowsky, D. and Miller, O.: Isotopic Composition and abundance of lithium in meteoritic matter. Geochim. et Cosmochim. Acta, Vol. 31, pp. 1831-1842.

316. Morgan, J. W. and Lovering, J. F.: Rhenium and Osminm abundances in chondrites meteorites. Geochim. et Cosmochim. Acta, Vol. 31, pp. 1893-1910.

317. Nichiporuk, W., Chodos, A., Helin, E., and Brown, H.: Determination of Fe, Ni, Co, Ca, Gr, and Mu, in stony Meteorites by X-Ray fluorescence - Geochim. et Cosmochim. Acta - Vol. 31, pp. 1911-1930.

318. Schmitt, R. A., Smith, R. H., Ehmann, W. D. and McKown, D., Silicon Abundances in Meteoritic Chondrules. Geochim. et Cosmochim. Acta, Vol. 31, pp. 1975-1986.

319. DeLaeter, J. R., and Jeffery, P. M, Tin: Its Isotopic and Elemental Abundance. Geochim. et Cosmochim. Acta, Vol. 31, pp. 969-985, (1967).

320. Greenland, L., The abundances of selanium, tellurium, silver palbadium, cadmium and zinc in chondrite meteorites; Geochim. et Cosmochim. Acta, Vol. 31, 5, pp. 849-860.

321. Mueller, Robert F. and Edward Olsen, The Olivine, pyronene and Metal Content of Chondritic Meteorites as a consequence of Prior's rule. Min. Mag., Vol. 36, No. 279, pp. 311-318, (1967).

322. Aherns, L. H., Notes on the fractionation of some of the abundant lithophib elements in chondrites with particular reference to LA and AL. Geochim. et Cosmochim. Acta, Vol. 31, pp. 861-868, (1967).

323. Larimer, John W., Chemical fractionation in Meteorites. I. Condensation of the Elements. Geochim. et Cosmochim. Acta, Vol. 31, pp. 1215-1238, (1967).

324. Larimer, John W. and Edward Anders, Chemical Fractionations in Meteorites. II. Abundance patterns and their interpretation. Geochim et Cosmochim Acta, Vol. 31, pp. 1239-1270, (1967).

325. Blander, M. and J. L. Katz, Condensation of Primordial Dust. Geochim. et Cosmochim.Acta, Vol. 31, pp. 1025-1034, (1967).

326. Urey, H. C., Parent Bodies of the Meteorities and the Origin of Chondrules Icarus, Vol. 7, pp. 350-359, (1967).

327. Glass, Bill, Microtektites in deep-sea sediments. Nature, Vol. 214, pp. 372-374, (1967).

328. Glass, Bill and Bruce Heezen, Tektites and Geomagnetic reversals. Nature, Vol. 214, p. 372, (1967).

329. Ninninger, H. H. and G. I. Huss, Tektites that were partially plastic after completion of surface sculpturing. Science, Vol. 157, pp. 61- , (1967).

330. Gentner, W., B. Kleinman and L. A. Wagner, New K-Ar and fission track ages of impact Glasses and tektites Earth Planet Sci. Letters, Vol. 2, pp. 83-86, (1967).

331. Kolbe, P., W. H. Pinson, Jr., John Saul and Elliott Miller. Rb-Sr study on country rocks of the Bosumtwi Crater. Geochim. et Cosmochim. Acta, Vol. 31, pp. 869-876.

332. Walter, L. S., Tektite compositional trends and Experimental Vapor fractionation of Silicate. Geochim. et Cosmochim. Acta. Vol. 31, pp. 2043-2063, (1967).

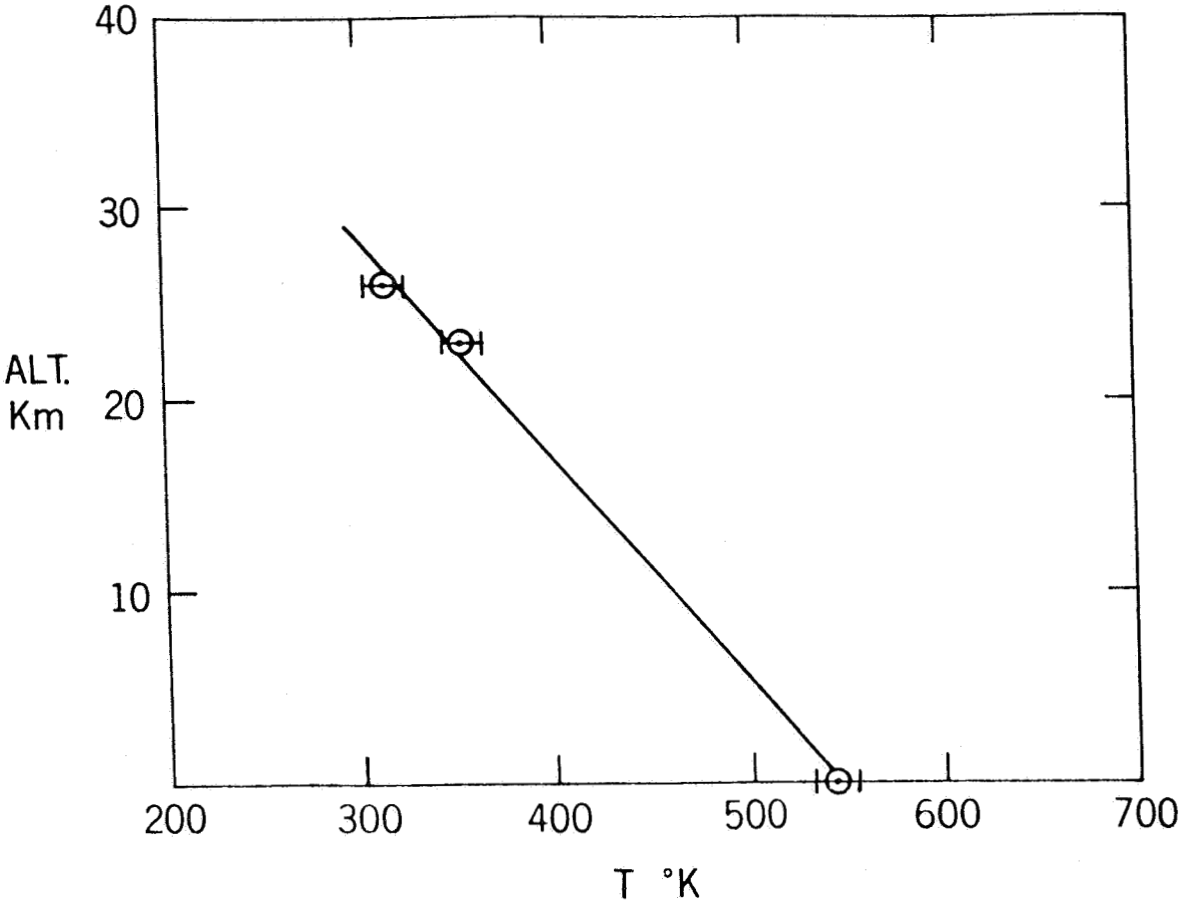

Figure 1–Temperature in the Venus atmosphere as a function of height above the surface.

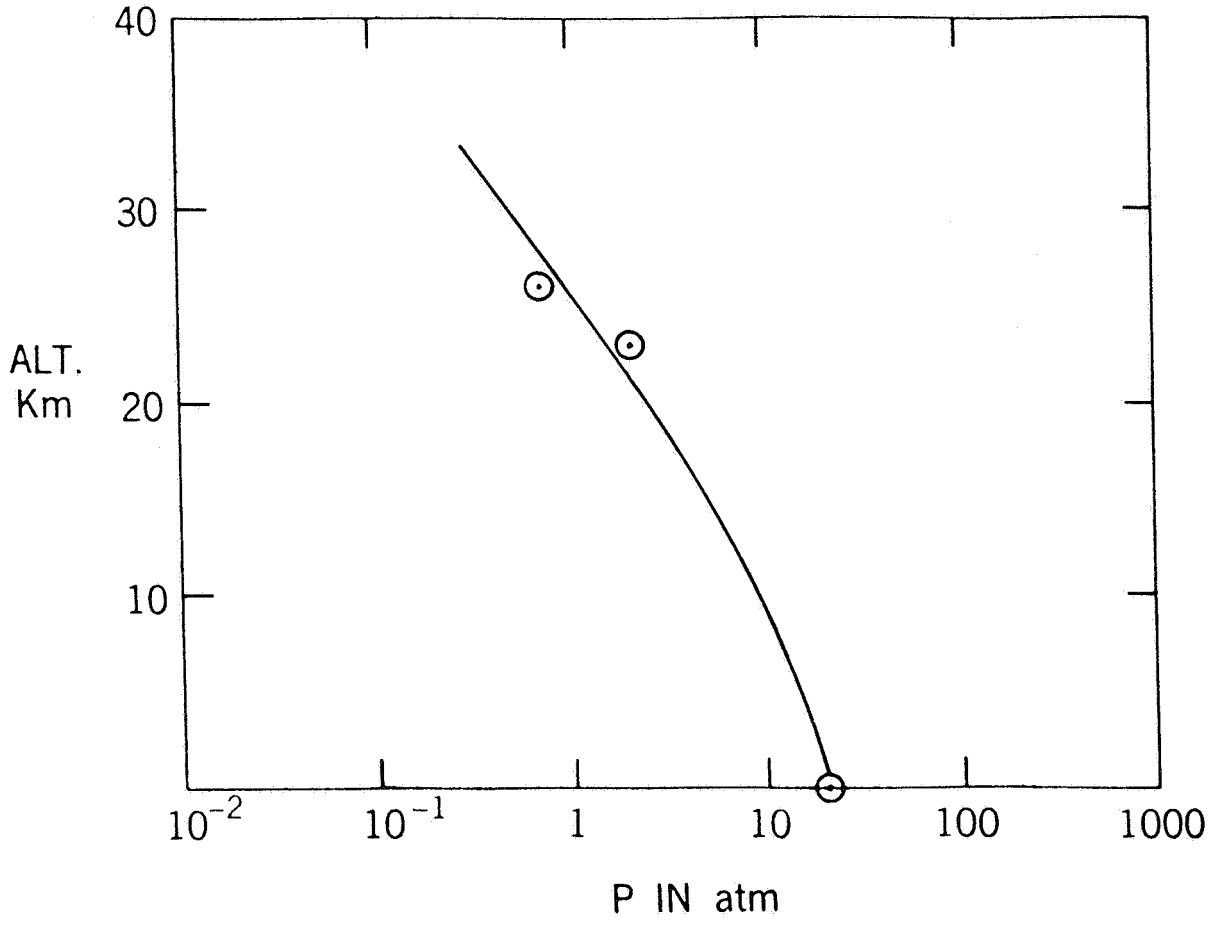

Figure 2–Pressure in the Venus atmosphere as a function of height above the surface.

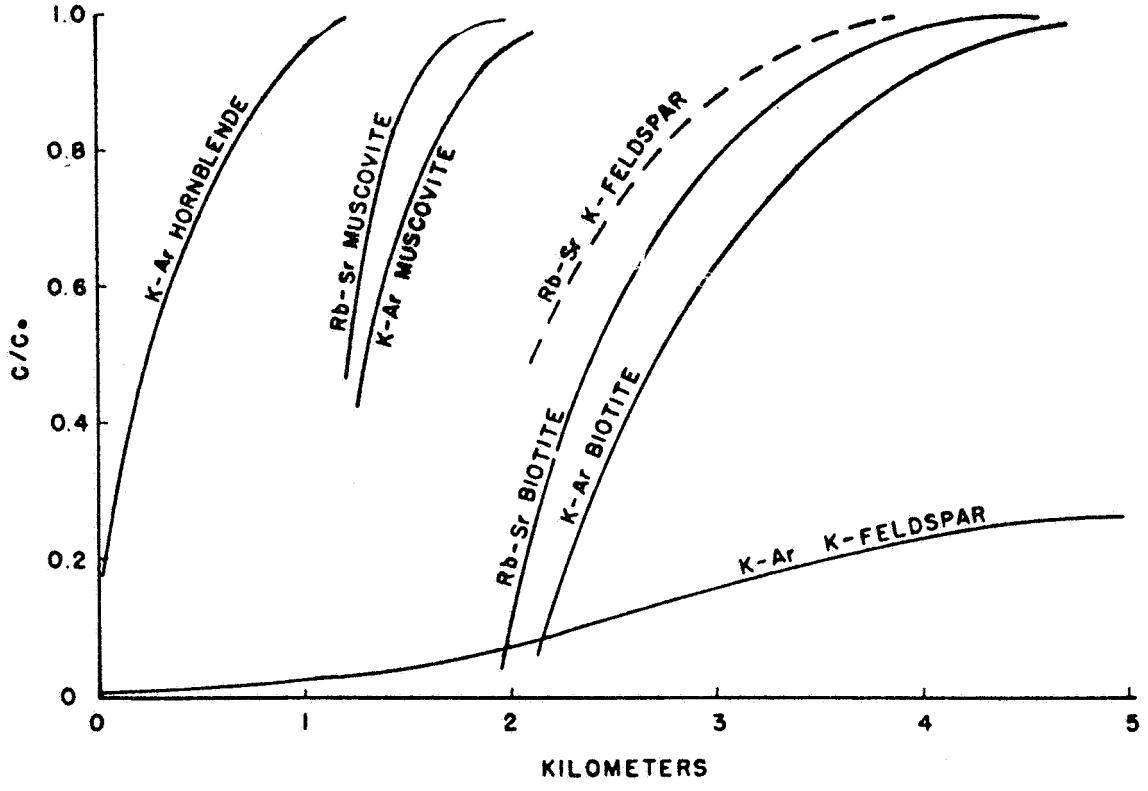

Figure 3–Generalized curves of C/C_o for Rb - Sr and K - Ar ages of biotite muscovite, and potassium feldspar and the K - Ar ages of Hornblende vs. map distance from the contact, Snowbank Lake. All curves have been drawn by visual best fit.

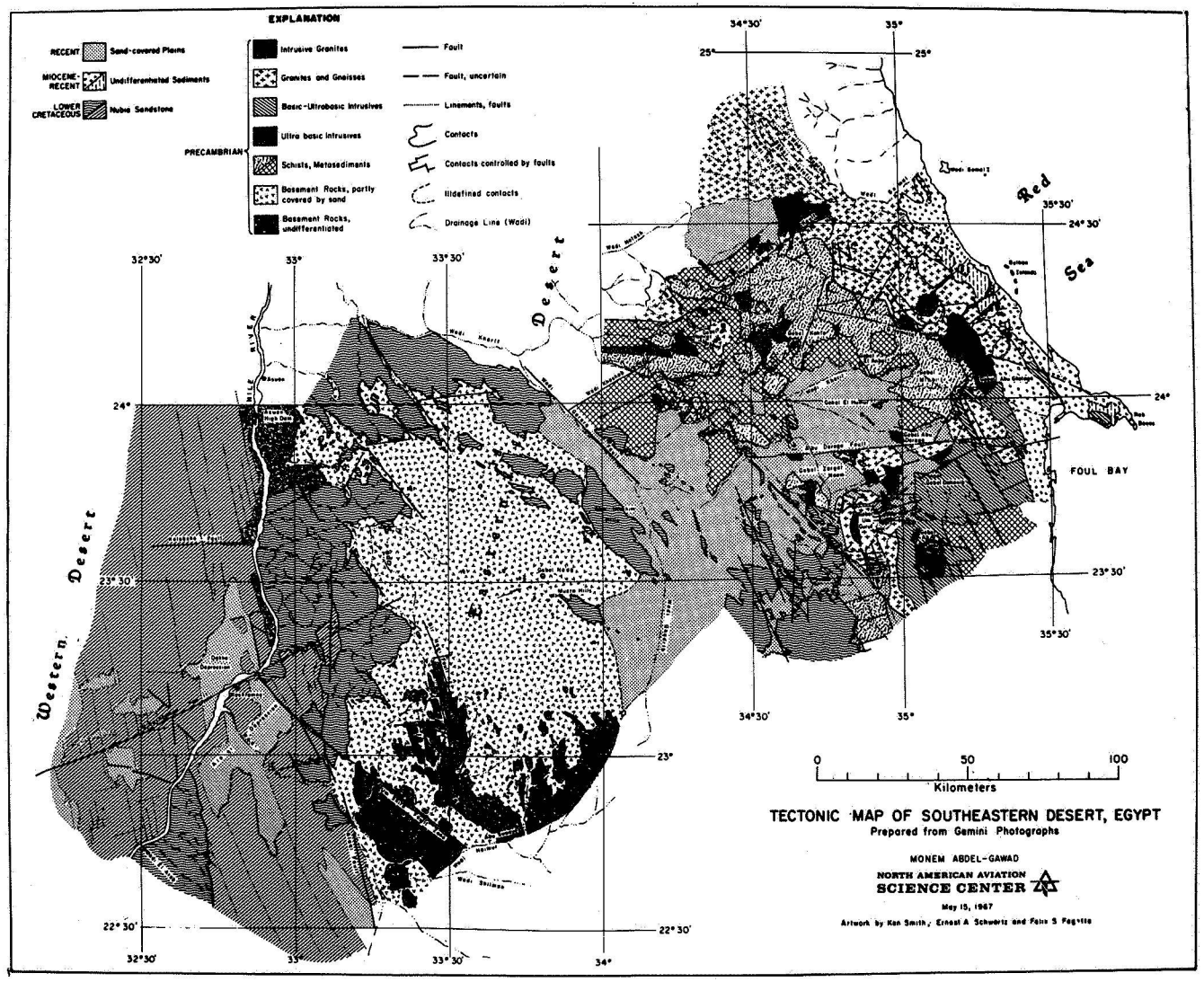

Figure 4–Tectonic Map of Southeastern Desert, Egypt. Prepared from Gemini Photograph.

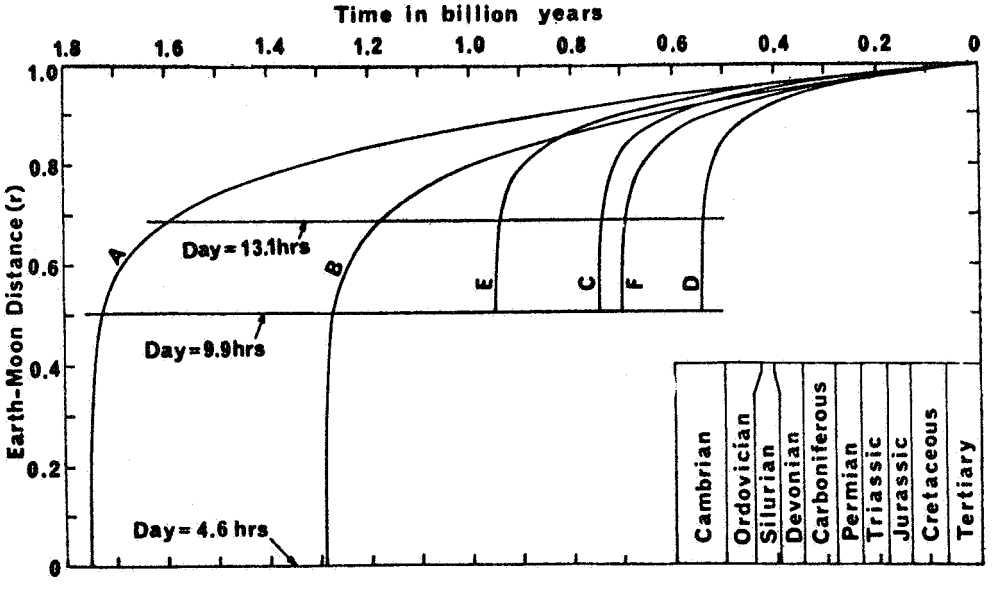

Figure 5–Variation of Earth-Moon distance during geologic time.

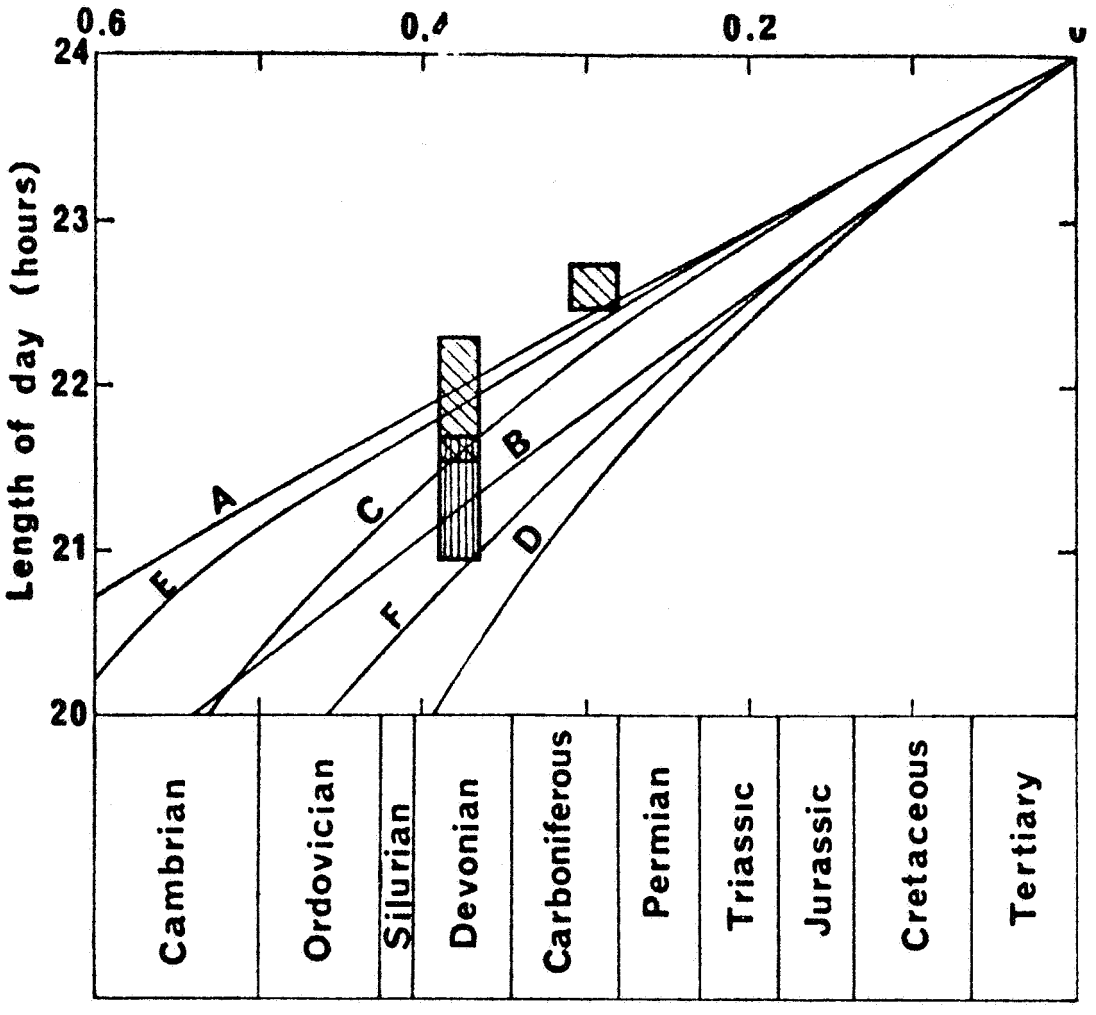

Figure 6–Variation in length of day showing Well's (diagonal lines) and Scrutton's (vertical lines) data on coral growth lines.

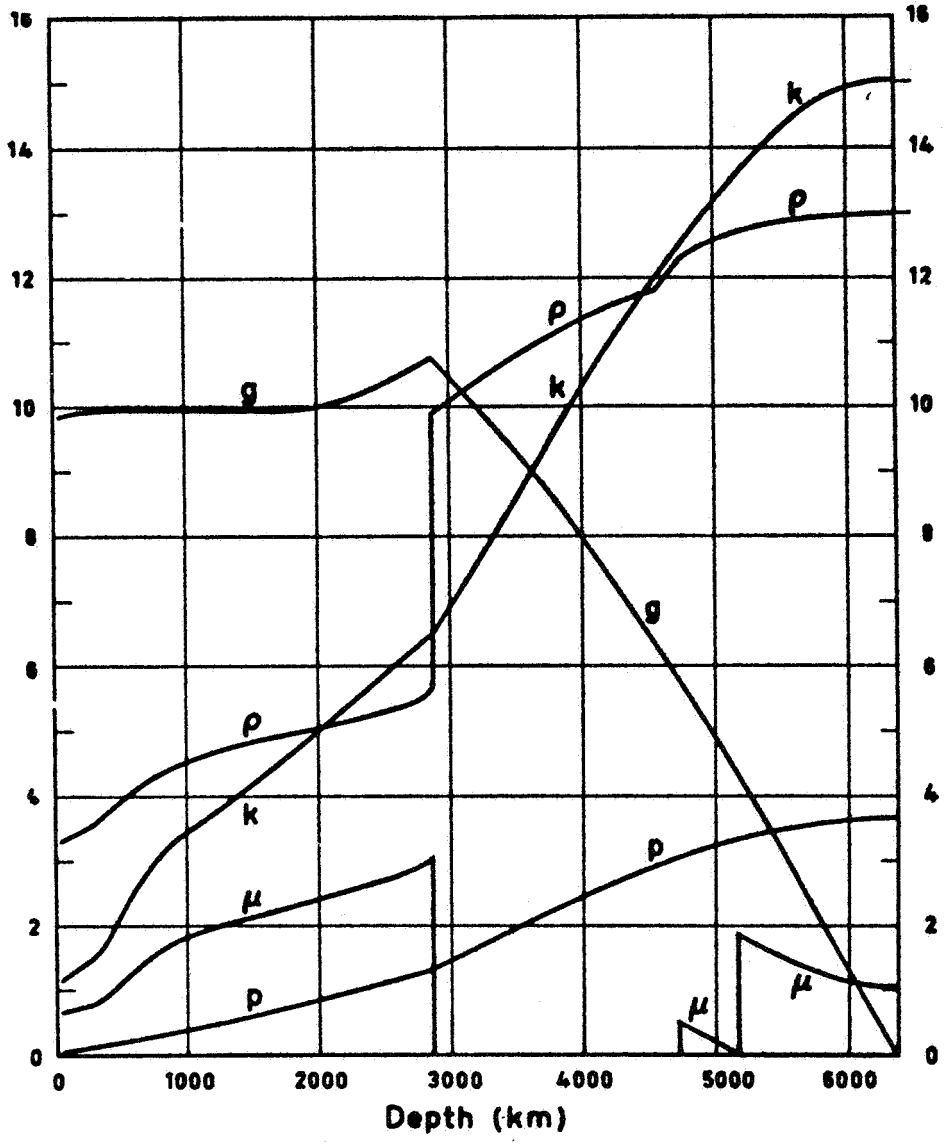

Figure 7–Variation of the pressure p, density ρ, incompressibility k, rigidity μ, and gravitational intensity g in the base Earth model B_1. (Units in vertical scale are as for Figure 8).

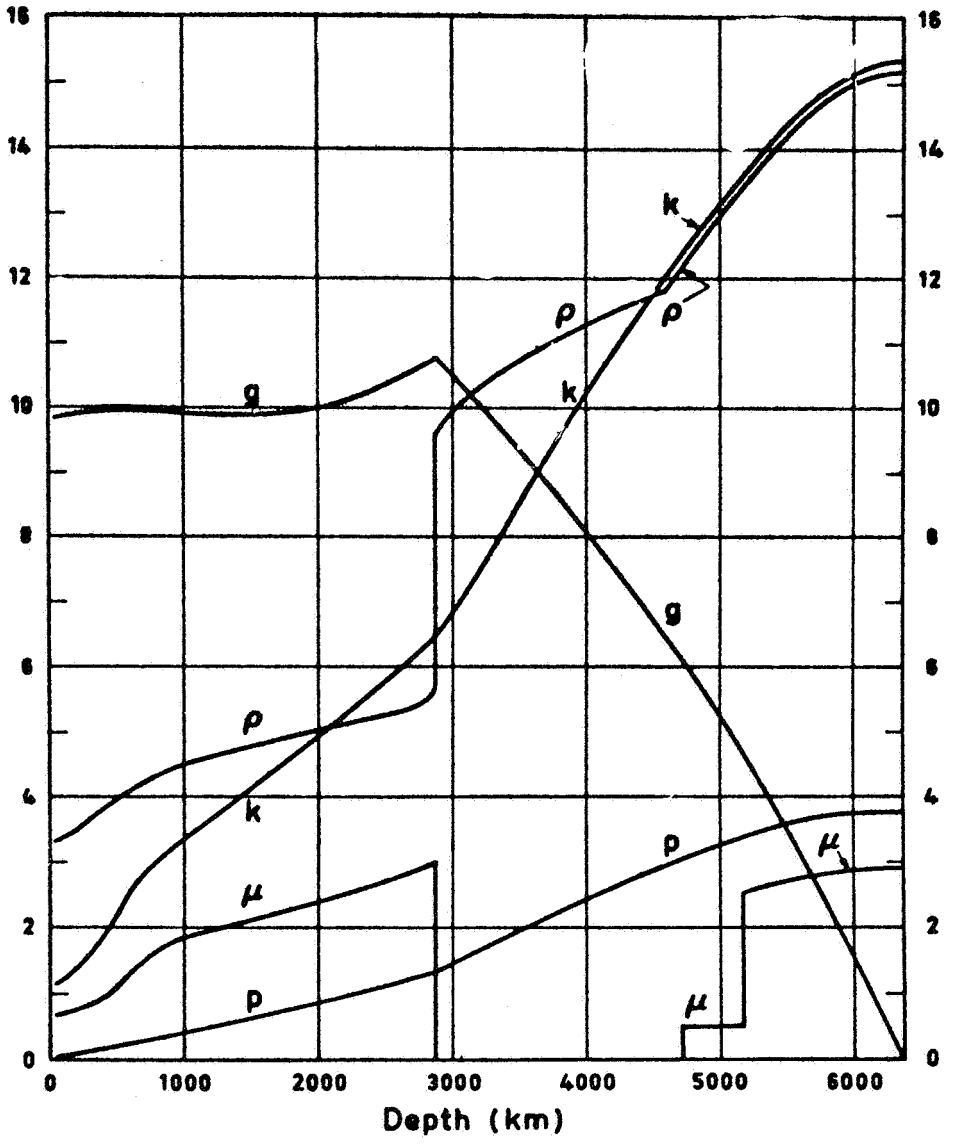

Figure 8–Variation of p, ρ, k, μ and g in the Earth model B_2. The units in the vertical scale are 10^{13} dyn/cm^2 for p, k and μ; g/cm^3 for ρ; and 100 cm/sec^2 for g.

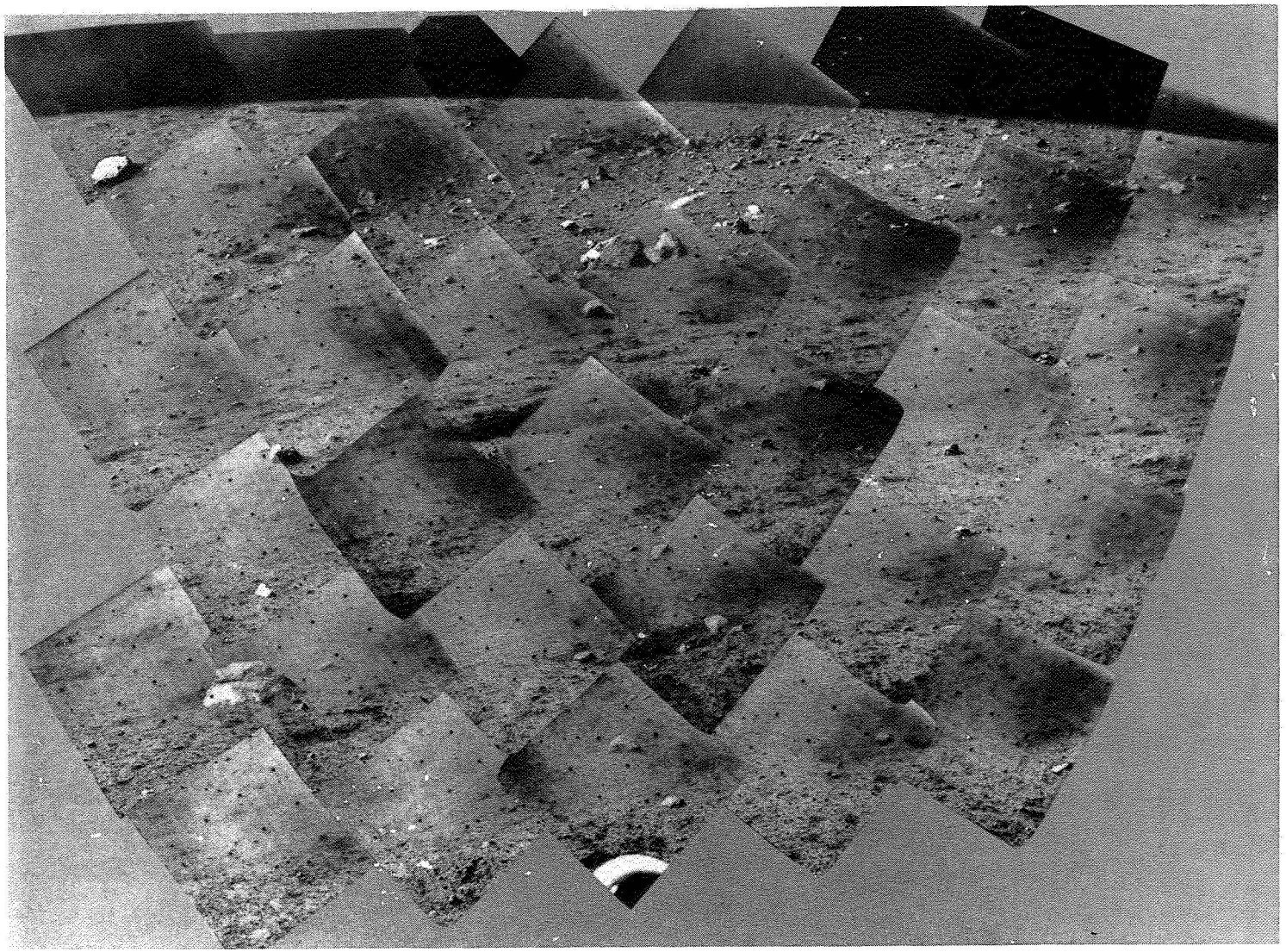

Figure 9–Mosaic of narrow-angle pictures taken by Surveyor III camera. View to north, showing mare terrain.

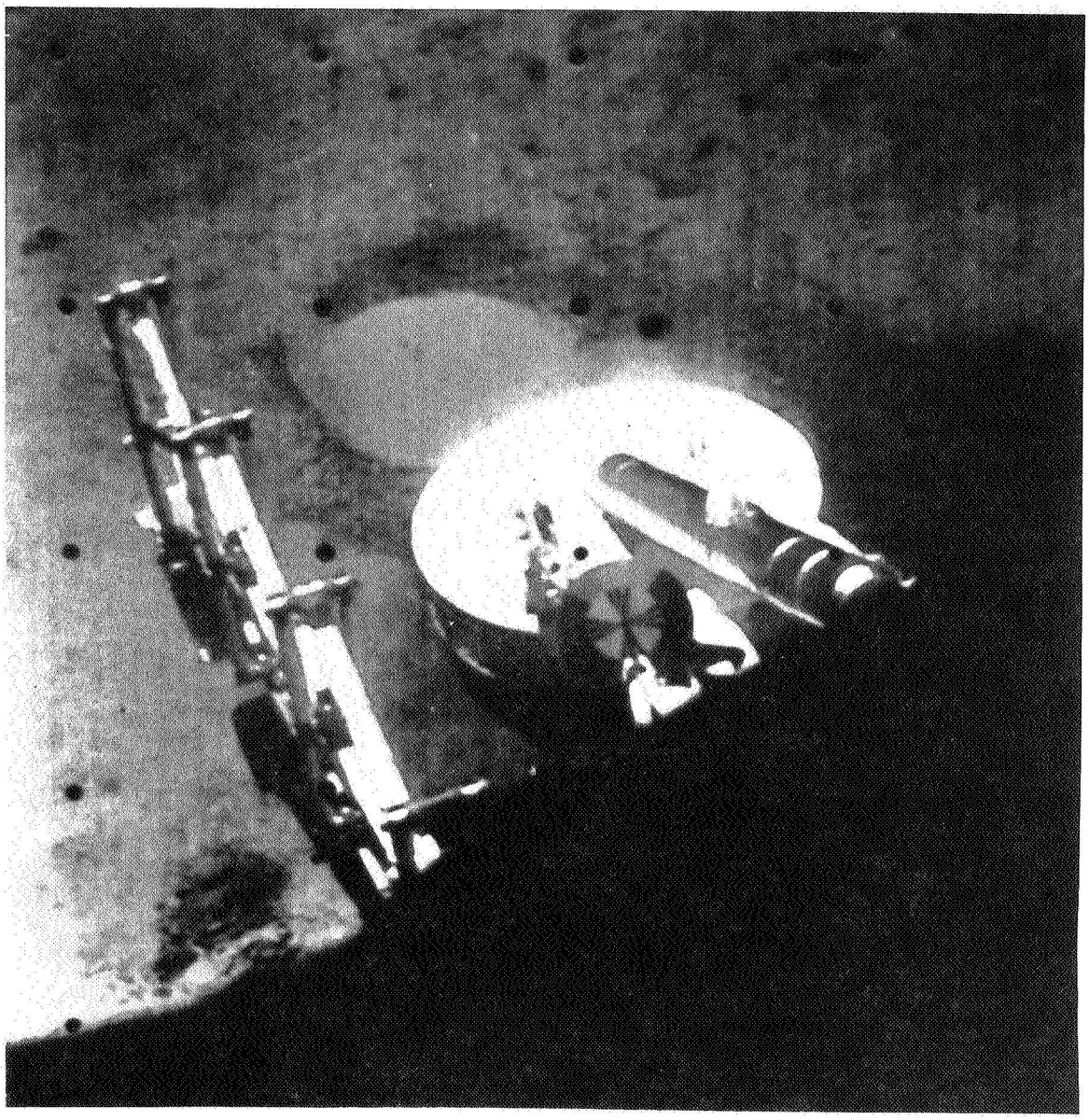

Figure 10—Close-up Surveyor III picture, showing footpad impression and dark material ejected footpad. Surface sampler at left has made impression at lower left.

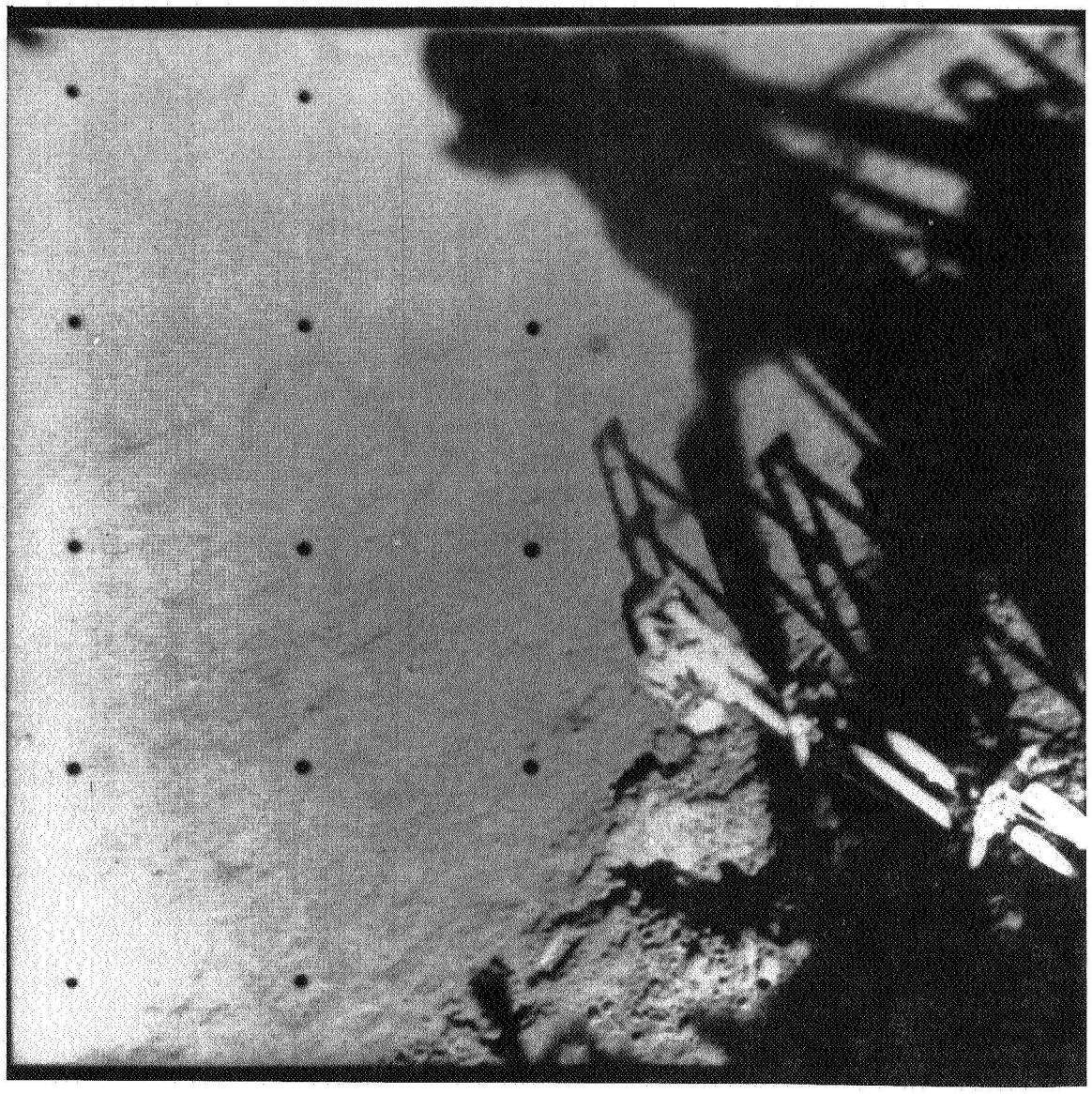

Figure 11–Surveyor III surface sampler embedded in lunar surface. Trench at lower bottom is about 2 inches wide, 10 inches long, and 5 inches deep.

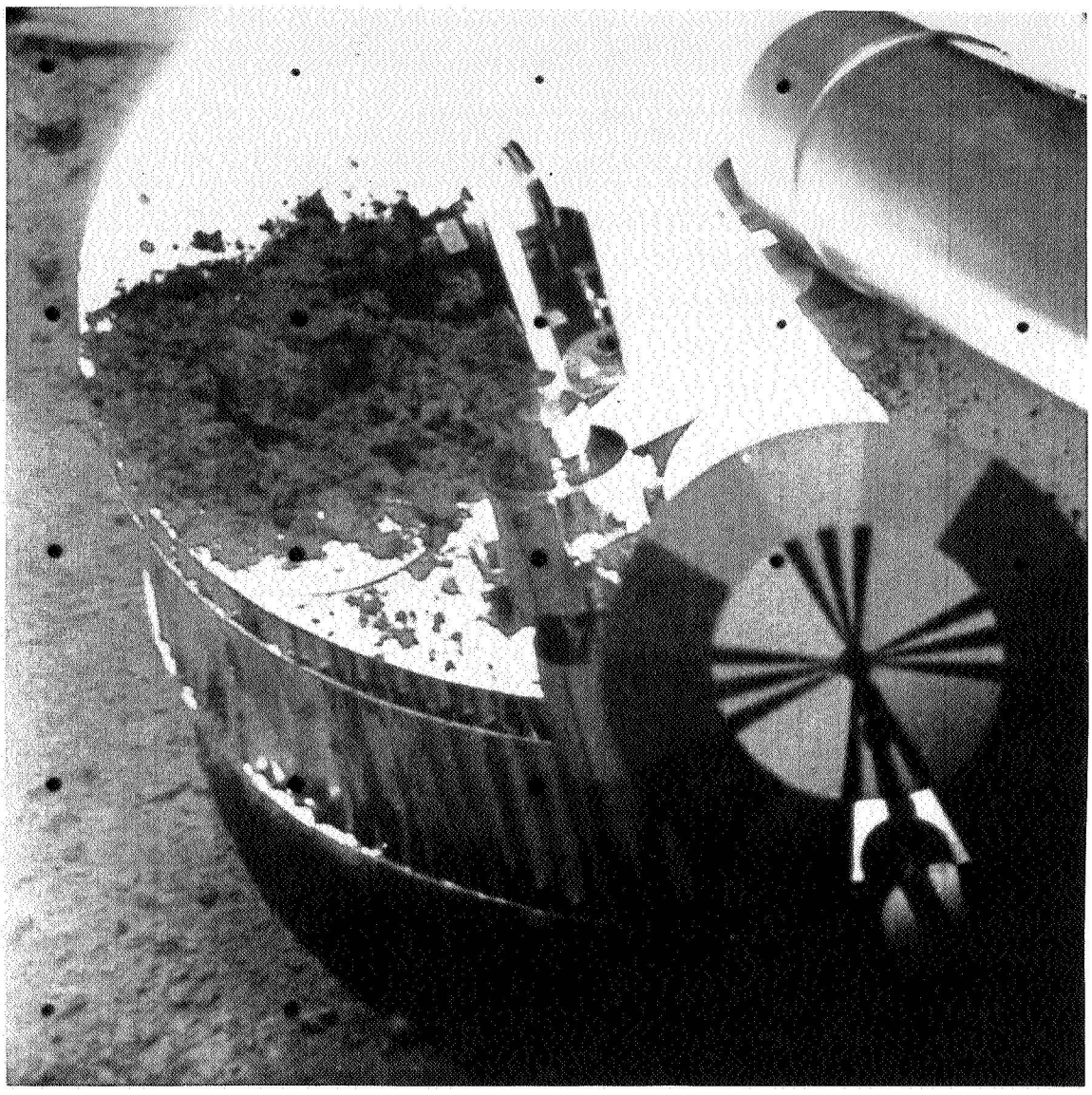

Figure 12–Lunar soil dumped on Surveyor III footpad by surface sampler to permit close examination. Note color calibration chart at lower right.

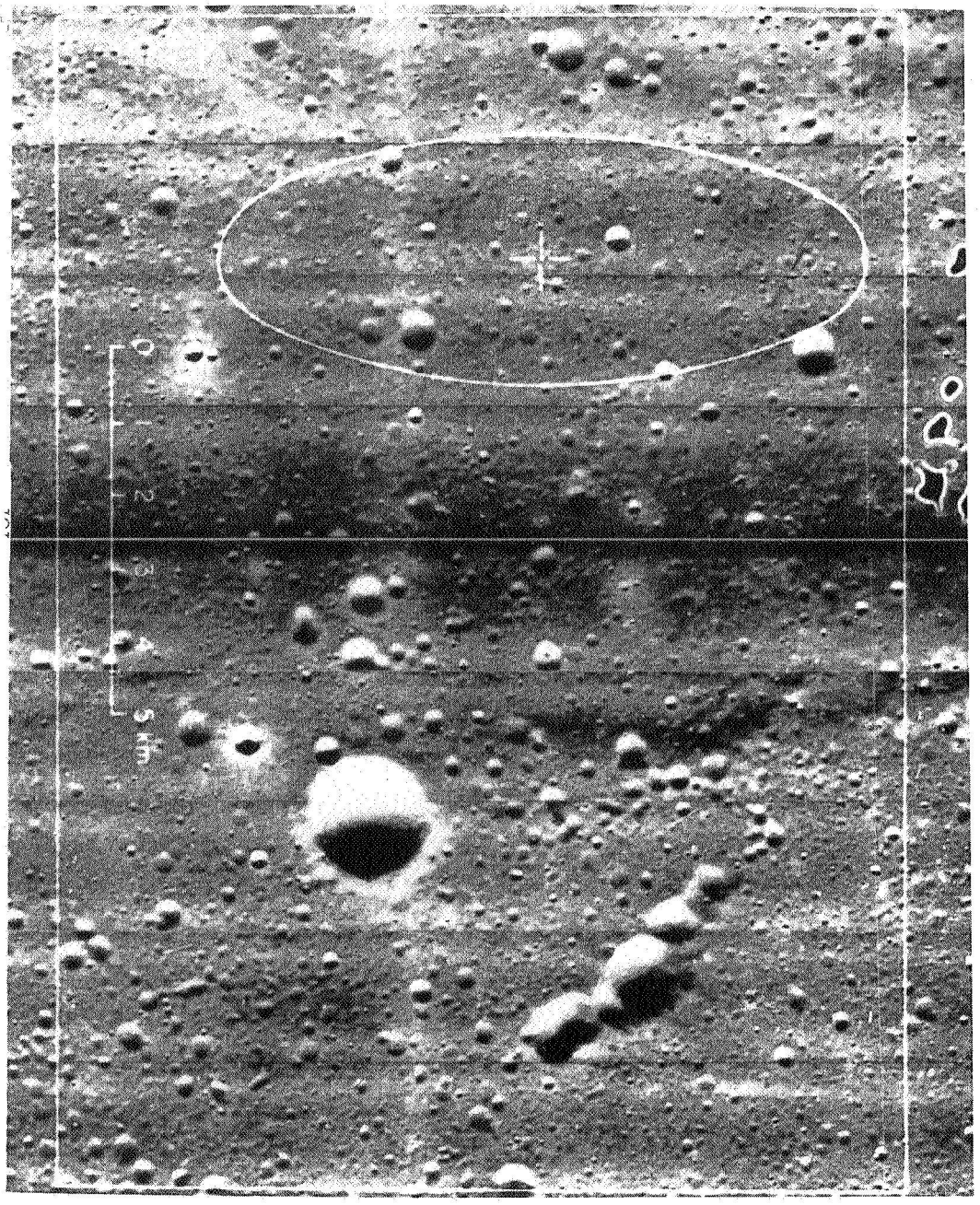

Figure 13–Surveyor V landing site, photographed by Lunar Orbiter V medium resolution camera, in southern Mare Tranquillitatis. Landing site lies in the ellipse to 99% probability. Large crater at lower right is Sabine D.

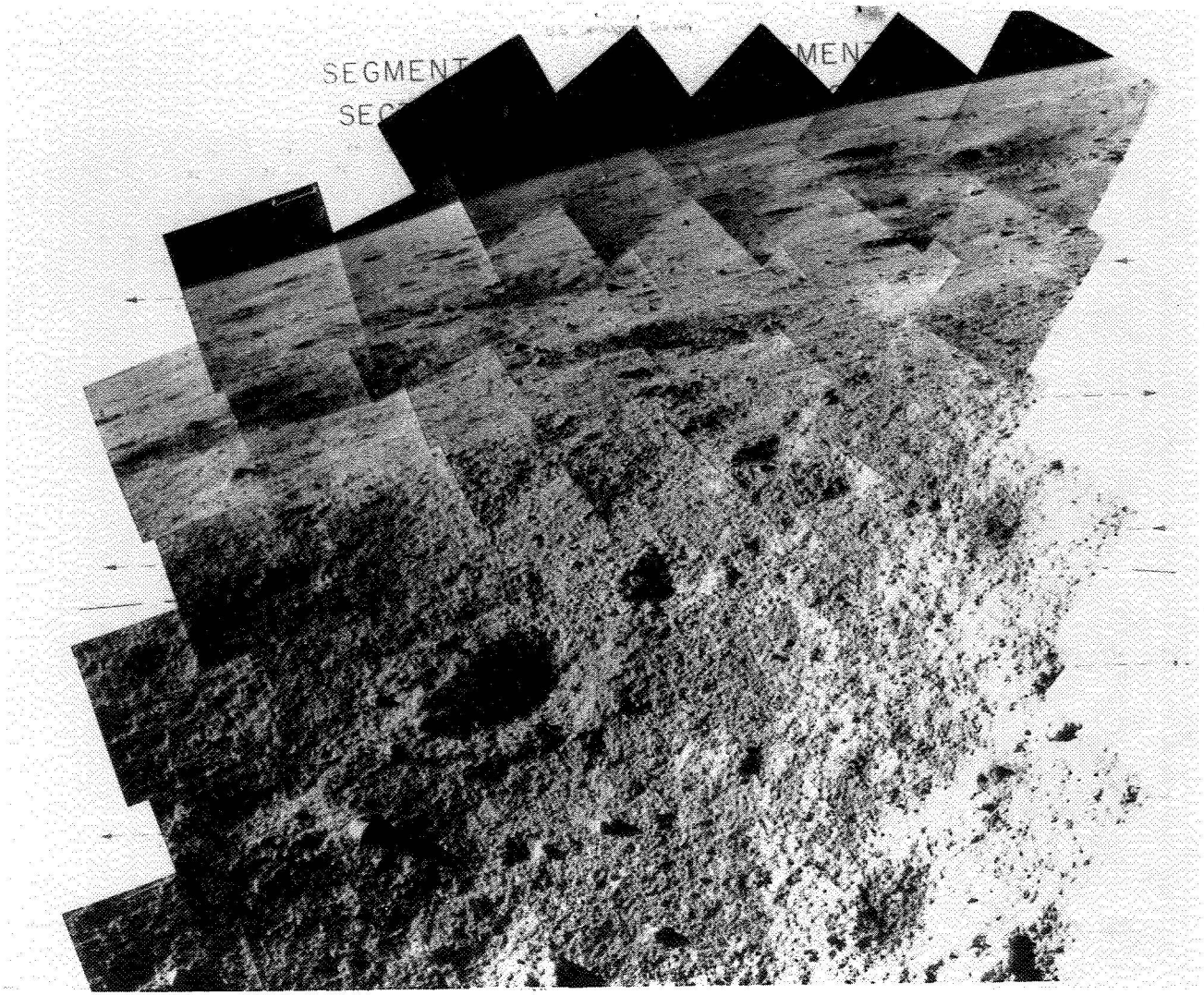

Figure 14–Mosaic of narrow-angle pictures from Surveyor V showing the northwest wall of the crater in which the spacecraft landed. Rim of the crater is about halfway up the picture, and is marked by change in apparent texture due to the change in slope and distance.

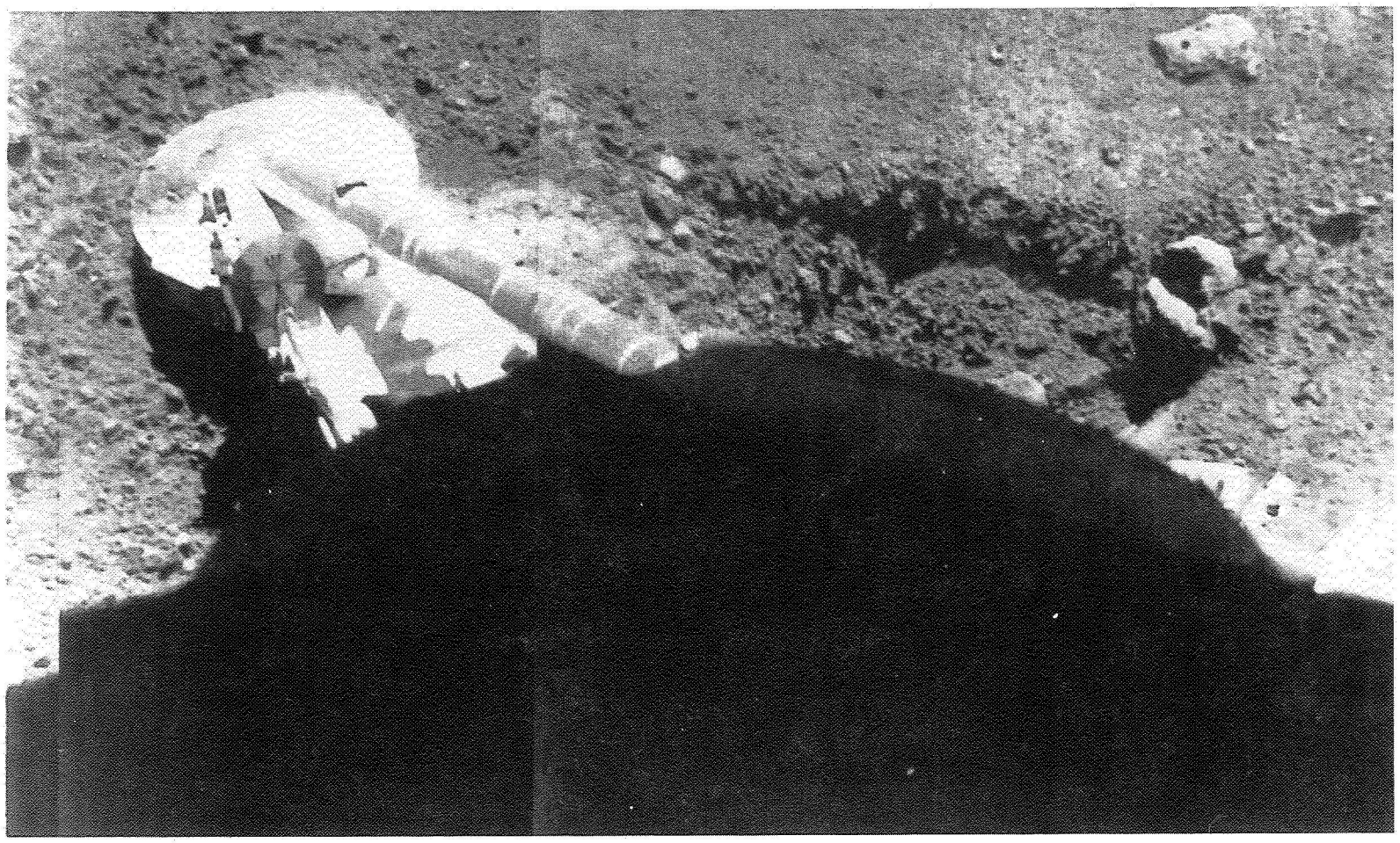

Figure 15–Trench dug by Surveyor V footpad during landing, as it slid downslope.

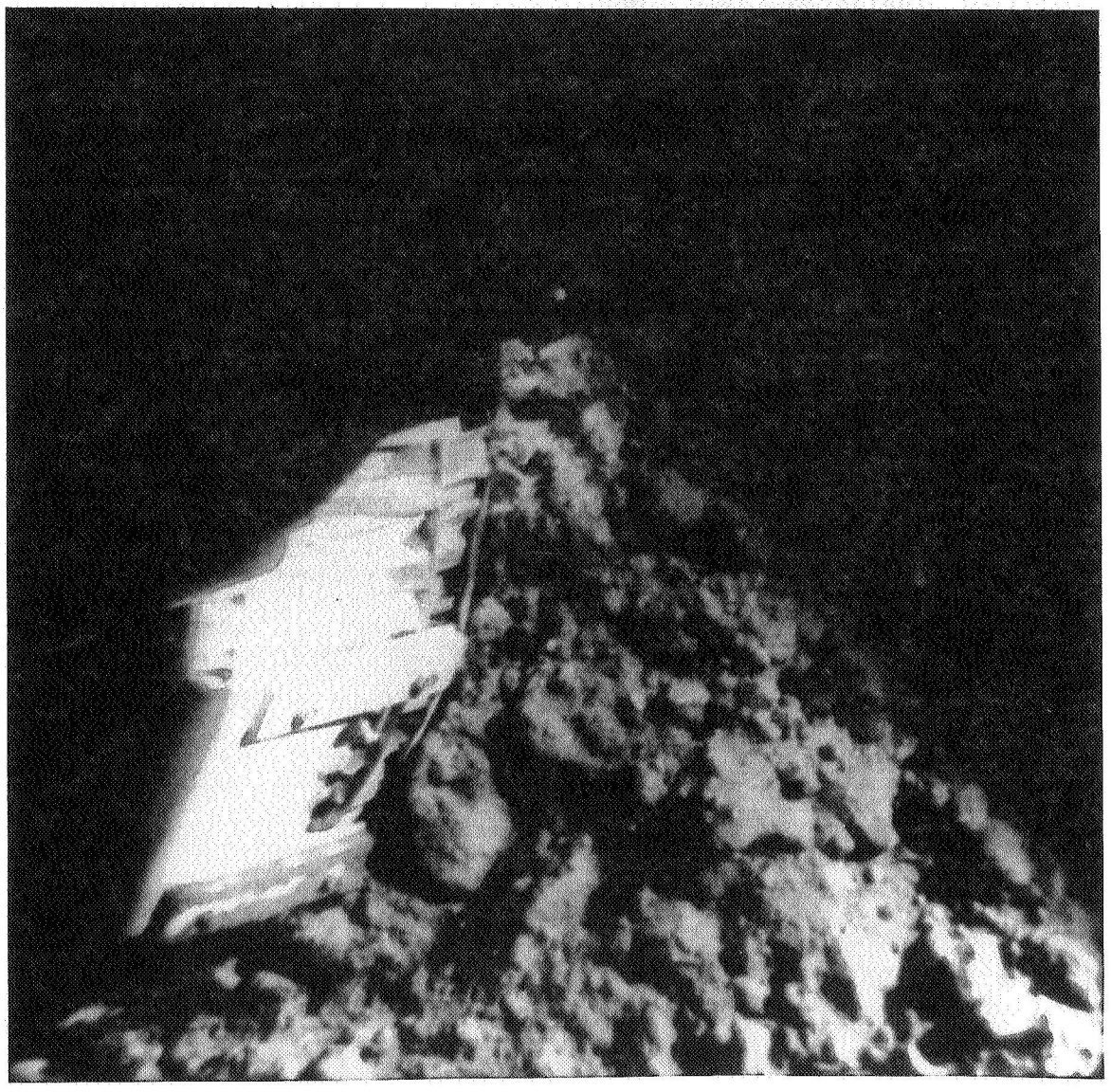

Figure 16–Surveyor V footpad with attached magnet (left) and control bar (right). Note the material sticking to the magnet; control bar is clean.

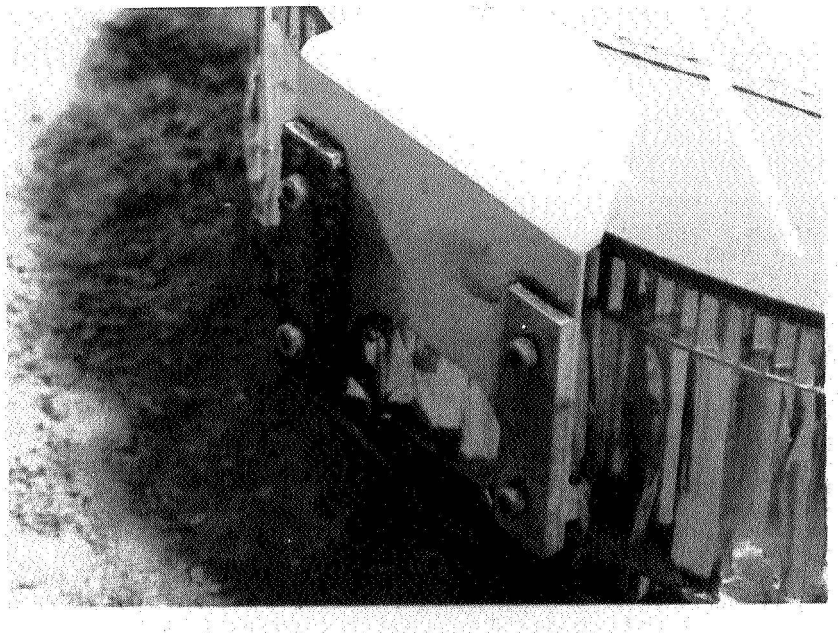

SCORIACEOUS BASALT

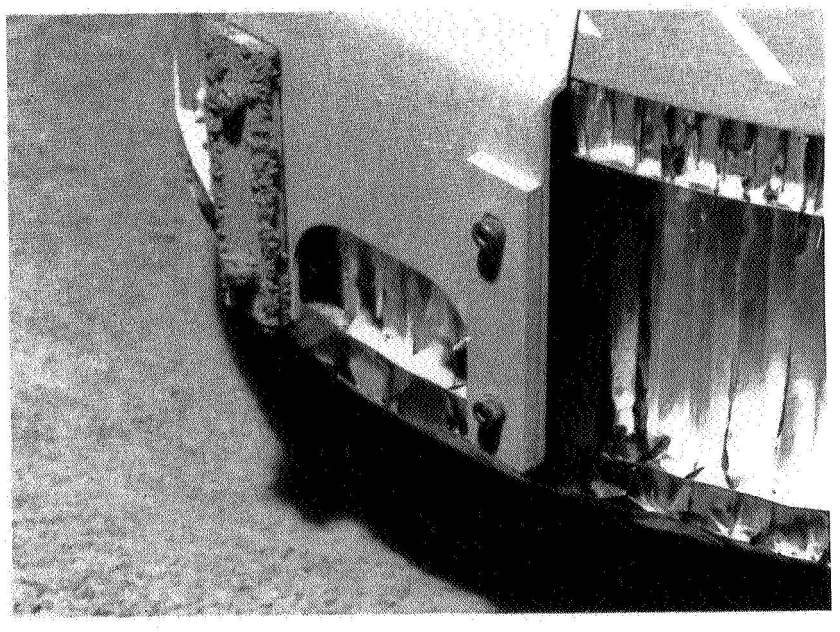

BASALT

Figure 17—Laboratory test of replicas of Surveyor V magnet and non-magnetic control bar. Footpad was impacted in 37-50 micron powders of scoriaceous basalt and basalt. Magnet (left) has material sticking to it.

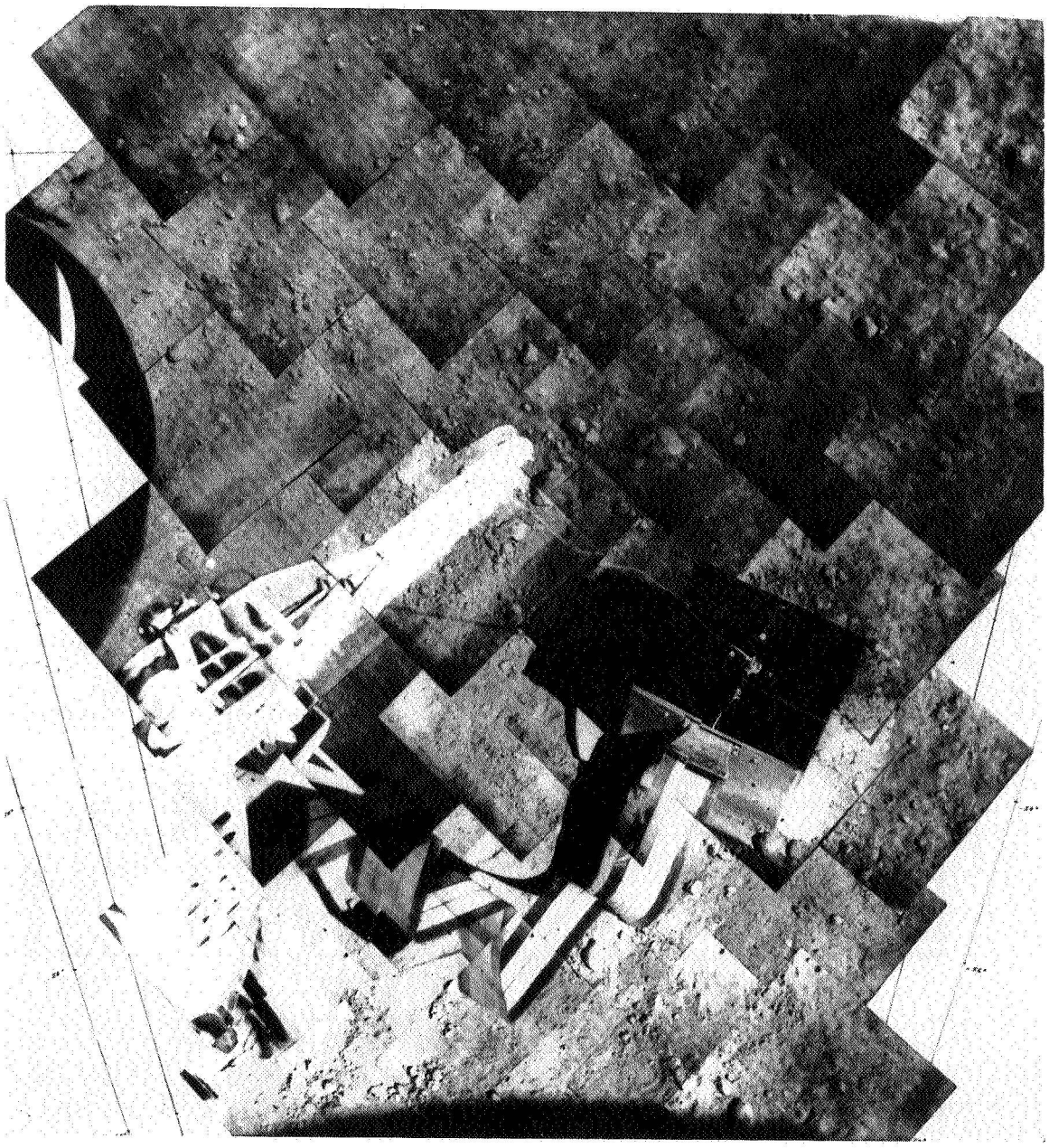

Figure 18—Surveyor V alpha scattering compositional experiment after firing of vernier engines, which moved the instrument.

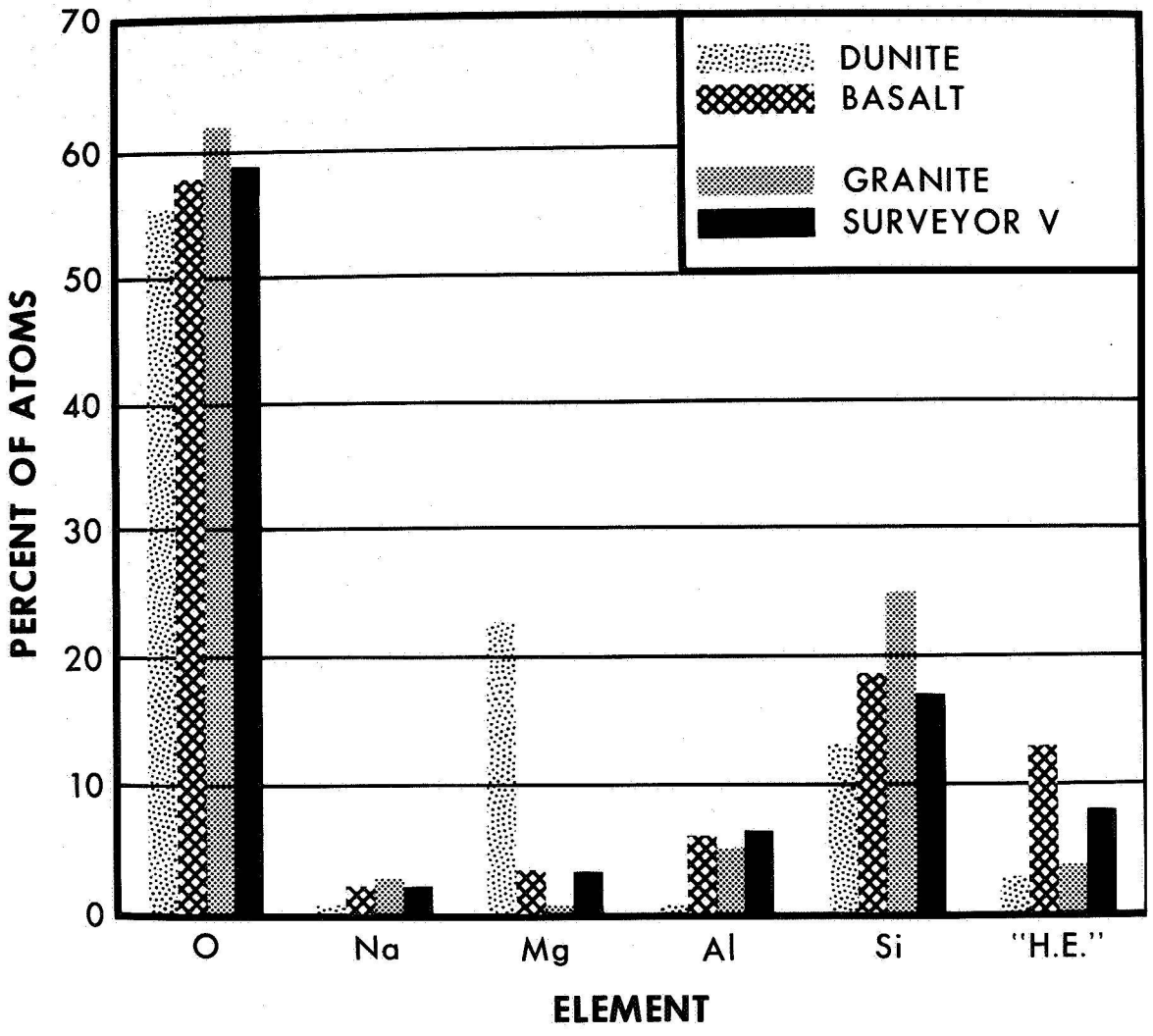

Figure 19–Comparison of Surveyor V alpha scattering experiment results, from first spot (before vernier firing), with dunite, basalt, and granite.

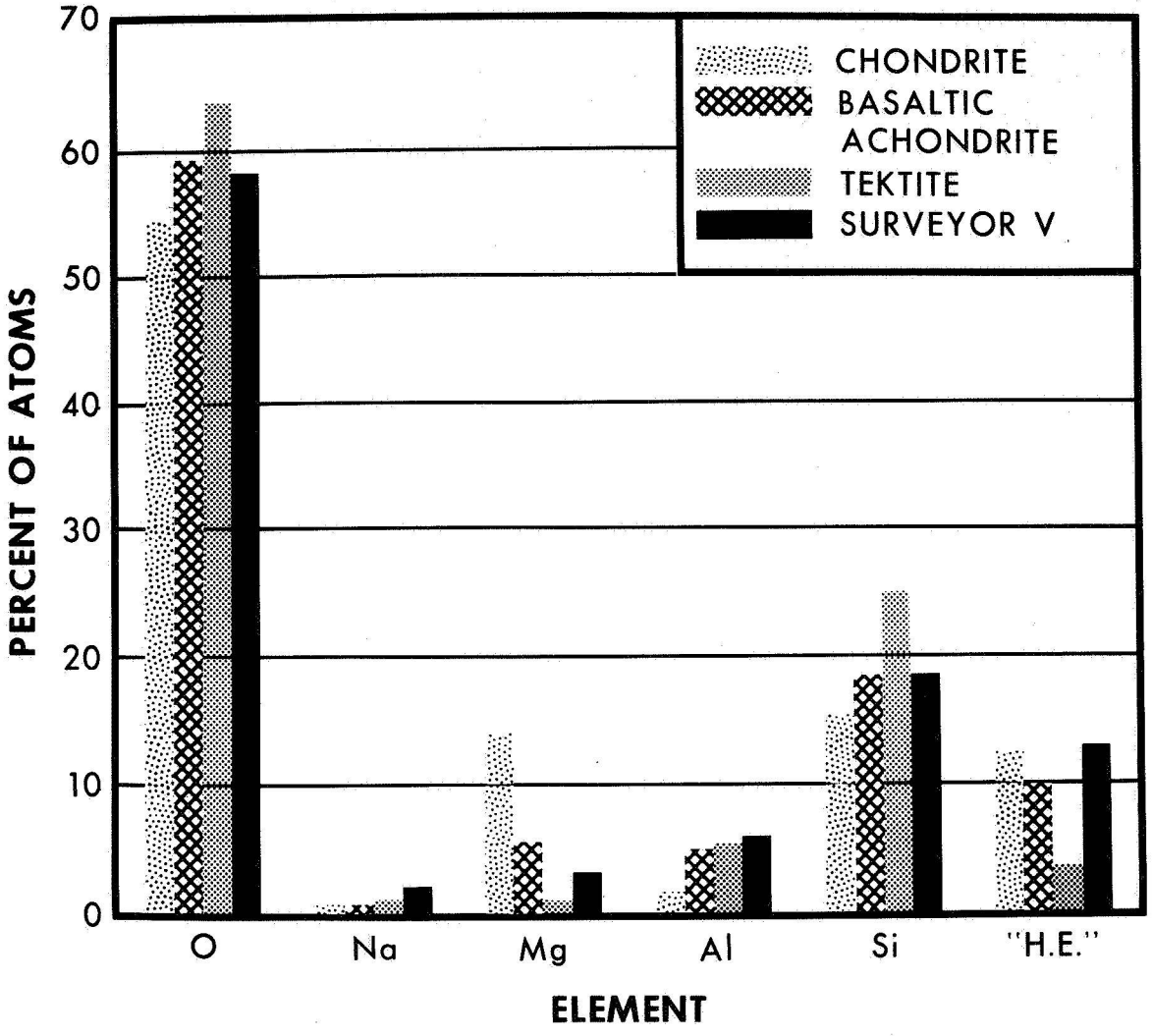

Figure 20–Comparison of Surveyor V alpha scattering experiment results from first spot (before vernier firing) with chondritic meteorites, basaltic achondrites, and tektites.

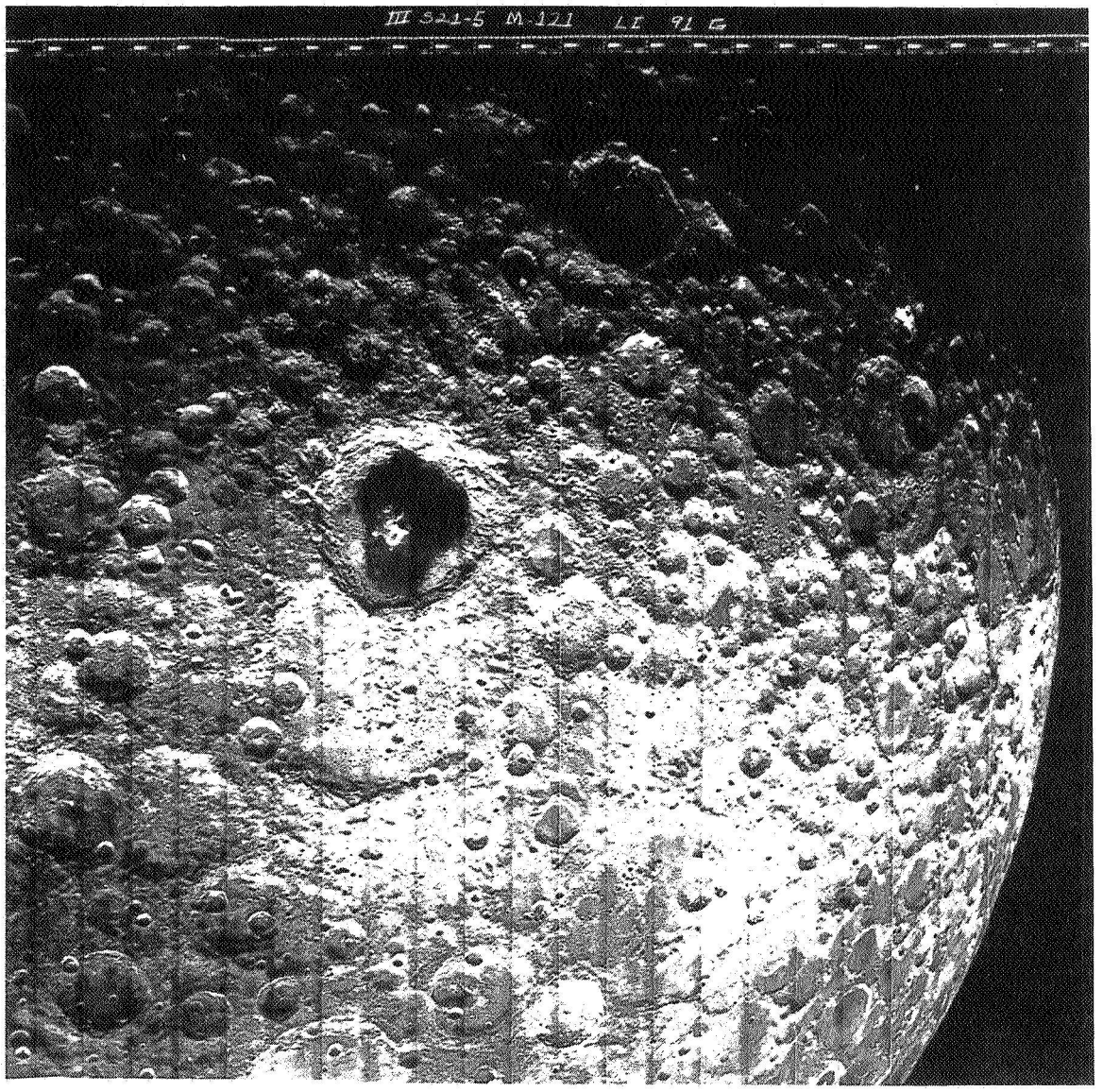

Figure 21–Lunar Orbiter III photograph from 907 miles altitude above the far side of the moon, showing the crater Tsiolkovsky, 150 miles in diameter.

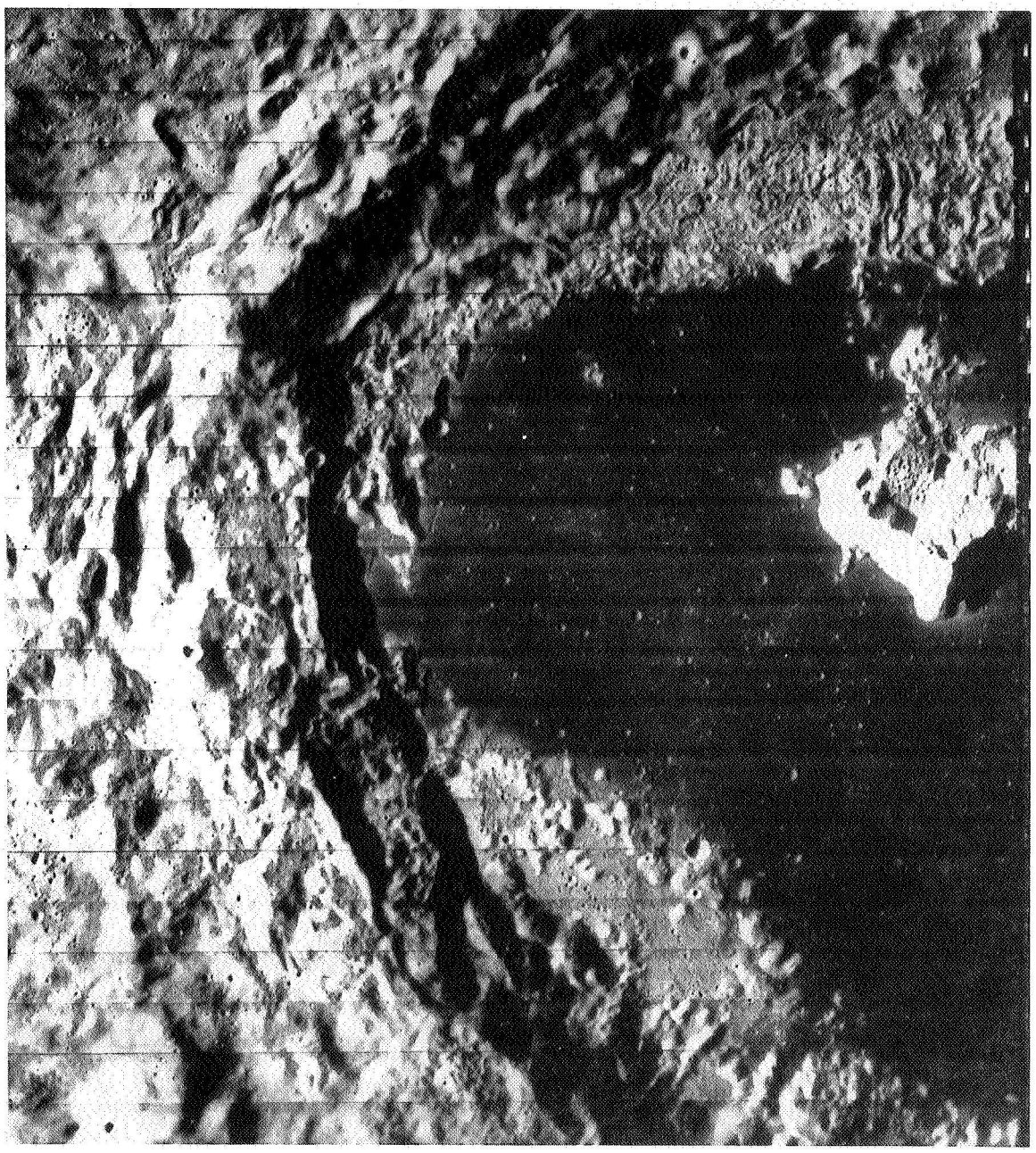

Figure 22–Close up view from Lunar Orbiter III with high-resolution camera of crater Tsiolkovsky. This crater apparently bridges the gap between craters such as Tycho and the mare-filled craters such as Archimedes.

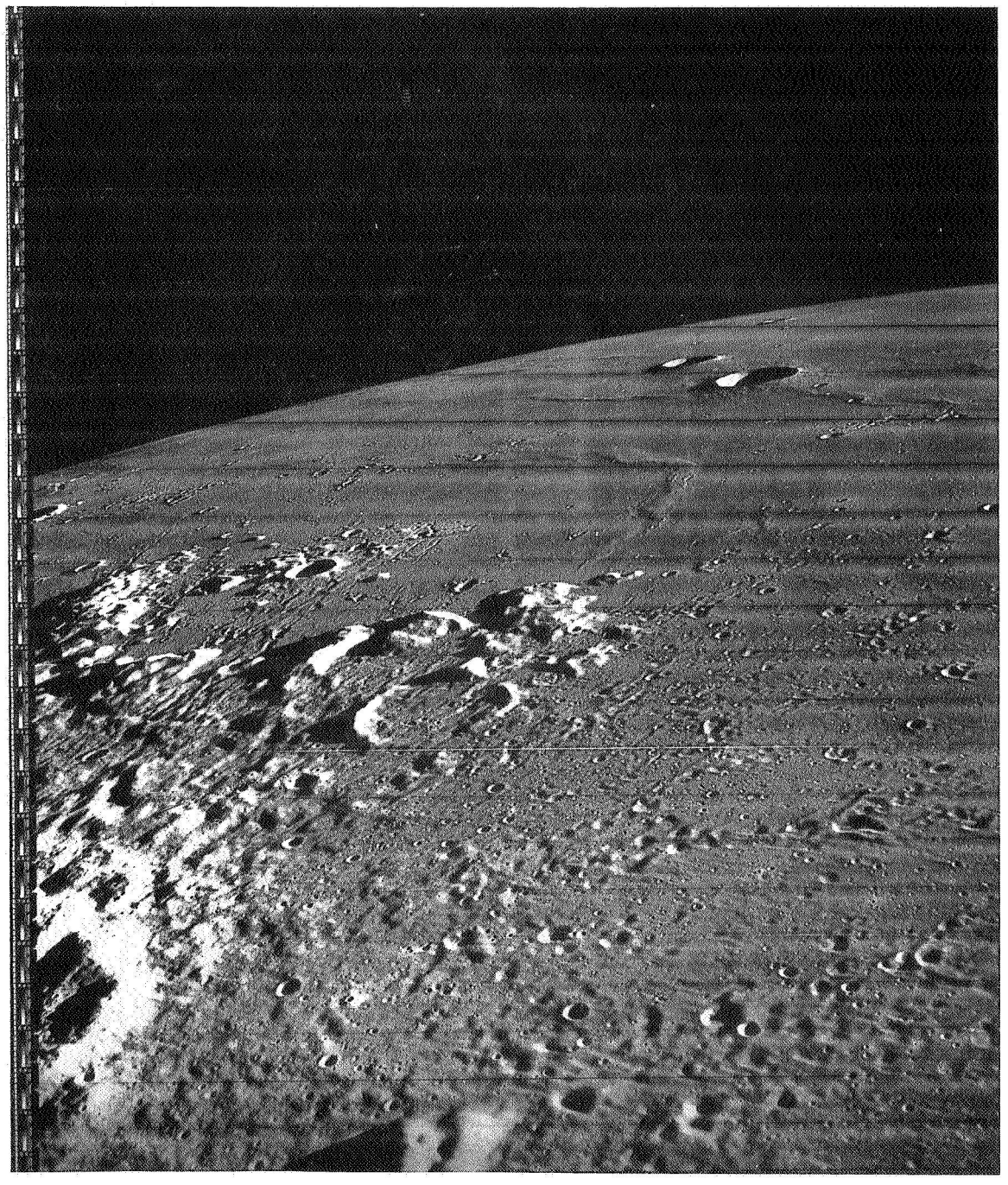

Figure 23–View to the north from Lunar Orbiter III showing part of Oceanus Procellarum, taken from 38 miles altitude. The landing site of Lunar IX, launched by the USSR in 1966, is at the center of the photograph near the highland-mare contact.

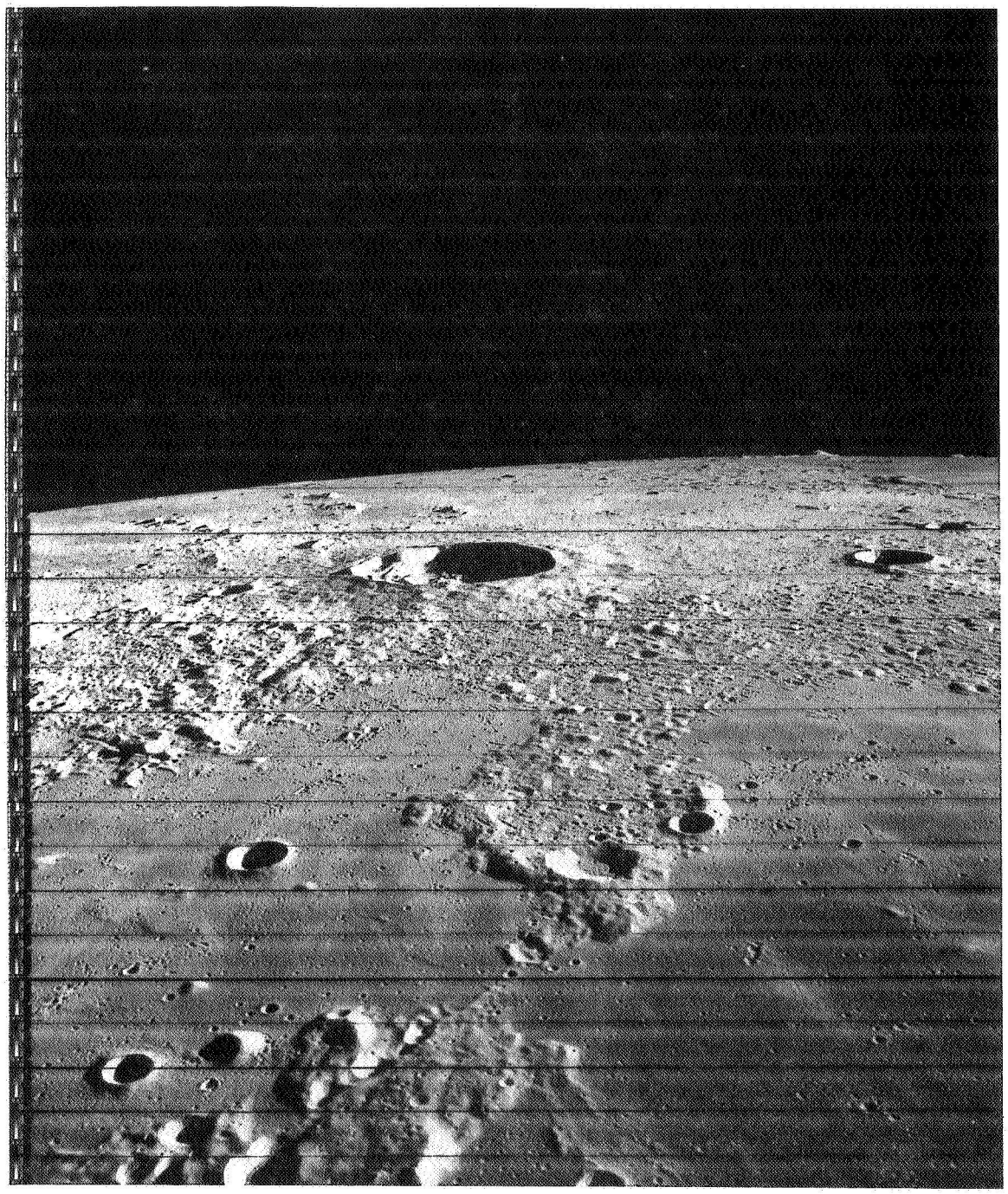

Figure 24–Lunar Orbiter III view to the north, showing the crater Kepler, in Oceanus Procellarum. Kepler is a Copernican age crater with a diameter of about 20 miles. Clearly visible are its hummocky ejecta blanket and secondary craters.

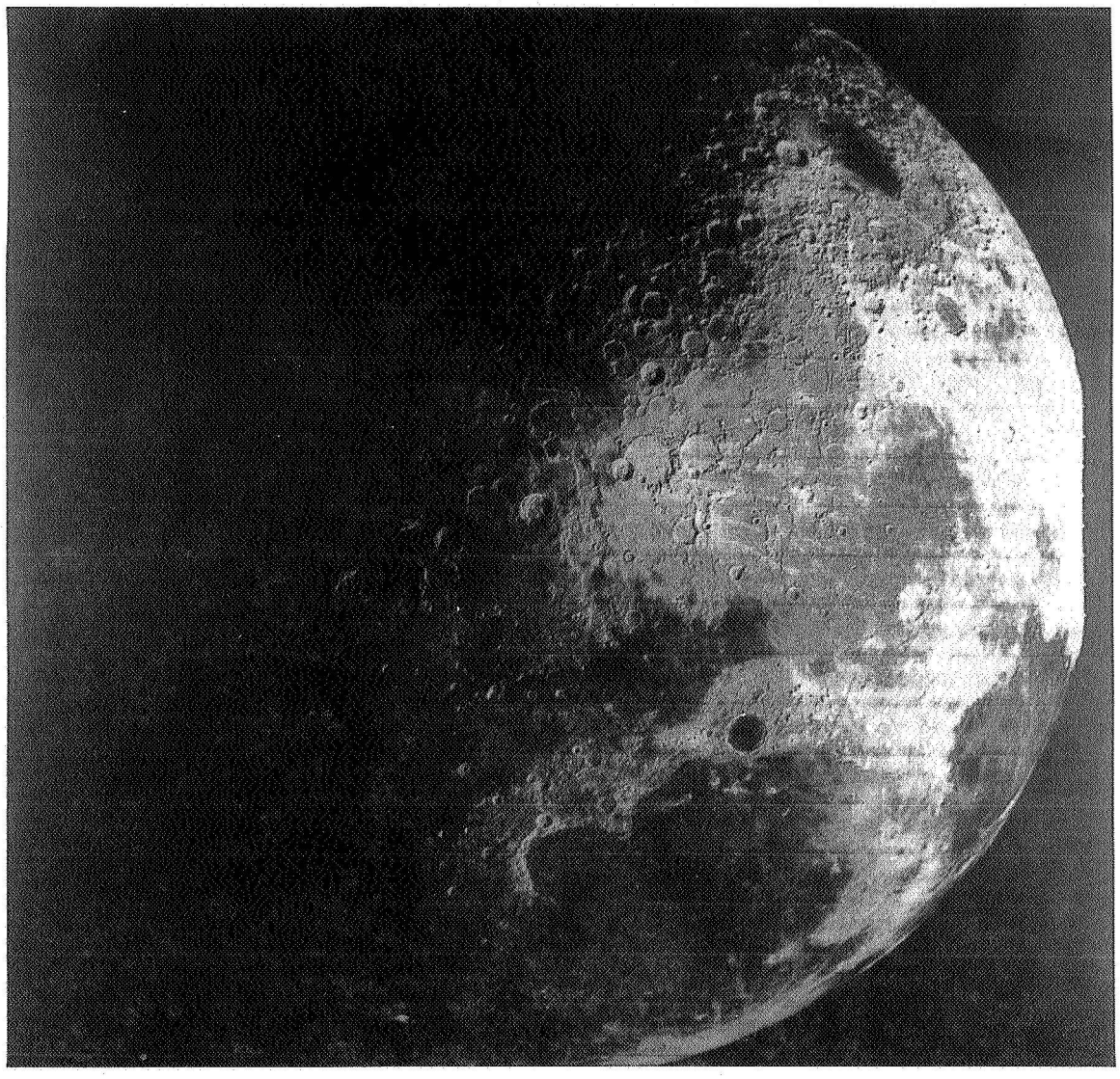

Figure 25–Lunar Orbiter IV taken from 2050 miles altitude over the moon's North Pole. The earthward hemisphere is at top; the large dark area is Mare Imbrium, with the mare-floored crater Plato on its north rim.

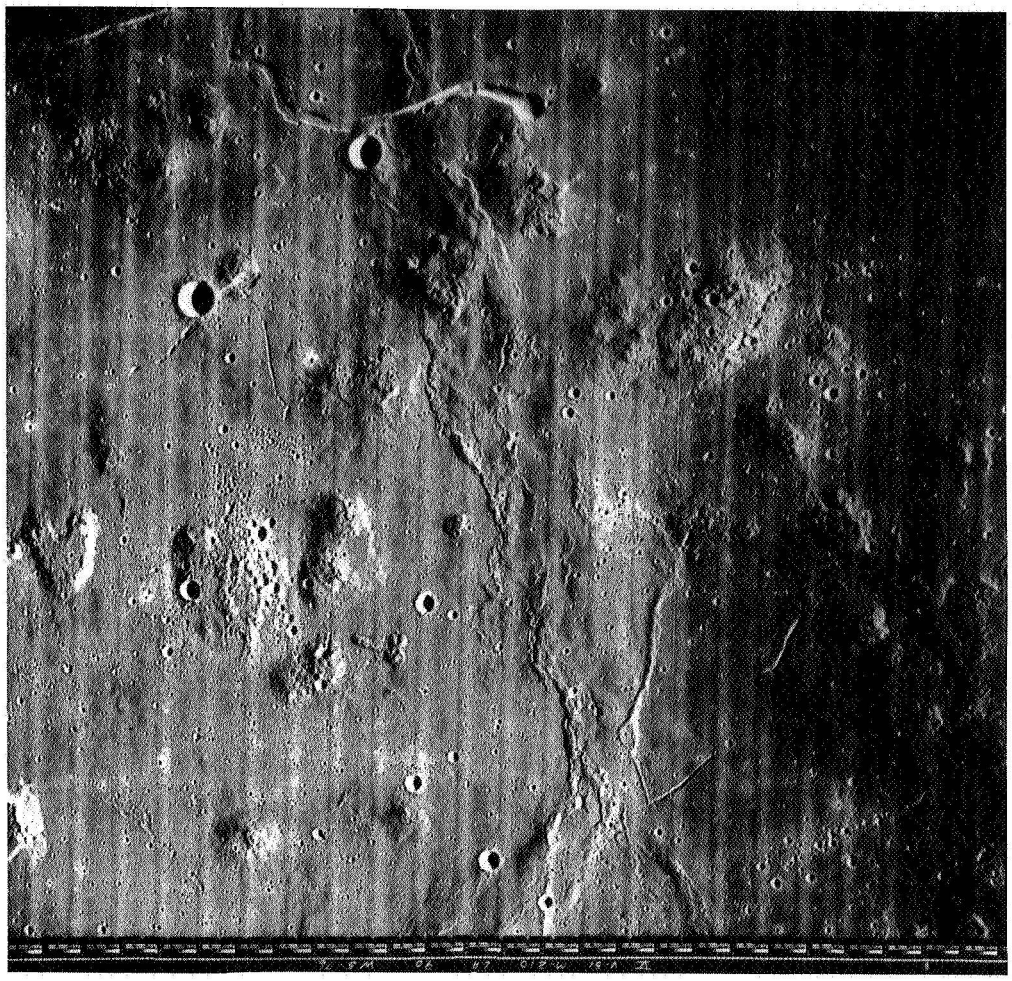

Figure 26–Lunar Orbiter V wide-angle photograph of the Marius Hills, with north at top. The various domes are considered volcanic features of some sort, possibly shield volcanoes. Notice the prominent mare ridges at center.

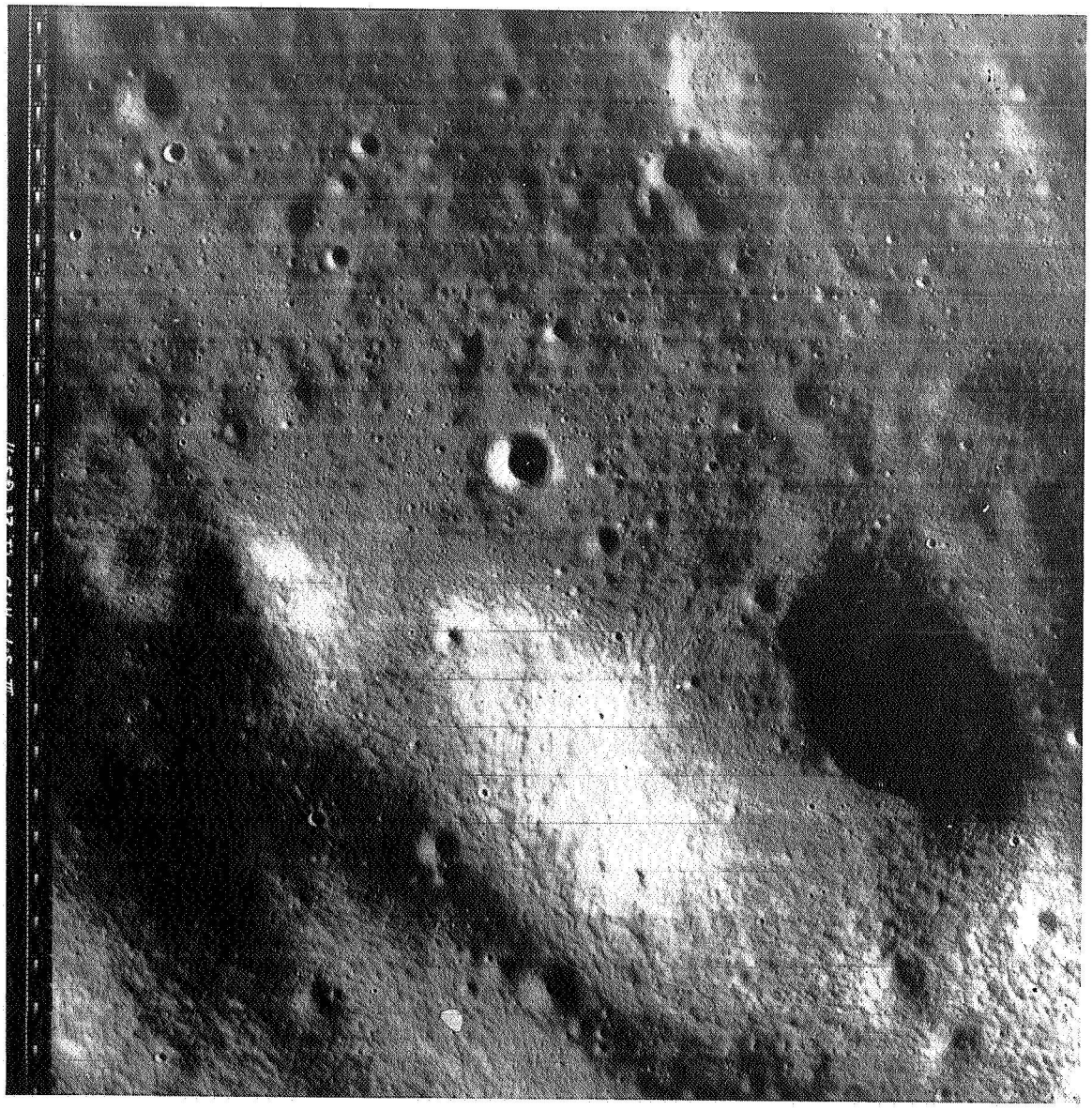

Figure 27–High-resolution photograph from Lunar Orbiter III of a 9-square-mile highland area near the crater Demboswki, at 6.6 °E and 4 °N on the visible hemisphere. Note "patterned ground," believed by some geologists to be the result of downslope movement.

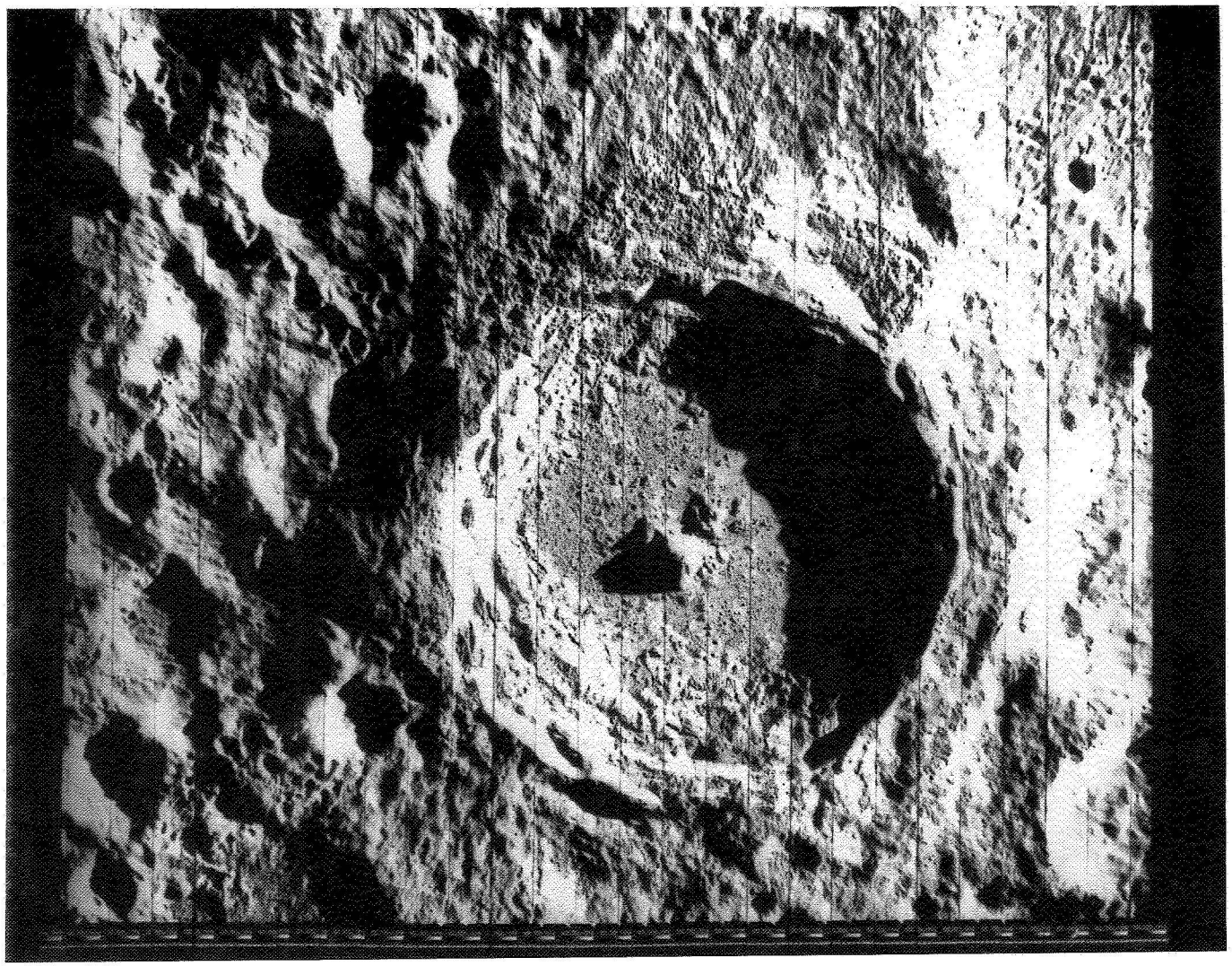

Figure 28–Lunar Orbiter V view of the crater Tycho, with north at top and sun at right. Tycho appears to be the youngest of the large craters.

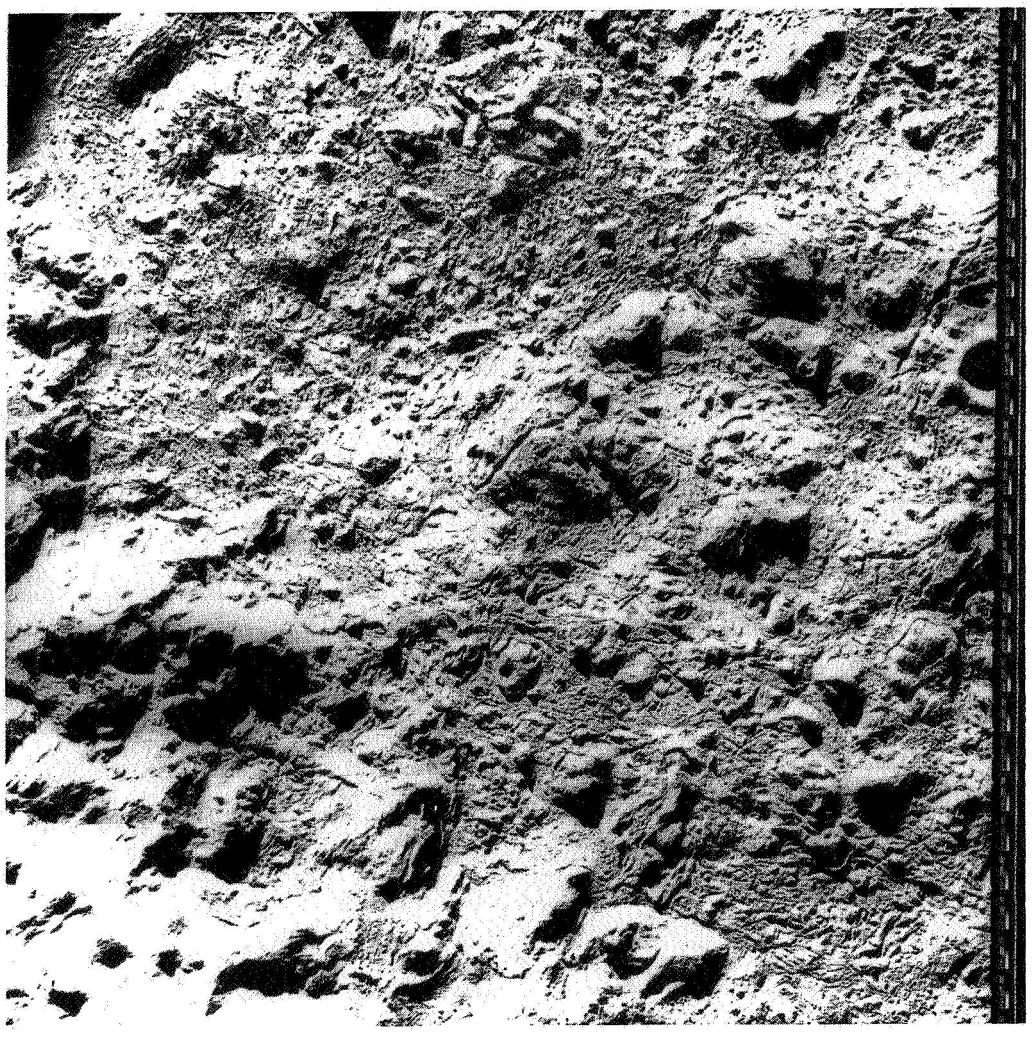

Figure 29—Lunar Orbiter V high-resolution view of the floor of Tycho, with north at top and sun at right. North-south distance in photo is about 14.7 miles. The ropy structure of the crater floor resembles that of terrestrial lava flows, and has almost certainly been formed by consolidation of some sort of liquid.

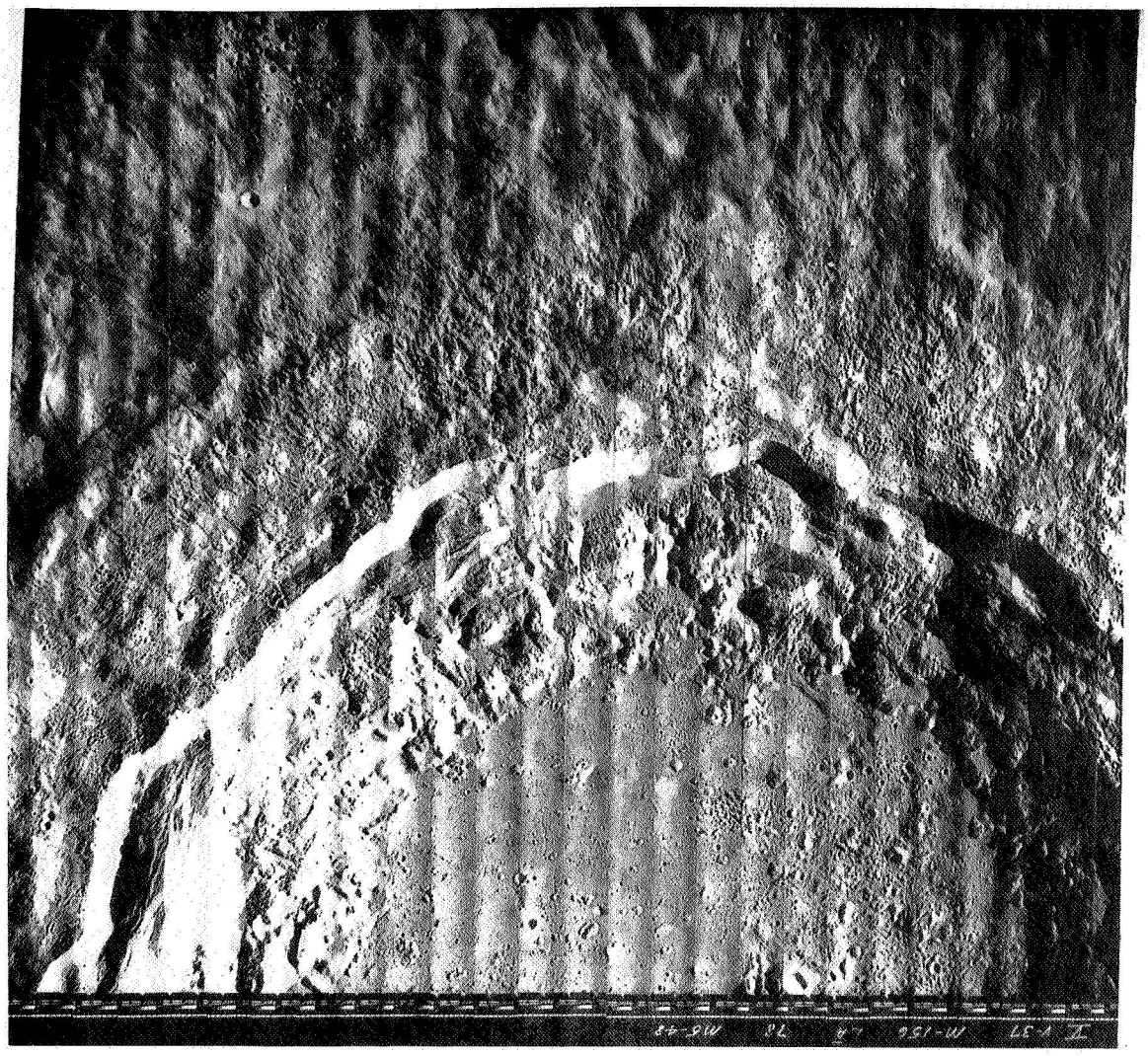

Figure 30–Lunar Orbiter V view of the northern part of the crater Copernicus, whose greatest diameter in the picture is about 55 miles. A number of typical crater features are shown exceptionally well, including the ejecta blanket and slump blocks produced by normal faulting of the crater walls.

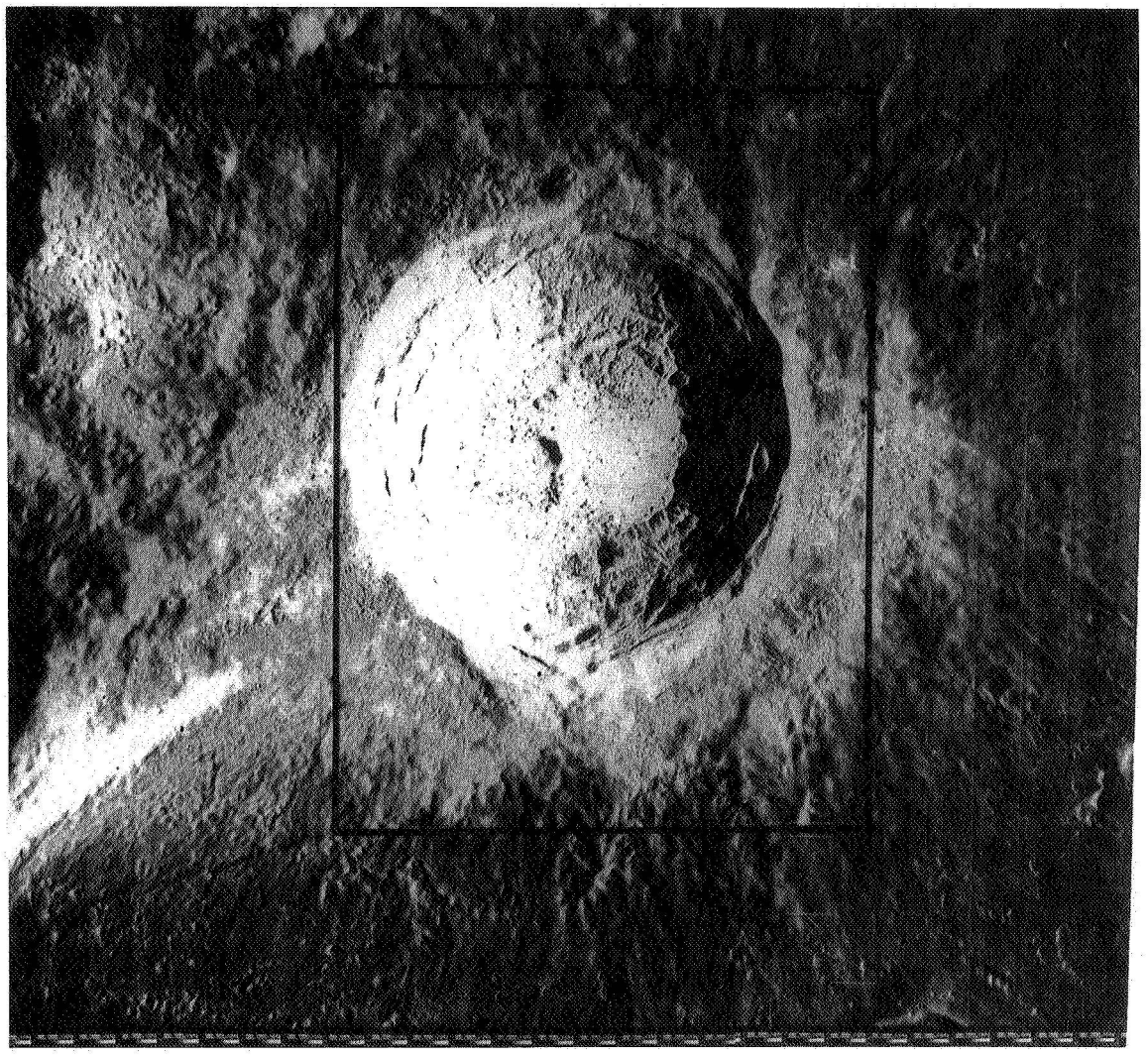

Figure 31—Lunar Orbiter V wide-angle photograph of the crater Aristarchus, from an altitude of about 80 miles. Aristarchus, the brightest large feature on the earthward hemisphere, is the site of several confirmed transient events, in particular the famous "red spots" seen by Greenacre and Barr in 1963.

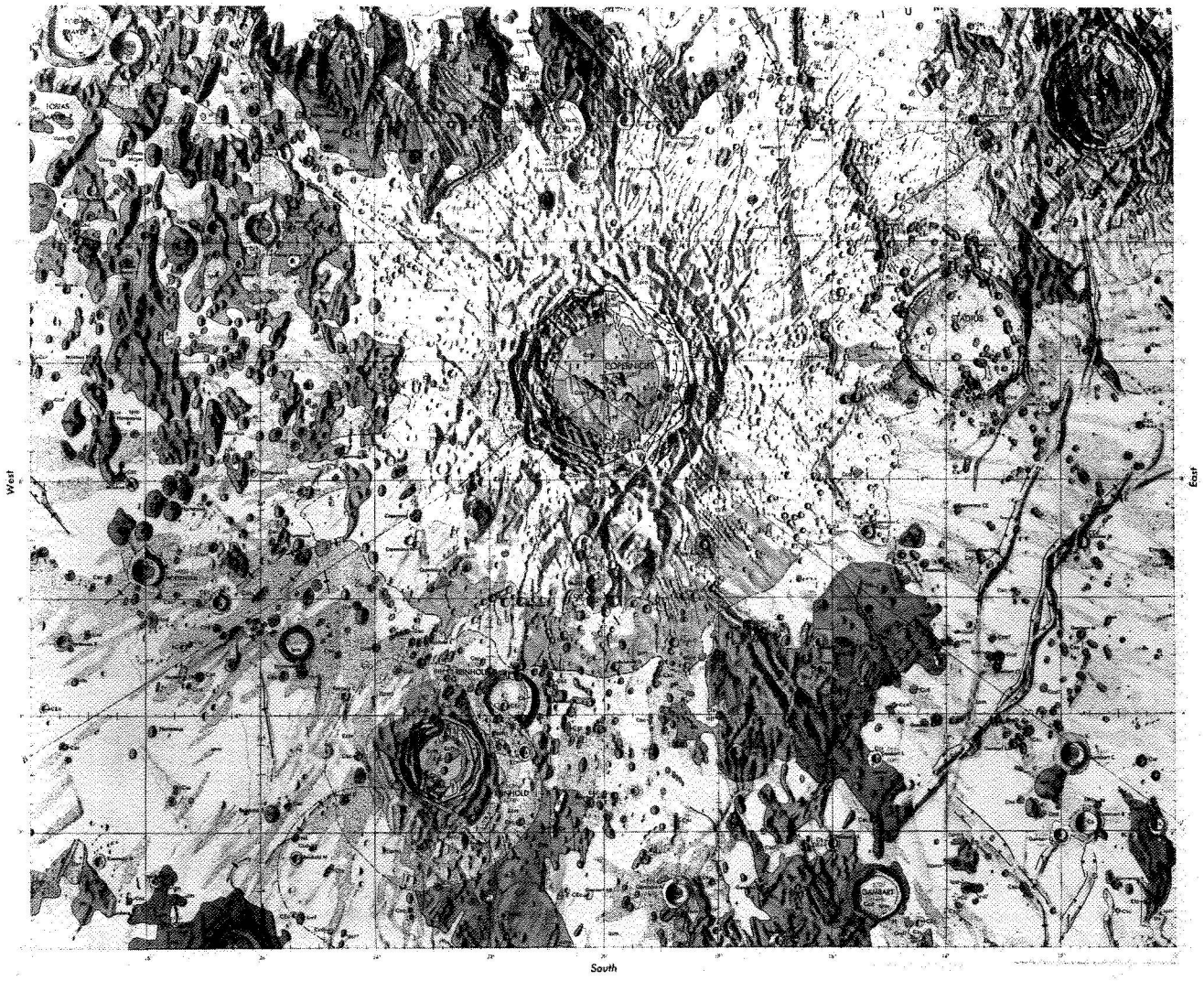

Figure 32–Geologic map of the crater Copernicus and vicinity, prepared by Schmitt, Trask, and Shoemaker. Scale is 1:1,000,000. Legend omitted.

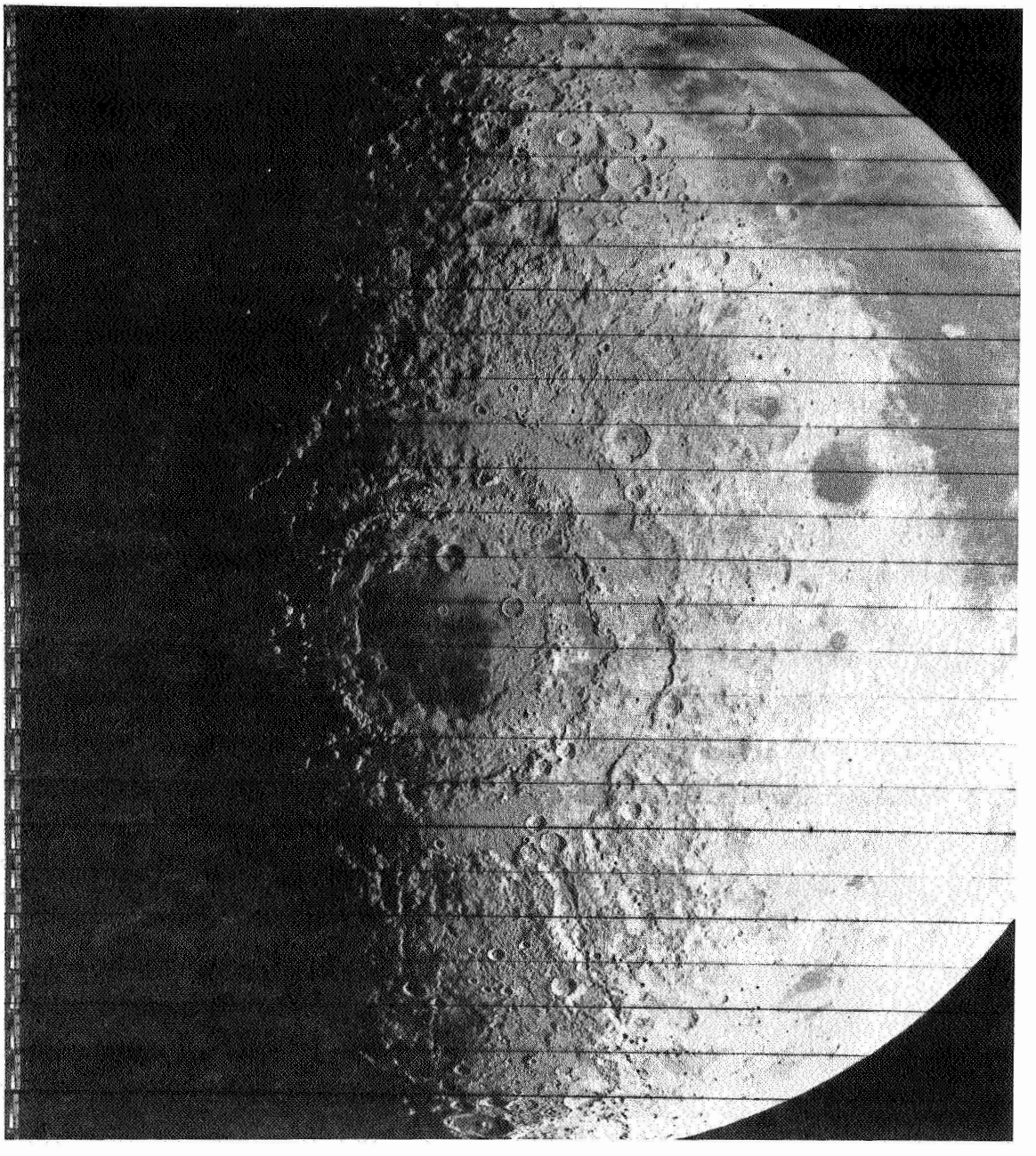

Figure 33–Lunar Orbiter IV view of Mare Orientale, on the western limb of the moon. This feature is only partly visible from earth. It is believed to be the youngest of the large maria, which may have resembled Mare Orientale at an early stage in their evolution.

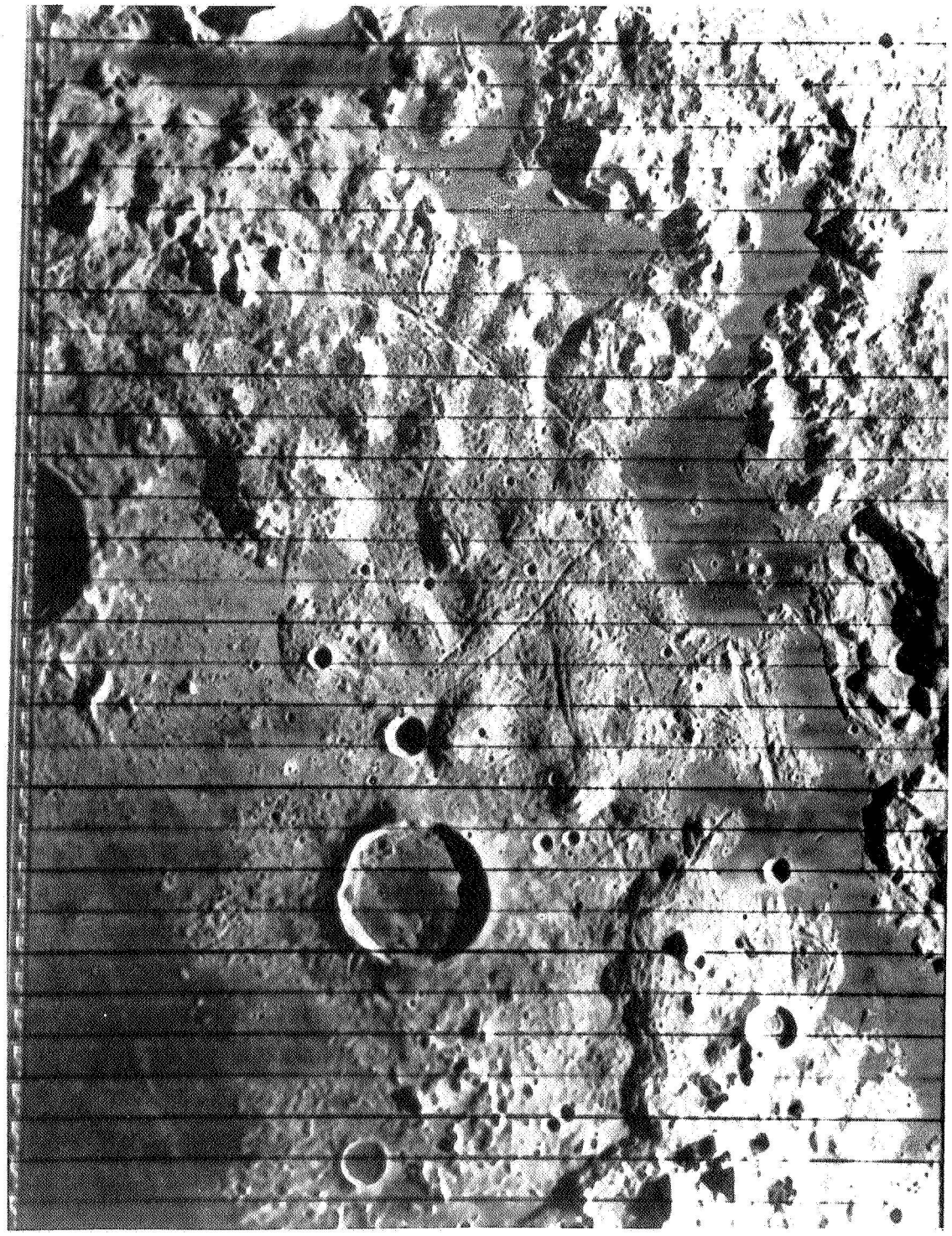

Figure 34–High-resolution Lunar Orbiter IV view of the eastern part of Mare Orientale (north at top). In addition to the additional structural details shown, this photograph illustrates the differences between craters believed to be of impact origin (left) and volcanic origin (lower center).

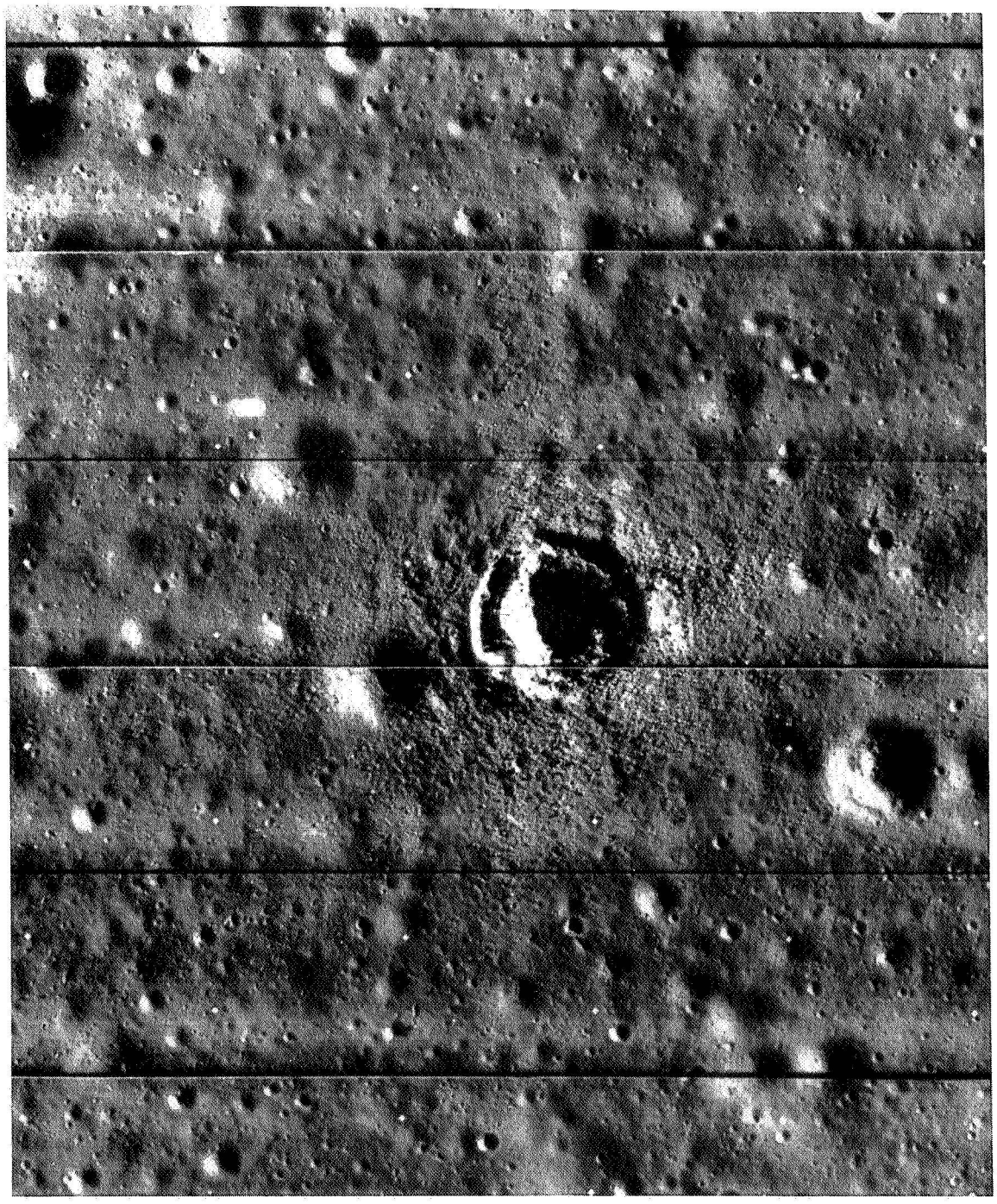

Figure 35–Lunar Orbiter III high-resolution photograph of part of Oceanus Procellarum. The area shown measures about 3,600 by 2,800 feet. The well-preserved impact crater is about 500 feet in diameter. Its shape has been changed by peripheral slumping after formation.

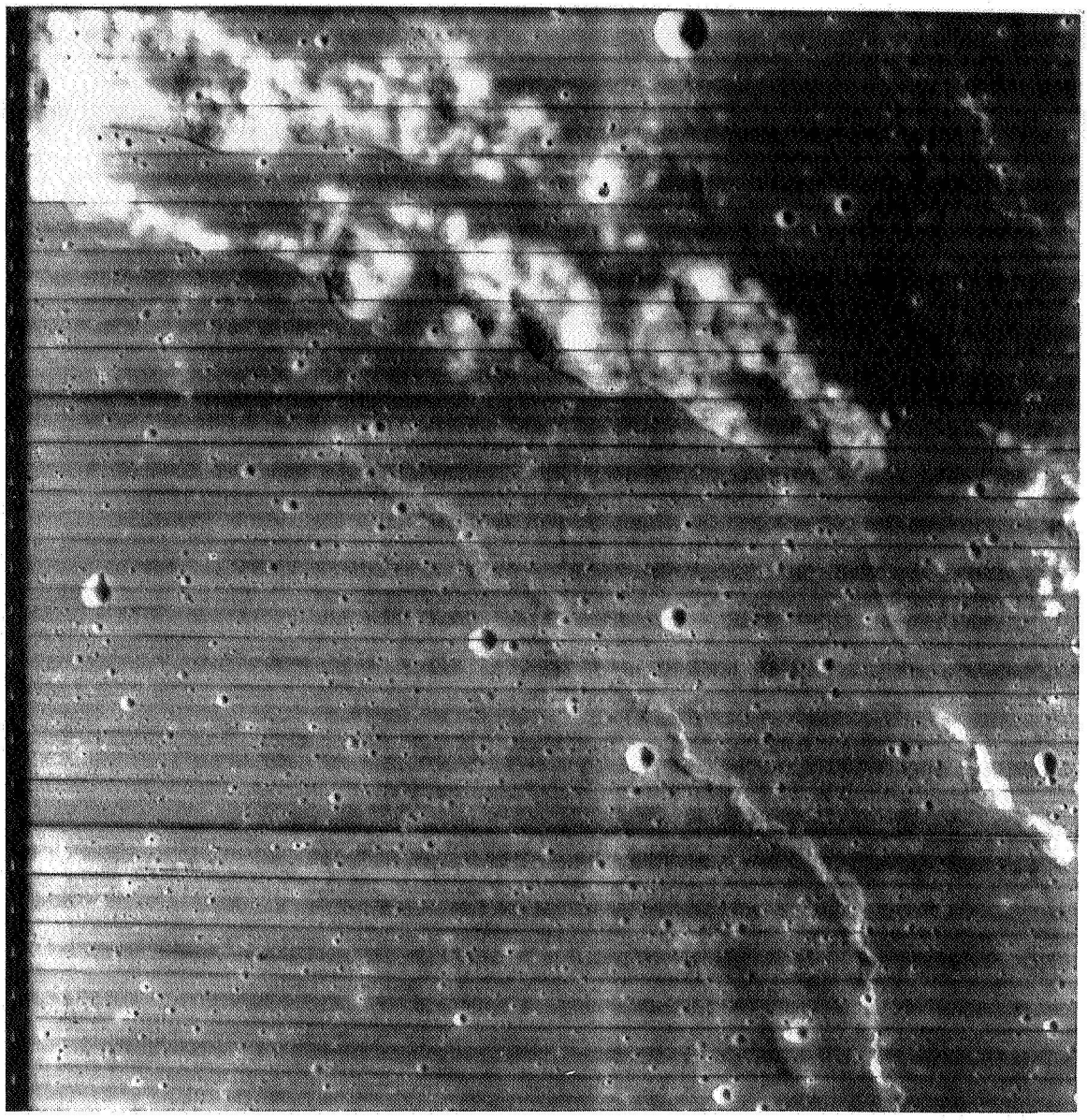

Figure 36–Moderate resolution photograph of the Flamsteed Ring taken by Lunar Orbiter I, with north at top. Only the northeastern part of the Ring is shown. Area is about 32 by 38 kilometers.

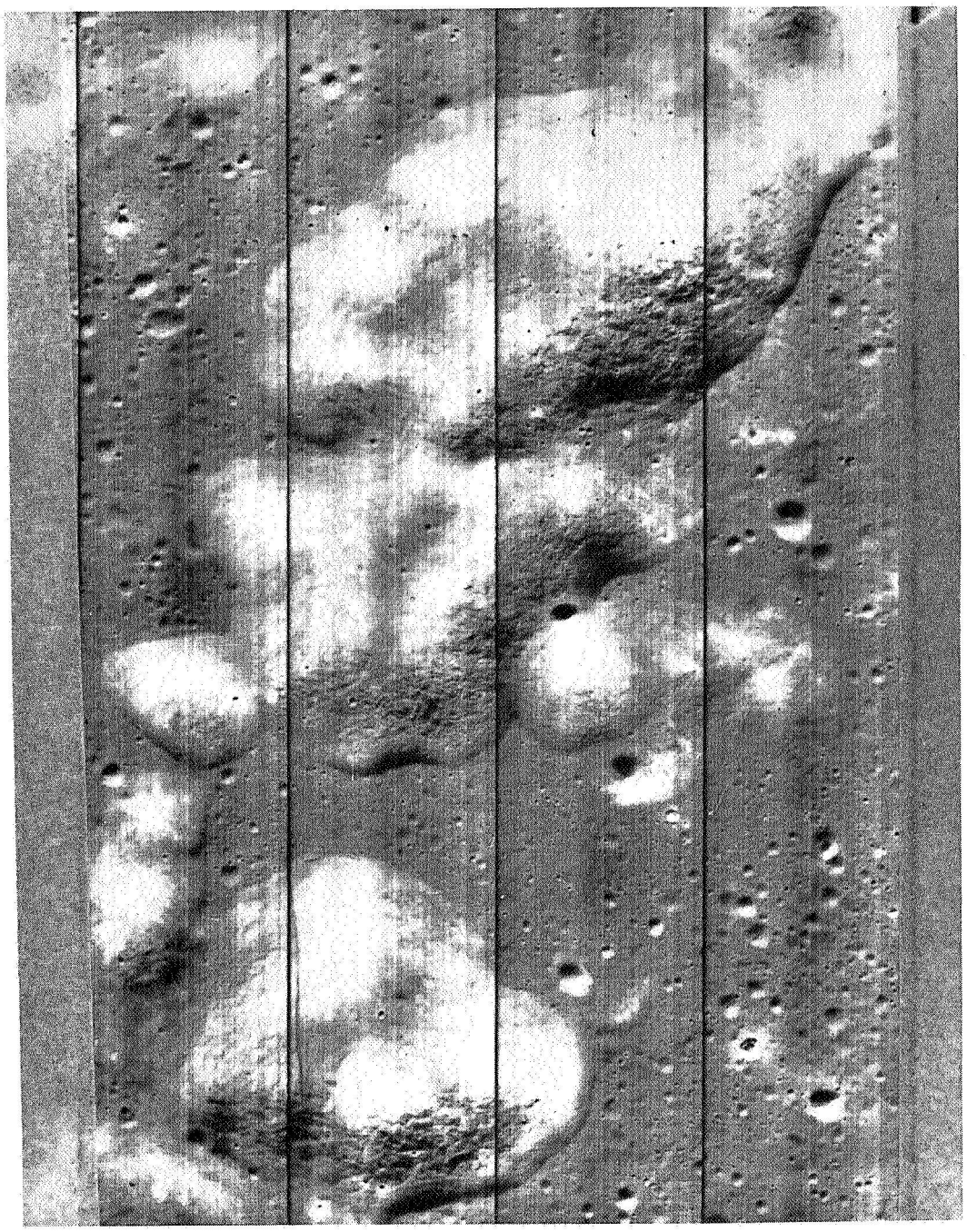

Figure 37—Enlarged portion of Figure 36, emphasizing morphology of the Flamsteed Ring. Of particular interest are the convex slopes, low crater density on the hills, and the "patterned ground."

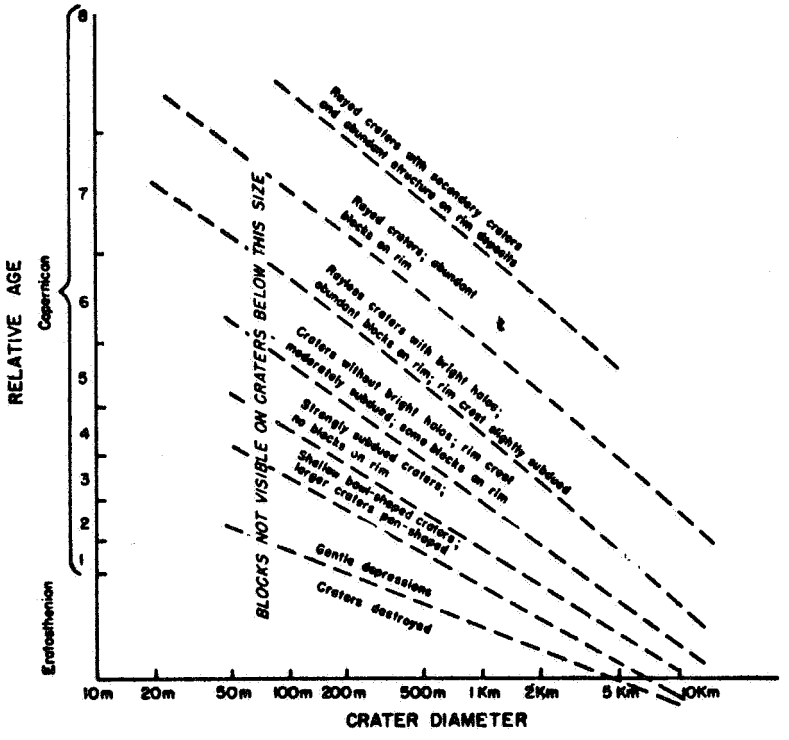

Figure 38–Relation between diameters properties and ages of craters. Categories are intergradational.

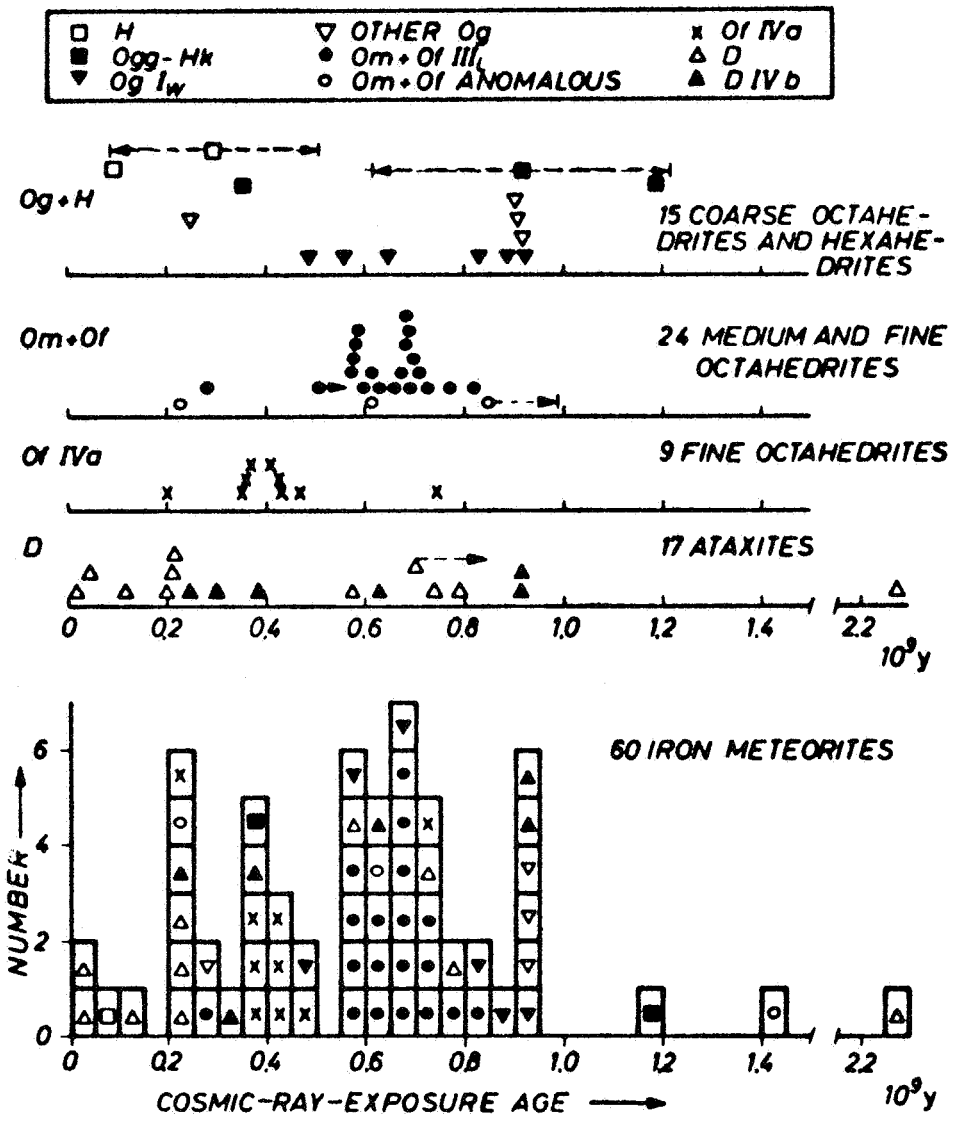

Figure 39—Distribution of cosmic ray exposure ages. Below: Histogram of the ages of 60 iron meteorites. Above: Age distribution of these 60 meteorites resolved into distributions of the various classes; in addition, some poorly determined ages are enclosed.

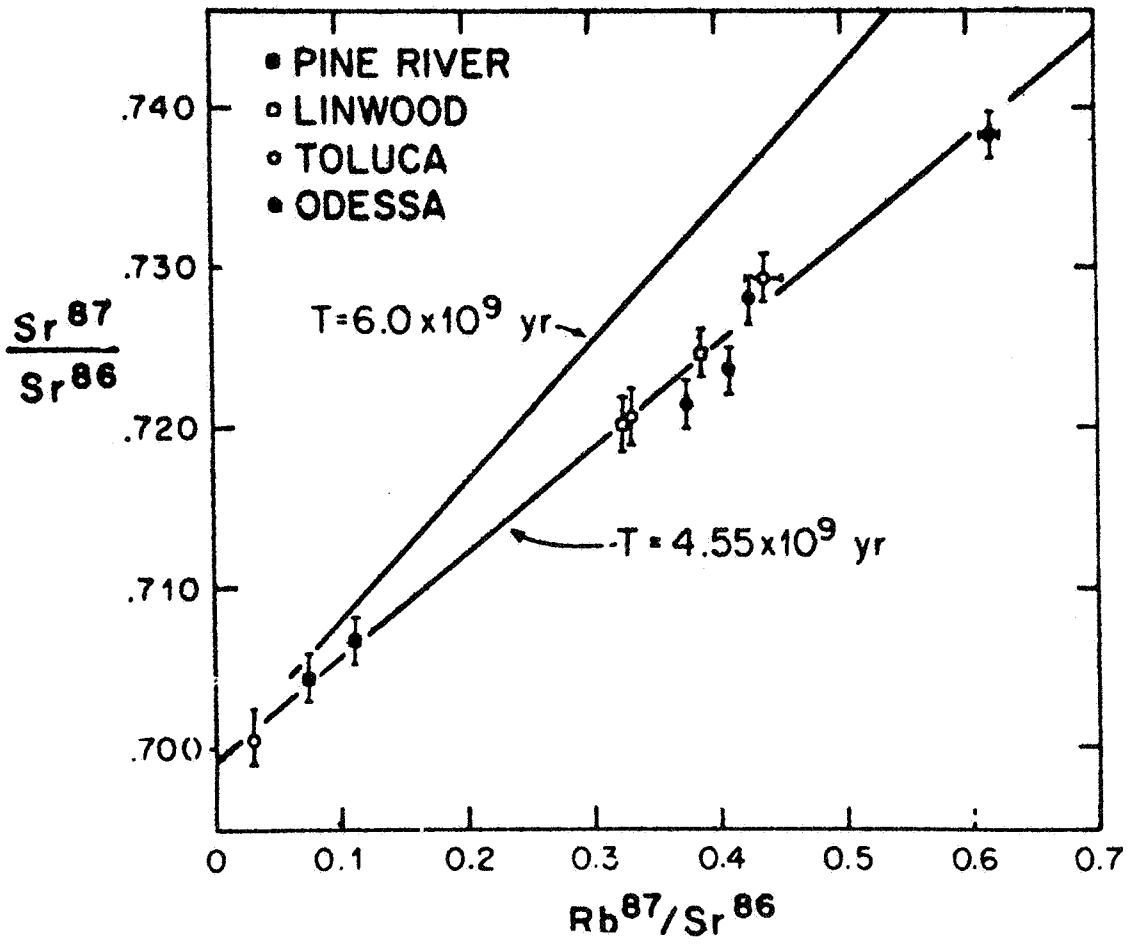

Figure 40–Strontium evolution diagram for silicate inclusions from four iron meteorites. Each of the meteorites in this representation should be considered singly as well as collectively.

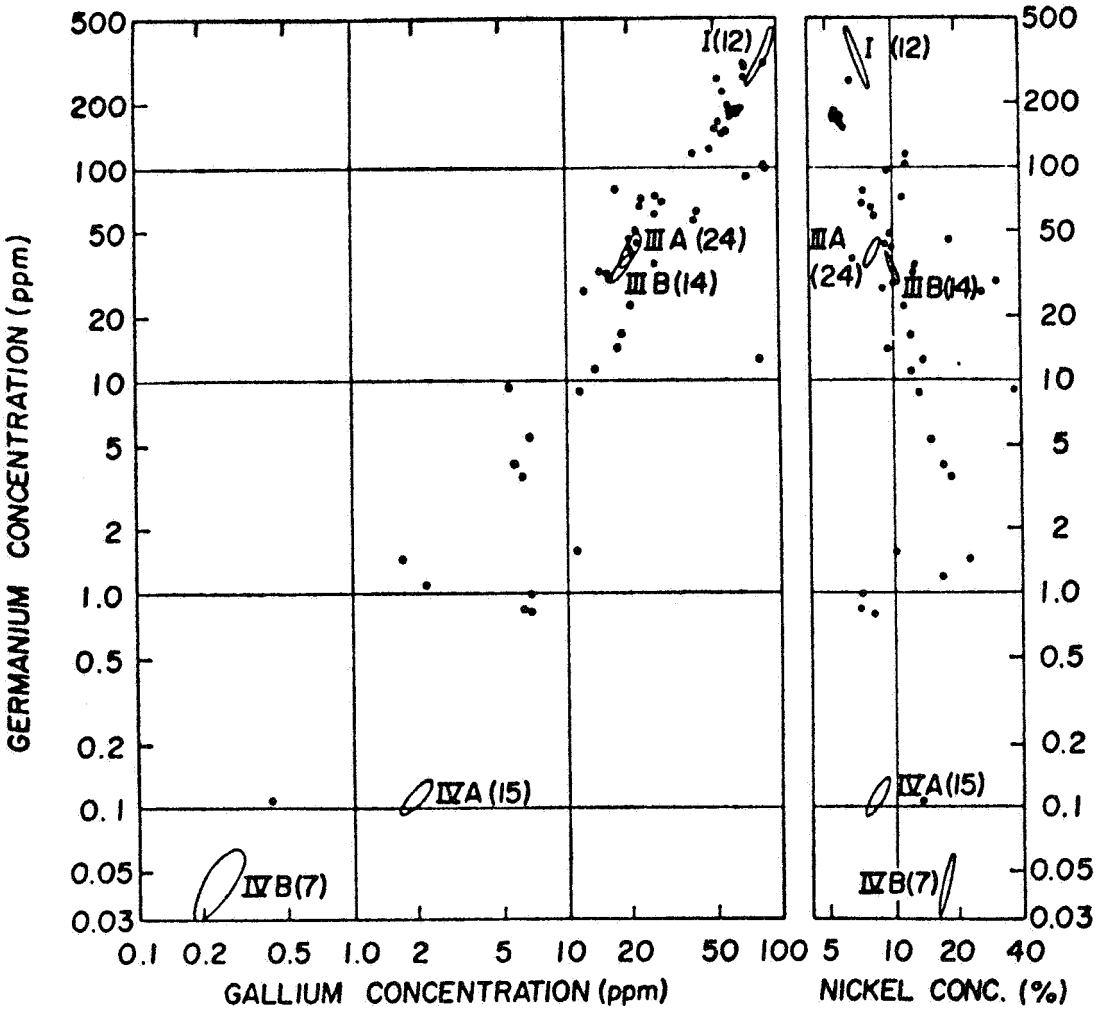

Figure 41–Plots of germanium concentration as gallium concentration for Ca. 150 iron meteorites and of germanium concentration as nickel concentration for Ca. 100 iron meteorites. The resolved chemical groups are encircled and labeled with the population of the group given in parenthesis.

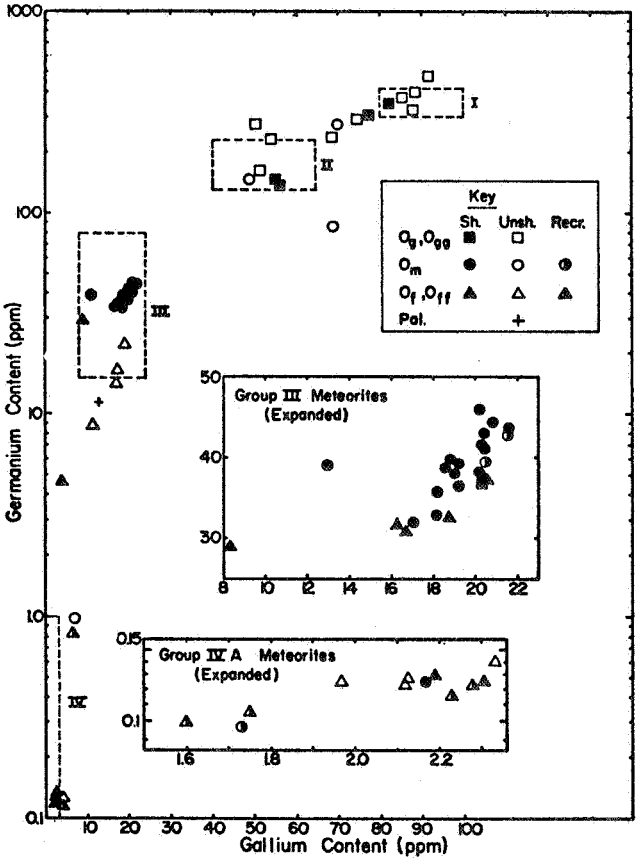

Figure 42–Germanium as gallium contents, shock histories, and structure of sixty-one octahedrites.

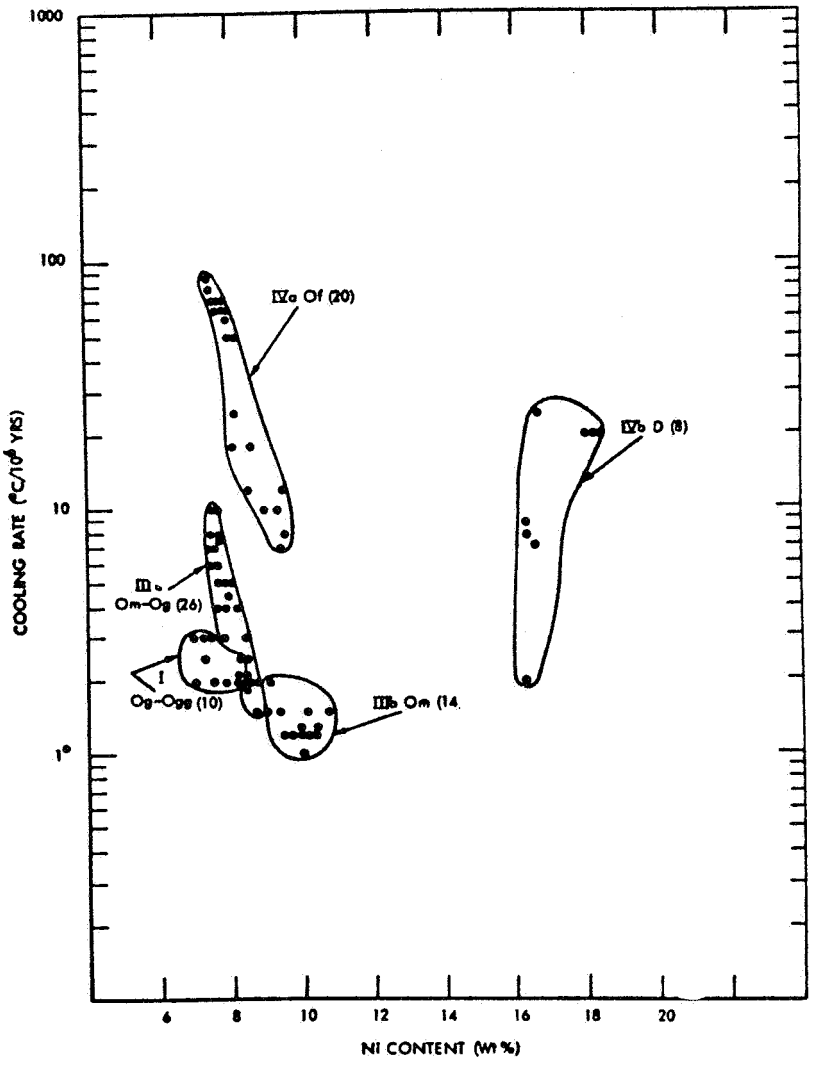

Figure 43–Variation of cooling rates and Ni content for meteorites in the five Ga-Ge groups numbers in parentheses indicate the number of meteorites studied in each group. Each cooling rate-Ge group plots coherently and is outlined on the graph.

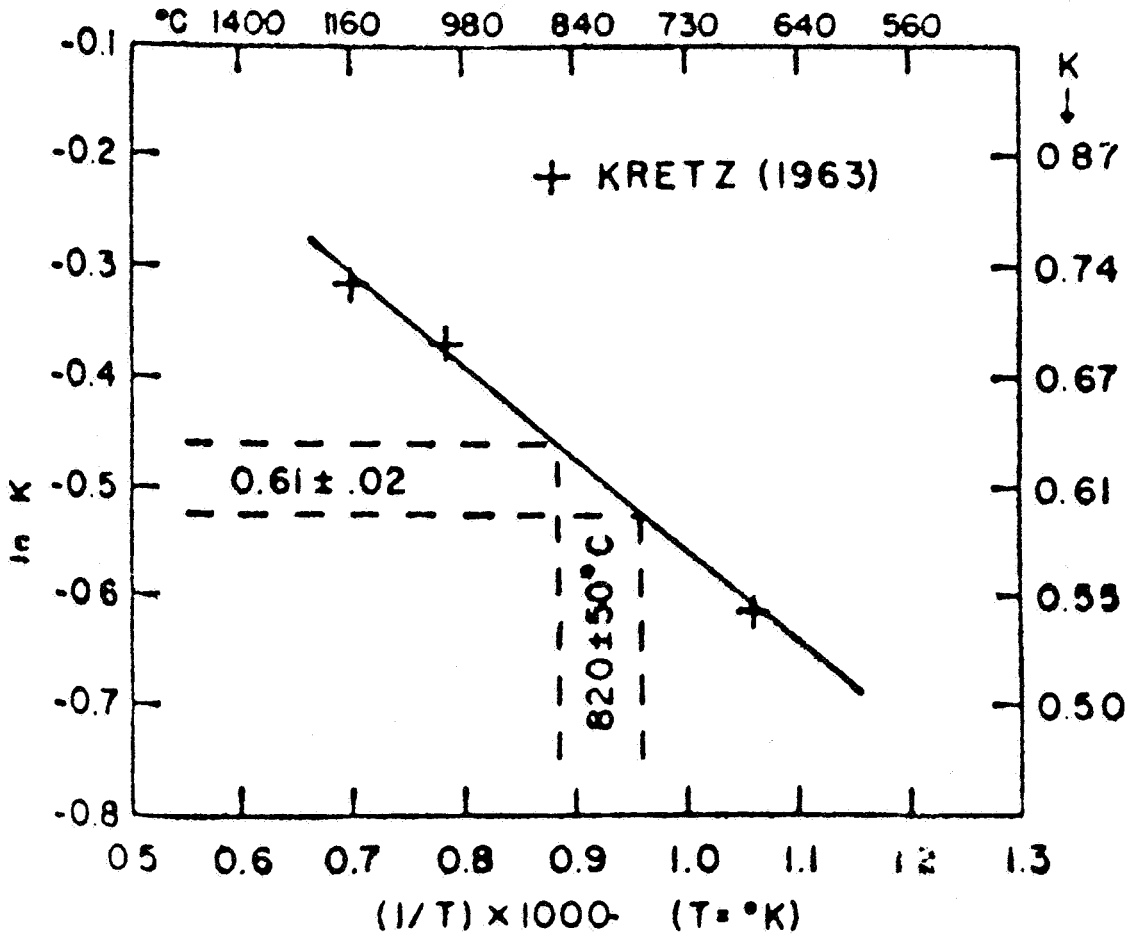

Figure 44–Estimated dependence of Kd_2 versus temperature.

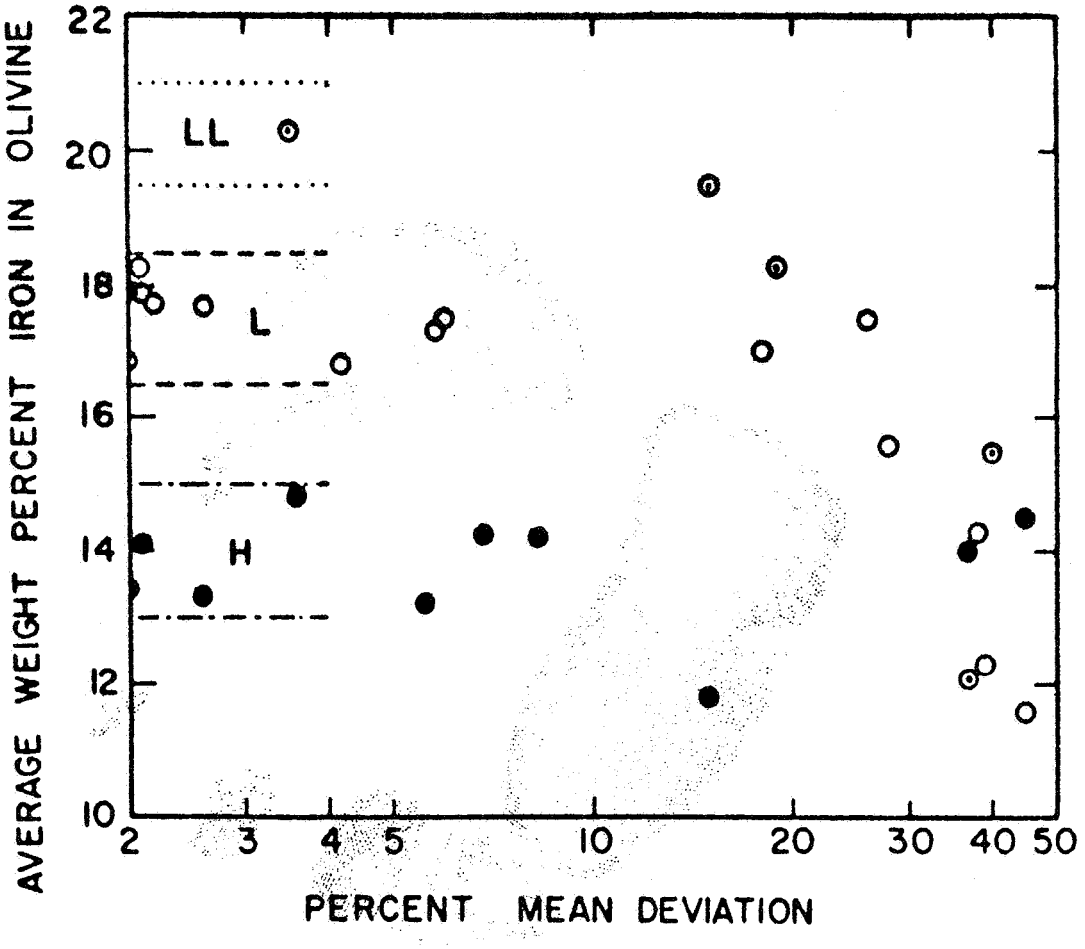

Figure 45–Plot of averave iron content of olivine versus percent mean deviation for chondrites. Note the trend towards lower iron contents for the olivine in the most unequilibrated L-L group chondrites (open circles with dot(and L group chondrites (open circles) olivine from the h group chondrites (solid circles) show little change. The dashed line pairs above and below "LL," "L," and H. denote the approximate range in compositions of olivine from equilibrated samples.

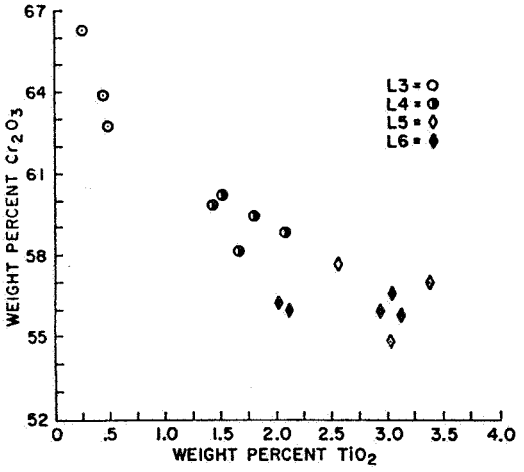

Figure 46–Correlation between chromite composition and petrographic subgroup classification. With decreasing Cr_2O_3 content, TiO_2 content of chromite from H and L, subgroups increase.

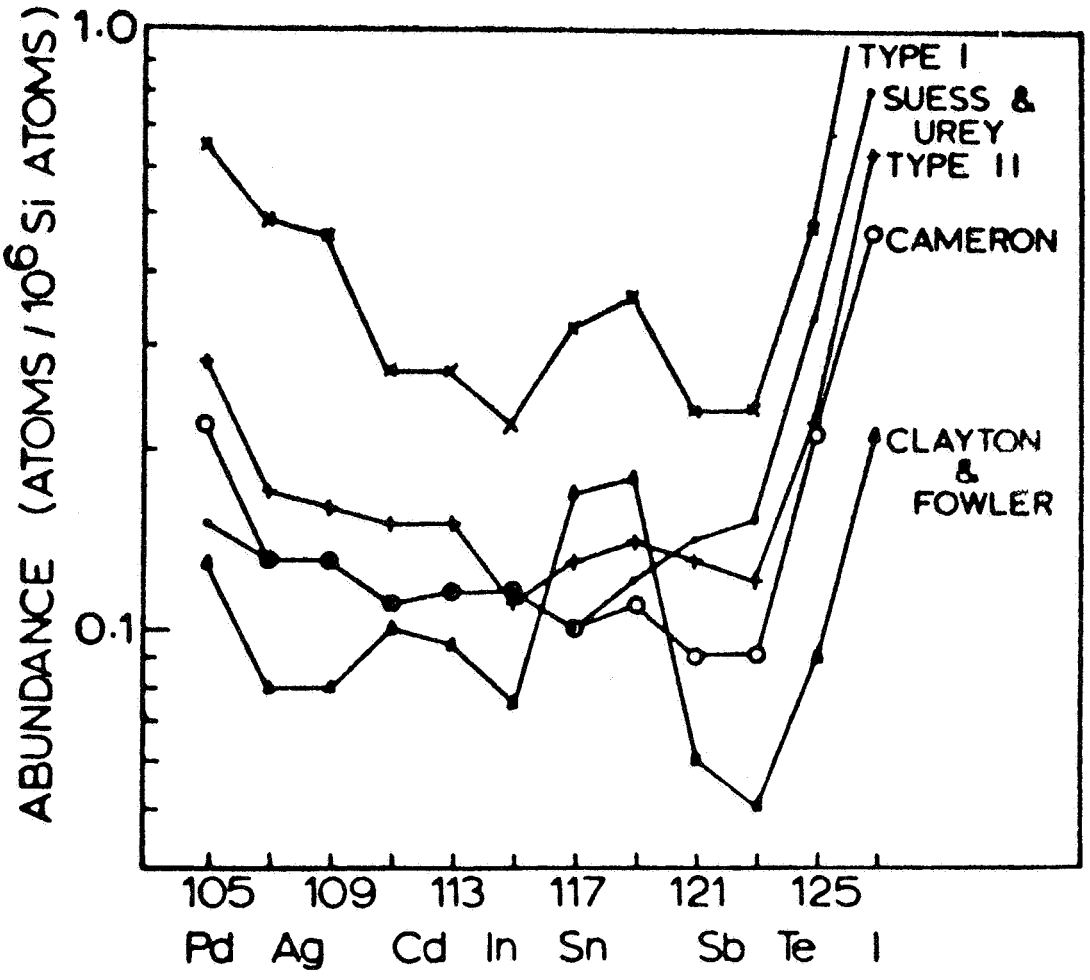

Figure 47–Experimental and predicted atomic abundances in the mass region 105-126. Predicted values are those of Suess and Urey, Cameron, Clayton and Fowler. Experimental abundances were derived from a compilation given by Larimer and Anders except for in Akaiwa and unpublished data summarized by Schmitt and Smith and Sb (this work).

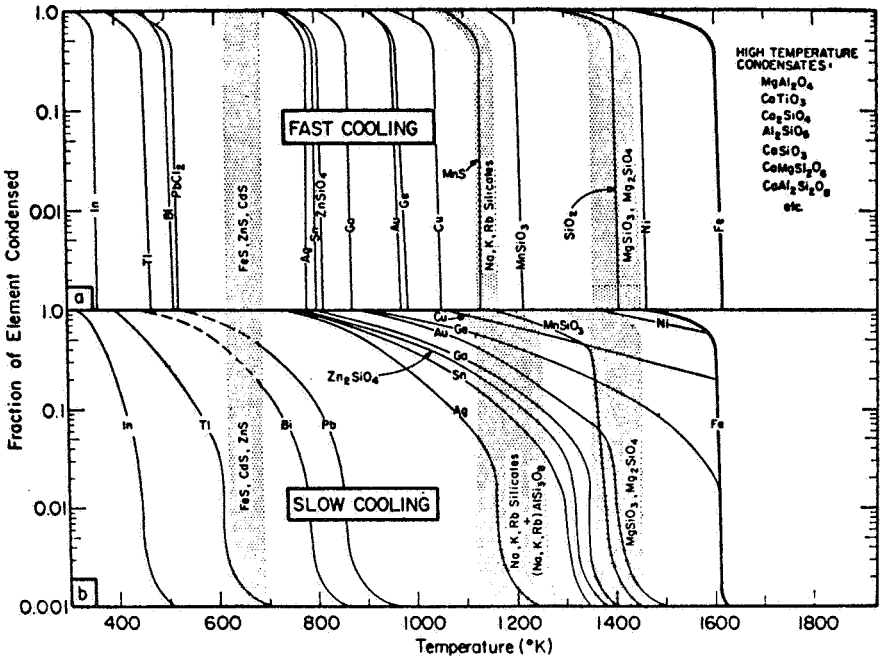

Figure 48—Condensation of the elements as a function of temperature and cooling rate. (a) Fast cooling; successive layers of pure elements or compounds condense on grain surfaces with little or no diffusion into the grain interior. Condensation range for each element is quite narrow. (b) Slow cooling; newly condensed elements diffuse into grain interior forming solid solutions. Activity in the condensed phase is lowered leading to higher condensation temperatures and broader condensation ranges.

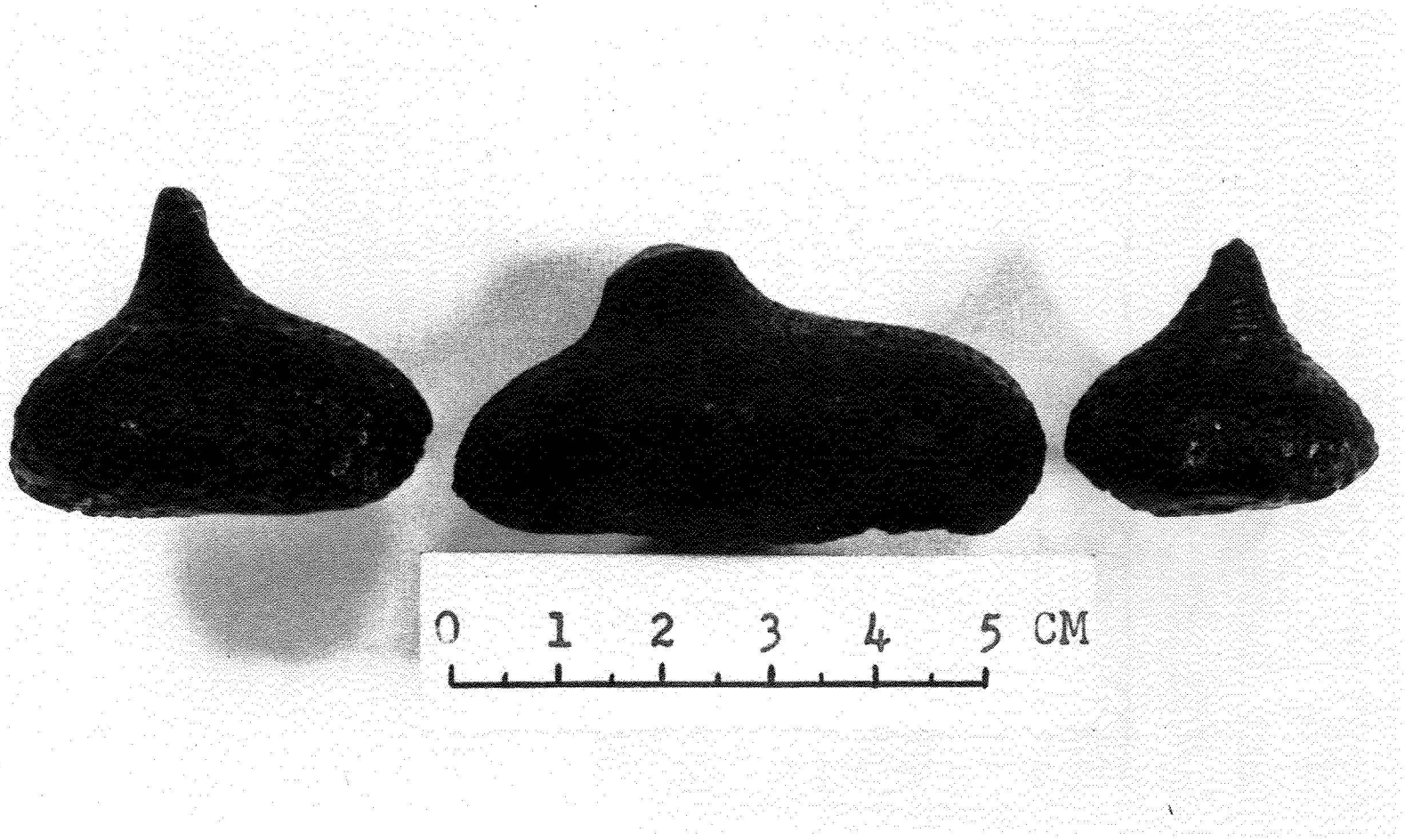

Figure 49–Bulbous drops that show plastic flattening and external spollation after completion of aerial sculpturing. Photograph courtesy of the American Meteorite Laboratory.

Figure 50–Tektites that suffered surface breaks and interior stretching during plastic bending. Note the lack of sculpturing within breaks. Photograph courtesy of the American Meteorite Laboratory.

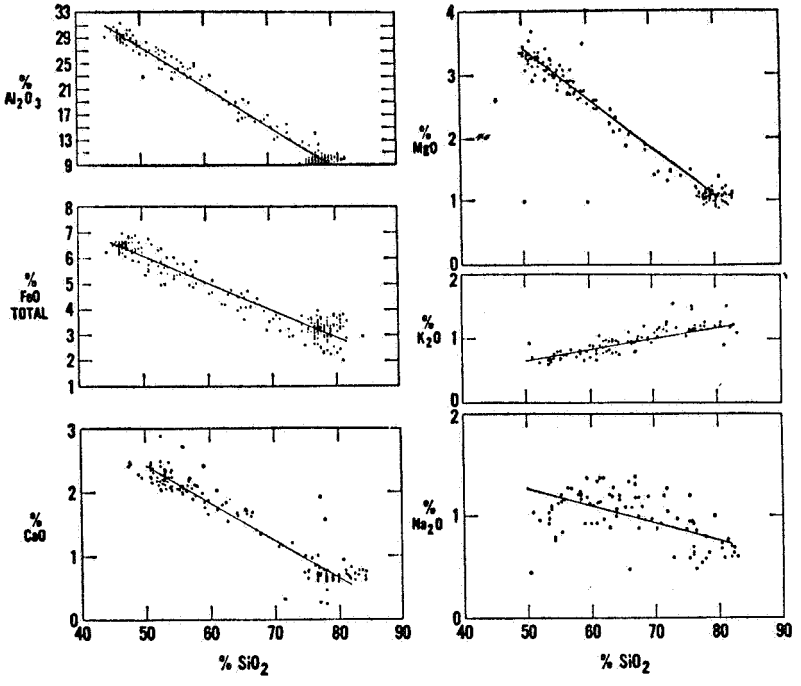

Figure 51–Vapor fractionation of Silicate containing 82% SiO_2 preformed at 2800 C°.

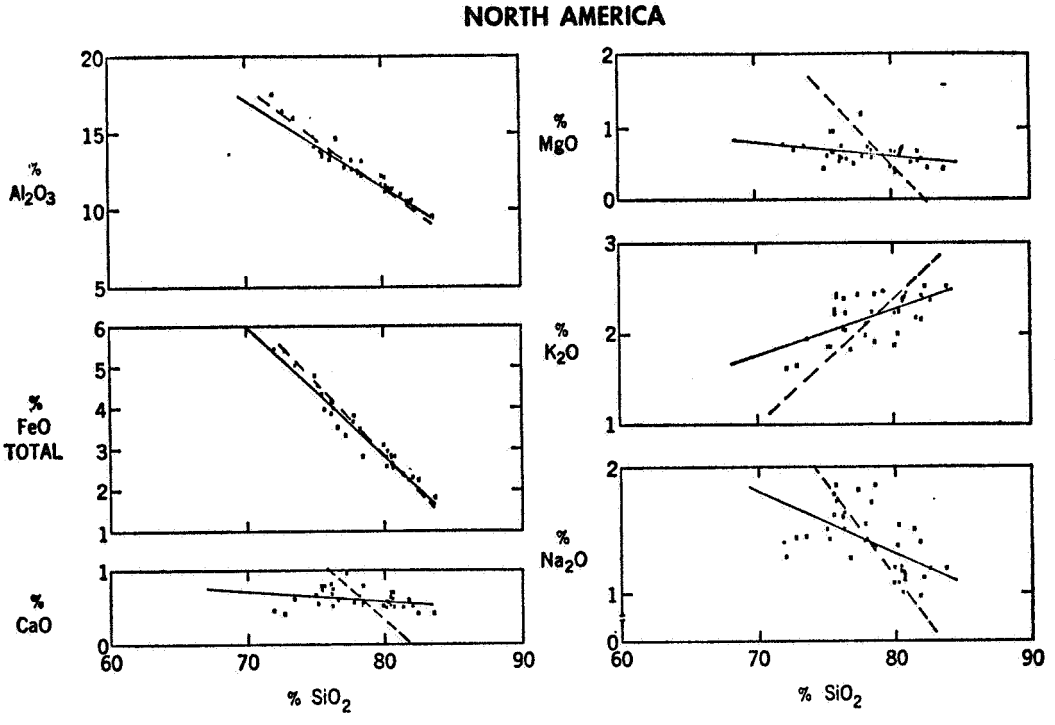

Figure 52–Major oxide-silica correlation for North American tektites.